REPORT MDC E0449

N71-38742

6792

HIGH TEMPERATURE INSULATION MATERIALS FOR RERADIATIVE THERMAL PROTECTION SYSTEMS (TPS)

CASE FILE COPY

YEAR END SUMMARY

MCDONNELL DOUGLAS ASTRONAUTICS COMPANY - EAST

MCDONNELL DOUGLAS CORPORATION

6'

COPY NO. 75

HIGH TEMPERATURE INSULATION MATERIALS FOR RERADIATIVE THERMAL PROTECTION SYSTEMS

10 AUGUST 1971

REPORT MDC E0449

YEAR END SUMMARY

Prepared for George C. Marshall Space Flight Center
Marshall Space Flight Center, Alabama 65812
Contract NAS 8–26115

Prepared by: T.A. Hughes
Materials and Processes Department

MCDONNELL DOUGLAS ASTRONAUTICS COMPANY - EAST
Saint Louis, Missouri 63166 (314) 232-0232

MCDONNELL DOUGLAS CORPORATION

TABLE OF CONTENTS

1.0 SUMMARY 1

2.0 INTRODUCTION 2

3.0 ENVIRONMENT SIMULATION AND TEST PROCEDURES 4

- 3.1 Acoustics 4
- 3.2 Vibration 5
- 3.3 Thermal 7
- 3.4 Test Fixture 11
- 3.5 Test Specimens 15

4.0 TEST RESULTS 19

- 4.1 Material Selection 19
- 4.2 1800°F Tests 20
- 4.3 2200°F Tests 35
  - 4.3.1 First Group - 2200°F 35
  - 4.3.2 Second Group - 2200°F 40
  - 4.3.3 Third Group - 2200°F 45

5.0 RIGIDIZING OF FELTED INSULATIONS 54

6.0 FOLLOW ON PROGRAM 56

7.0 CONCLUSIONS 57

- 7.1 Metal Foil Packaging 57
- 7.2 Insulations 57
- 7.3 Rigidizing of Felted Insulations 58
- 7.4 Test Procedures 58

8.0 REFERENCES 59

APPENDICES -

- A Entry Thermal Environment for Shuttle TPS High Temperature Insulations A-1
- B Density-Conductivity Trade-off Study B-1
- C Oxidation Resistance of Metal Foils C-1
- D Trade Names D-1

LIST OF PAGES

Title Page
ii through v
1 through 59
A-1 through A-14
B-1 through B-3
C-1 through C-12
D-1

ABSTRACT

Results are presented of a program to evaluate thermal insulations for use under a radiative TPS of a shuttle orbiter vehicle. Evaluations were made for survival under the multimission requirements of shuttle acoustic/vibration loads and thermal profiles with peak temperatures of 1800°F and 2200°F. During the first year of the program a total of 1100 specimen-cycles were completed using metal foil packaged refractory fiber insulations.

FOREWORD

This report was prepared by McDonnell Douglas Astronautics Company - East, under Contract No. NAS8-26115, National Aeronautics and Space Administration, Marshall Space Flight Center, Alabama. It was administered under the direction of the Materials Division of the Astronautics Laboratory, with Mr. H. M. King acting as the Contracting Officer's Representative. The valuable contributions made to this program by the following people are gratefully acknowledged: H. E. Christensen, Thermodynamics; J. R. Suhre, Dynamics; B. G. Cox, thermal testing; and H. S. Bieniecke, acoustic and vibration testing.

This report covers the period 30 June 1970 to 29 June 1971.

1.0 SUMMARY

The objective of this program is the development and evaluation of high temperature insulations and packaging materials for use under the radiative metal skin of a reusable shuttle vehicle. The insulation has to be capable of surviving the thermal loads and the acoustic/vibration loads associated with launch and reentry, for a minimum of 20 missions, and an ultimate goal of 100 missions. Minimum weight and cost are also important criteria.

A total of 1100 specimen-cycle tests were conducted on 20" x 4" specimens during the first year of this program, simulating mission launch acoustics/vibrations, and reentry heating to peak temperatures of 1800° and 2200°F. As a result of those tests the following evaluations were made:

Packaging Materials: *Inconel 702, Inconel 601, or Hastelloy X, 0.002 to 0.005 inch thick have demonstrated acceptability to 1800°F. At 2200°F peak temperature only TD-NiCr (0.003 inch) of the foils tested has demonstrated acceptability.

Insulations: Certain silica felts such as Astroquartz, Refrasil A-100, and Irish Refrasil have performed satisfactorily. Dynaflex was unsatisfactory at less than 6 lb/ft^3 density, borderline at 6 lb/ft^3, and satisfactory at 12 lb/ft^3. Microquartz also demonstrated a deficienty, pronounced shrinkage, that creates reservations about its use. Flexible Min-K demonstrated satisfactory performance to 2200°F, and would be a desirable material for volume limited applications.

This program has been extended for an additional year. Future work will include studies of venting and moisture accumulation in packaged insulations, evaluations of low weight insulations for 1000°F service, testing flight configuration specimens at maximum temperatures, and some development of HCF block insulation.

* Trade name owners are identified in Appendix D.

2.0 INTRODUCTION

The thermal protection system (TPS) is one of the most important space shuttle systems, and has a large impact on weight, development cost, and operating cost. It is also one of the major contributors to the uncertainties in weight and reuse predictions. In a metallic radiative TPS approach, the high temperature insulation, which must be placed between the metal heat shield panel and the primary structure, is a most important item.

The study described herein was performed to compare insulation materials and packaging techniques, and to provide information and data to assist the shuttle program in the selection and design of thermal insulations. To accomplish this, selected insulations were cyclically exposed to the shuttle environment of acoustic/vibration loads and thermal exposure at reduced pressure. The peak temperatures of primary interest in this program during the first year were 1800°F, 2200°F and 2500°F. A total of 400 specimen-cycles were completed in 1800°F tests and 700 specimen-cycles in 2200°F tests. No tests have yet been run at 2500°F because the packaging problems which arose at 2200°F were not resolved until late in the report period.

The primary requirements for shuttle insulations as defined in the scope of work for this contract are that it have the lowest density and thermal conductivity consistent with mechanical durability and thermal stability to withstand repetitive exposure to the shuttle operating environments, including acoustic, vibrational and thermal loads. Since the radiative skin will not be weathertight, the insulation must not absorb moisture, or it must be protected from it. The insulation should be capable of withstanding at least 20 cycles of exposure to nominal ascent and reentry loads, with an ultimate goal of withstanding 100 cycles of exposure.

The insulation concepts examined in this program were generally low density refractory fiber felts (1 to 12 lb/ft^3) enclosed or packaged in thin gage, oxidation resistant metal foil; and rigid blocks, either in metal foil packages or incorporating a water-resistant refractory coating. The metal foil packaging concept has many advantages, including effective support and containment of light, nonrigid felts, protection from moisture, and versatile means of attachment to the structure. An impermeable membrane, such as metal foil, however, must be vented to accommodate the rapid pressure changes associated with launch and reentry.

The evaluation program was conducted by mounting five specimens (20 x 4 in) in a fixture, subjecting the assembly to either launch acoustics or vibration at ambient room temperature, and then to a thermal cycle at 10 torr pressure. To expedite testing, five cycles of each environment were run consecutively so that in each sequence five simulated missions were completed. All specimens were either 1.5 or 2.0 inches thick, and no attempt was made to optimize thicknesses as this portion of the program was primarily for comparative evaluation.

The environmental definition for establishing the test parameters initially reflected the then current primary interest in the low cross-range orbiter. As the program progressed, however, the primary interest shifted to the high cross-range orbiter, and which would influence principally the thermal test profile. In establishing our thermal profile we had given considerable weight to the possible long cross-range reentries, and therefore the change in emphasis did not cause any perturbations to the program.

In addition to the flight simulation testing of commercial insulations, an investigation was also conducted on the rigidizing of prefelted insulations by impregnation with ceramic binders. This investigation did not produce a useful product and was suspended in favor of HCF block insulation which was at a more advanced state of development.

3.0 ENVIRONMENT SIMULATION AND TEST PROCEDURES

The insulation test specimens were subjected to a block of 5 cycles of launch vibration/acoustic environment, followed by a block of 5 cycles of reentry thermal exposure. The launch mechanical loads were applied by vibration in the initial sequence, and following the subsequent thermal test, the next sequence employed acoustic exposure, in lieu of vibration. This procedure was employed because of some uncertainties in the internal environment and response of the insulation to that environment.

The most severe acoustic loads occur during the ascent phase, in conjunction with a very modest heating period. During reentry, the situation is reversed, a severe thermal pulse of considerable duration, and with a moderate acoustic load. To simulate these environments, the test specimens were subjected to acoustic/vibration loads at ambient room temperature and pressure, and to thermal loads at reduced atmospheric pressure, reflecting the low ambient pressures associated with the high altitude of entry.

3.1 Acoustics

The major source of mechanical excitation on the shuttle vehicle is the noise from the main propulsion engines, which results in an acoustic load on the TPS skin. The acoustic environment experienced by the internal insulation is modulated by the vehicle skin, though the degree of modulation is uncertain. In addition, response of the skin to the acoustic excitation may be transmitted to the insulation via the structural supports in the form of mechanical vibration.

Peak lift-off noise external to the aft portion of the booster was estimated from empirical considerations to be 169 dB (0.82 lbf/in^2), and the transonic buffeting near the booster-orbiter interface, 155 dB (0.164 lbf/in^2). The most significant excitation ends before appreciable heating of the insulation occurs. Peak noise external to the orbiter is estimated to be 0.33 lbf/in^2 (161 dB), at lift-off, decaying to 0.13 lbf/in^2 (153 dB). Because use of internal insulation is expected to be primarily in the orbiter, the maximum power available from the test equipment (156 dB) was considered a reasonable average simulation for evaluation purposes. It was assumed that the mated vehicles would pass through Mach 1.0 at about 30 seconds, after which time the vehicles would be essentially free of the acoustic noise field.

Reentry acoustic excitation for the orbiter is estimated to be 113 dB (0.0013 lbf/in^2), or less than 0.2% of that occurring during launch. This peak occurs about 10 minutes after peak reentry heating (low cross-range) when the surface temperature has cooled considerably. The estimate for noise level during reentry was based on data from the ASSET reentry (Reference 1) and from the NASA-Langley wing stall flutter and buffet response study (Reference 2).

The acoustic noise spectrum specified for test purposes is shown in the table below, and was applied for 150 seconds in each test, representing 5 launch cycles.

RANDOM ACOUSTIC NOISE SPECTRUM

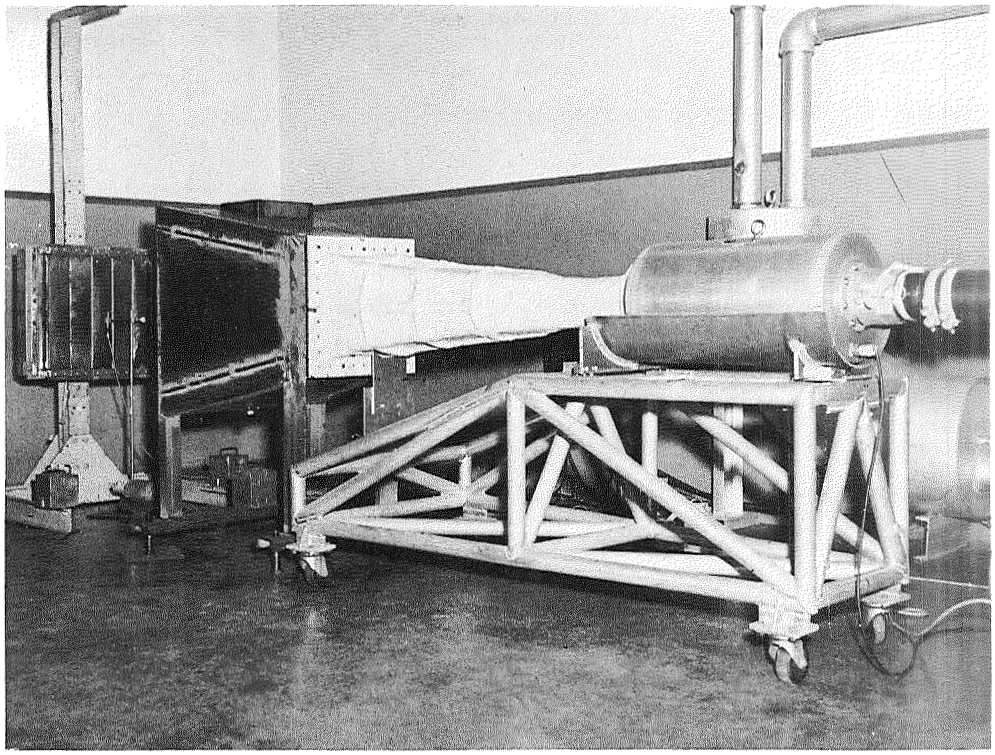
Octave Band Hz	dB Re 0.002 $dynes/cm^2$ rms	Tolerance dB
23.8 - 47.2	133.7	+6, -2
47.2 - 92	139.3	+6, -2
94 - 188	142.7	+5, -1
183 - 375	146.8	+4, -1
375 - 750	150.7	+4, -1
750 - 1500	144.0	+5, -1
1500 - 3000	139.7	+6, -2
3000 - 6000	133.2	+6, -2
Overall	154.0	+4, -0

The noise source consisted of a Wyle WAS-3000 airstream modulator coupled to an exponential horn having a 50 Hz low frequency cut-off. The modulator was rated at 10,000 acoustic watts. A general view of the acoustic test arrangement is shown in Figure 1. The 20 inch dimension of the specimens was purposely placed in the vertical plane to simulate launch orientation and which provides for representative excitation and resultant settling of the insulation.

The acoustic spectrum and power level achieved during testing was monitored with a reference microphone. Representative data is shown in Figure 2 along with the tolerance permitted under the approved plan. A traverse across the opening of the exponential horn indicated that the spectrum-power level was uniform across the face within the tolerance band.

3.2 Vibration

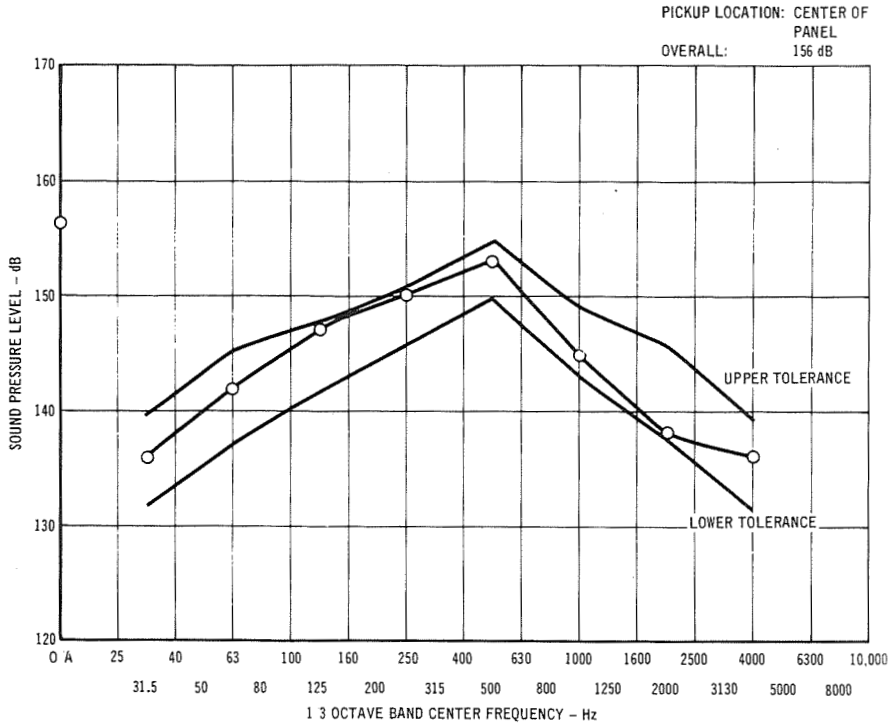
As stated previously, vibration response of the shuttle structure during launch and reentry is primarily caused by the acoustic pressure acting on the



ACOUSTIC TEST SET-UP WITH SPECIMENS IN PLACE

457-1127

Figure 1



OCTAVE BAND SPL DISTRIBUTION

457-1126

Figure 2

external surface. Based on predicted acoustic loads the random vibration spectrum shown in the table below was used in the program. The vibration load was applied for 150 seconds in each test, representing 5 launch cycles.

RANDOM VIBRATION SPECTRUM

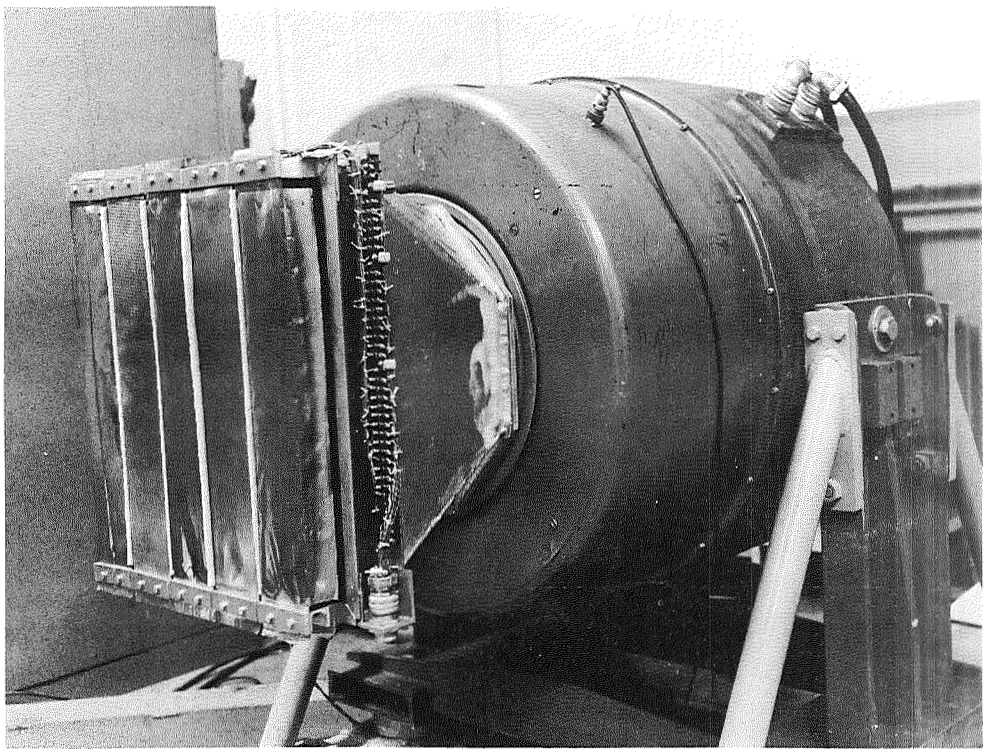
20 - 200 cps	+6 dB/octave
200 - 600 cps	0.25 g^2/cps
600 - 2000 cps	-6 dB/octave

The vibration test equipment consisted of an MB/C25 HB electromagnetic exciter powered by a 20 KVA Ling amplifier. The signal to the amplifier was wide band random with the power spectrum shaped by a filter set (MB-388) having constant bandwidths of 25 cps over the range of 20-2000 cps. In operation, the specimens were oriented with their principal surfaces in the vertical plane, with the primary axis of excitation at right angles to the surface of the insulation specimens as shown in Figure 3. Accelerometers mounted at the fixture attachment face were used to monitor excitation levels at various locations on the test fixture.

The vibration spectrum (Figure 4) was within tolerance except for a resonance at 1300 cps, and antiresonance at 1450 cps. Transmissibility plots indicated that the response was fairly uniform across the face of the fixture, and thus each specimen was subjected to essentially the same spectrum. It was not believed that the resonance adversely affected the validity of the test results because the motion was uniformly applied to all test specimens, and because of the design of the test specimens, high frequency response was expected to be drastically attenuated. Cause of the resonance was traced to the shaker armature. It was impractical to change to another shaker or to remove the armature from service as unacceptable delays would have been incurred in the test program.

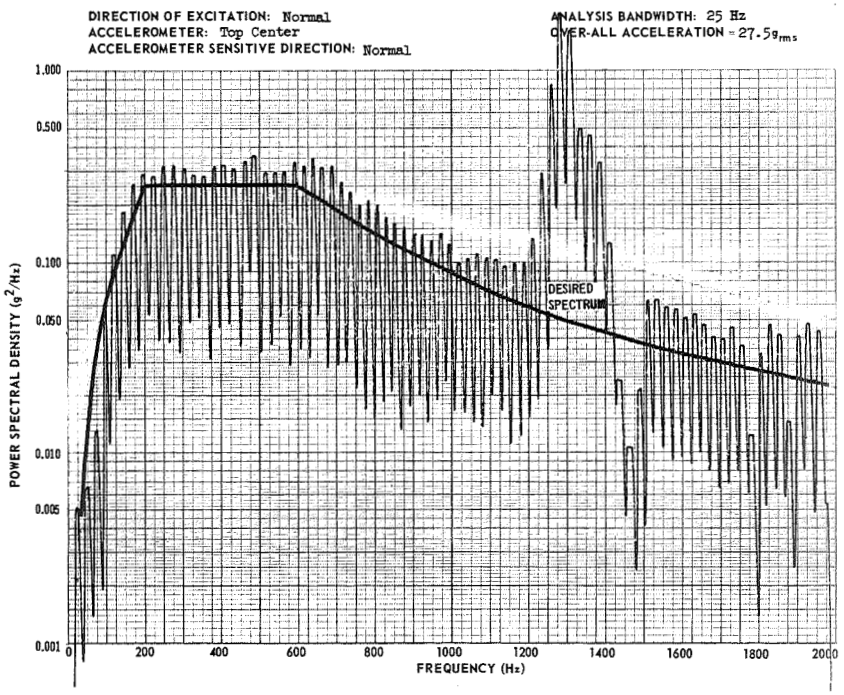
3.3 Thermal

There is a wide range of time-temperature histories possible by virtue of the various shuttle entry trajectories, vehicle stations and configurations. For the purposes of this program, one general time-temperature profile was selected that would adequately test the response of the insulation to its environment, be reasonably representative of current and foreseeable heat pulses, and be economical in time as many repetitive cycles were required in the test program.



TEST SPECIMENS IN VIBRATION TEST
(AFTER 30 CYCLES)

Figure 3



457-1129

POWER SPECTRAL DENSITY ANALYSIS

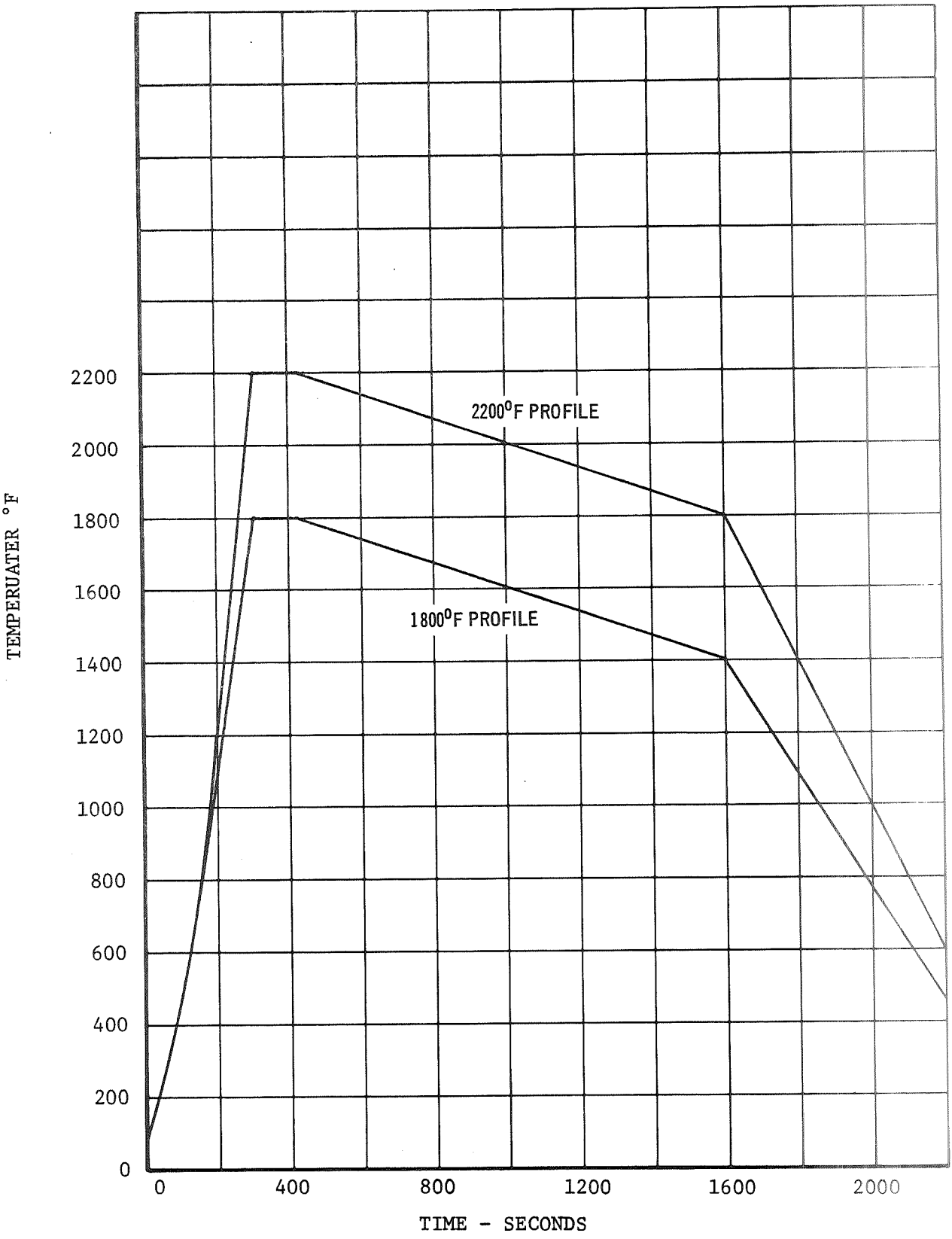
Figure 4

From an insulation materials viewpoint, the precise shape of the thermal pulse is not as important as the time at or above various temperatures. The initial heating rate should also be representative of the actual thermal shock the insulation will experience in service. By utilizing a generalized time-temperature profile that is not unique to any specific trajectory or body station, insula- performance comparison can also be applicable to a broader range of uses.

An extensive analysis was made of the various heat pulses that would be encountered by shuttle orbiters, and which provided a basis for a simplified thermal profile for test purposes. This profile was most strongly influenced by the long cross-range delta orbiter. Details of this analysis are reported in Appendix A. Because of practical considerations, the resultant profile was shortened by about 400 seconds during the cool-down phase to provide the profile shown in Figure 5, and which was used for testing. The reason for shortening the time was to reduce the total time required for cycling. This also provided an additional dividend in that the total heat input to the specimens was reduced at a noncritical temperature, additionally reducing the necessary cooling time after the heat input is terminated. The length of time required for the interior of the insulation to cool before it can be recycled is a very significant portion of total test time. To recycle a thermal test before the interior of the insulation had cooled sufficiently would result in progressive buildup of temperature in the interior of the insulation, distorting its thermal response.

It has not been possible to define closely the ambient pressure of the atmos- phere surrounding the insulation, due to lack of adequate data on heat shield air leakage rates. Prior to entry into the atmosphere, the insulation will be in a high vacuum environment, and the pressure environment external to the vehicle will build up at a slower rate than the thermal pulse. However, the rate at which the increased air density penetrates the interior of the vehicle cannot be predicted accurately at this time. For test purposes, we have utilized a constant pressure of 10 torr.

The test equipment for thermal testing was essentially a heated superalloy metal panel radiating to the test specimens within a vacuum chamber. The heater consisted of 24 graphite strip heaters wired in series-parallel, radiating to an Inconel plate which simulates the radiative TPS (a coated columbium plate was used for 2200°F tests). The Inconel plate also closed off the graphite heater cavity from the specimen area. The graphite heaters were bathed in nitrogen to prevent



457-1130

TIME-TEMPERATURE PROFILE
FOR THERMAL TESTING

Figure 5

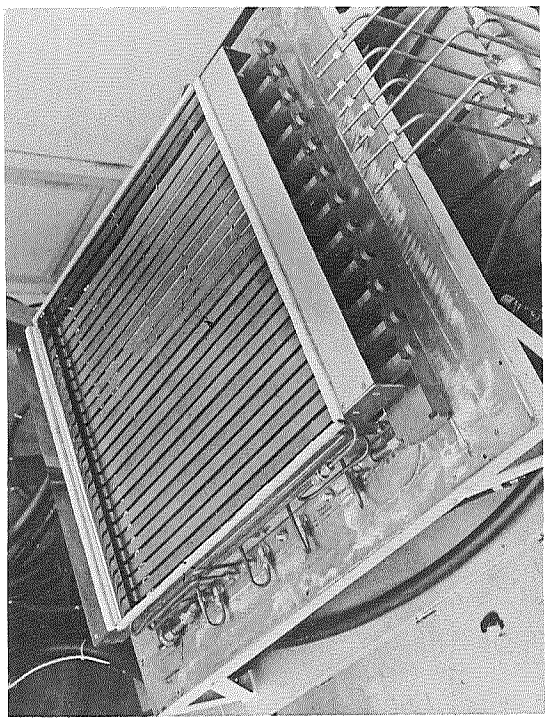
oxidation, while the specimens were in a positive flowing air atmosphere to permit oxidation of the metal foil packaging. The interior of the heater cavity was chrome plated to reduce losses, and also water cooled for protection. Figures 6 and 7 show the heater before the radiant susceptor plate was mounted. The susceptor plate (simulated TPS metallic heat shield) was mounted in a water cooled picture frame with an area slightly larger than the test area exposed (Figure 8). In operation, the specimens in the test fixture are suspended over the radiant panel. Figure 9 shows the fixture and test specimens in place above the radiant panel with some of the edge insulation removed.

The thermal test was run in a 5.5 ft. diameter vacuum chamber at 10 torr (air) pressure. The time-temperature profile of the radiant panel was continuously controlled by a function generator, with the temperature response of the panel and of the specimens sampled every 60 sec. and recorded on tape with a simultaneous digital print-out. Automatic data plots were available for each cycle as desired. Views of the chamber and instrumentation are shown in Figures 10 and 11.

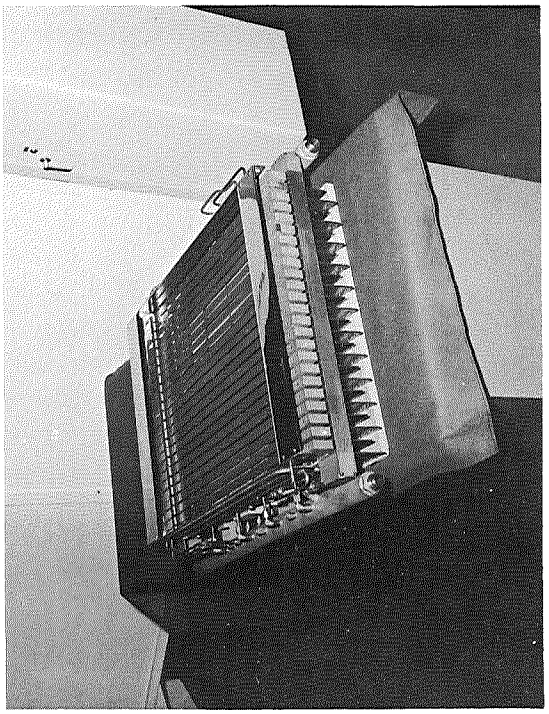
It was recognized that the duration of the cool down portion of the thermal cycle would have an influence on the reproducibility of the thermal histories. If the specimens were not sufficiently cool at the conclusion of one cycle, the succeeding cycle would tend to "pump-up" the temperature of the insulation. To eliminate problems of this nature, the internal temperature of the slowest cooling specimen was monitored (in our first five specimens, this was the Flexible Min-K, due to high density and low conductivity) and recycling was not initiated until its temperature had fallen below 150°F. To expedite cooling during the temperature decay period of the test, cooling air was introduced across the specimens. This also resulted in a gradual buildup of air pressure within the chamber, which was pumped out before the next cycle. A plot of the temperature history of Flexible Min-K over the entire fifth cycle of the first sequence is shown in Figure 12. As noted, the interior temperature of this specimen at initiation was just below 150°F. All other specimens at that time were about 70°F.

3.4 Test Fixture

The test specimens were mounted in a test fixture and remained undisturbed during testing. The test fixture with its five specimens was mounted on the vibration table, acoustic horn, and on the heater in the vacuum chamber as an assembly to avoid nontest damage. When mounted in the test fixture, the specimens were held by both the upper and lower end tabs for the vibration and acoustic test,



GRAPHITE HEATER BEFORE INSTALLATION OF RADIATION SUSCEPTOR PLATE Figure 6



HEATER WITH SUSCEPTOR MOUNTED IN WATER COOLED FRAME Figure 7



THERMAL TEST WITH SPECIMENS IN PLACE EDGE INSULATION REMOVED FOR CLARITY Figure 8

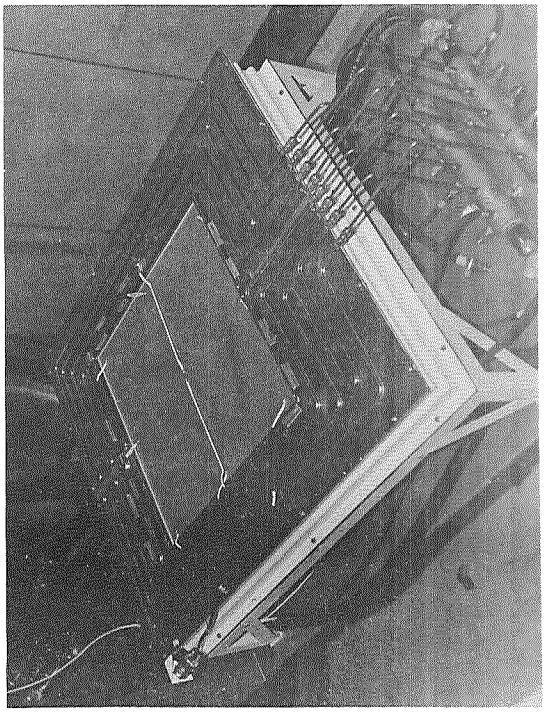


Figure 9

457-1131

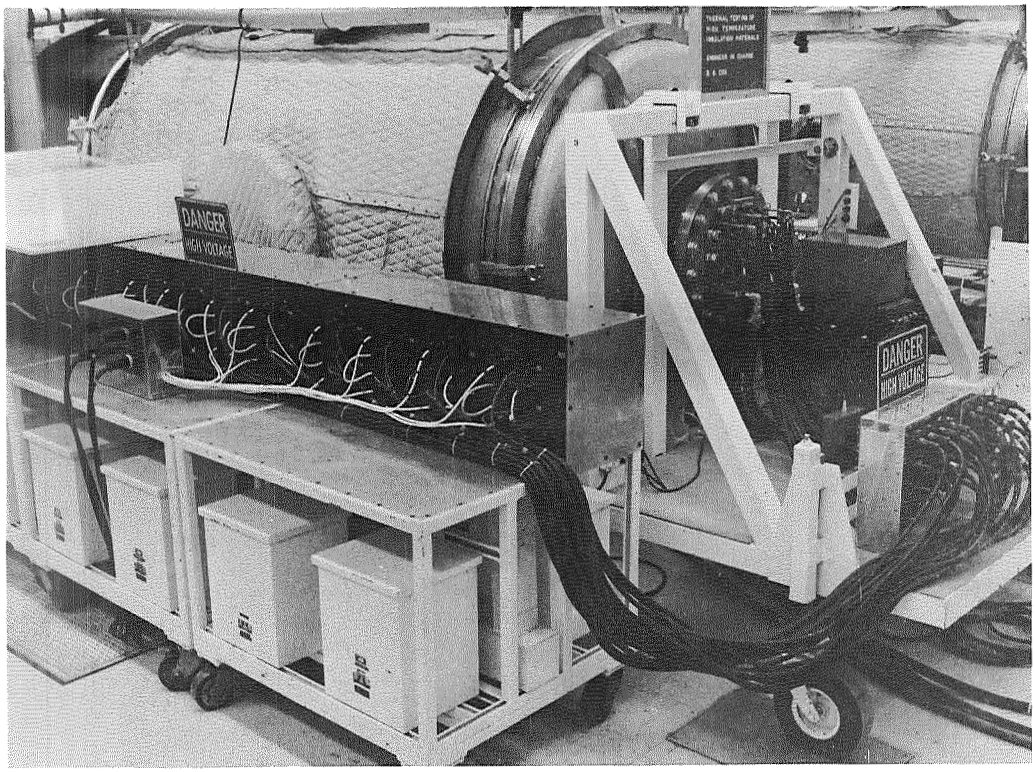
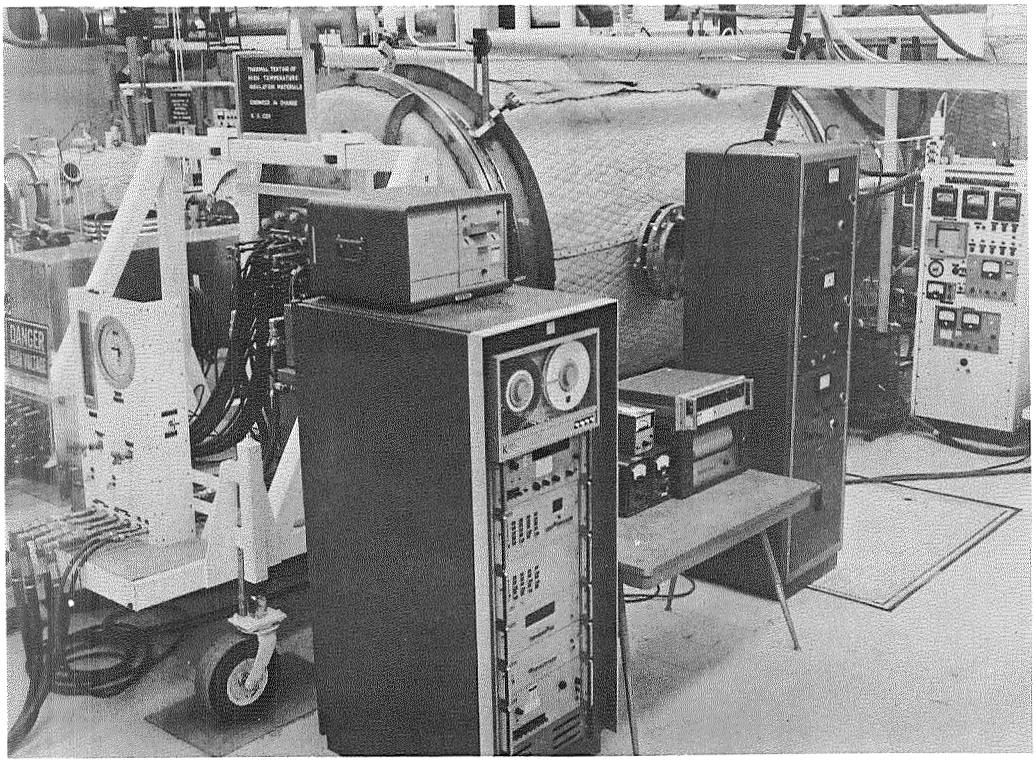


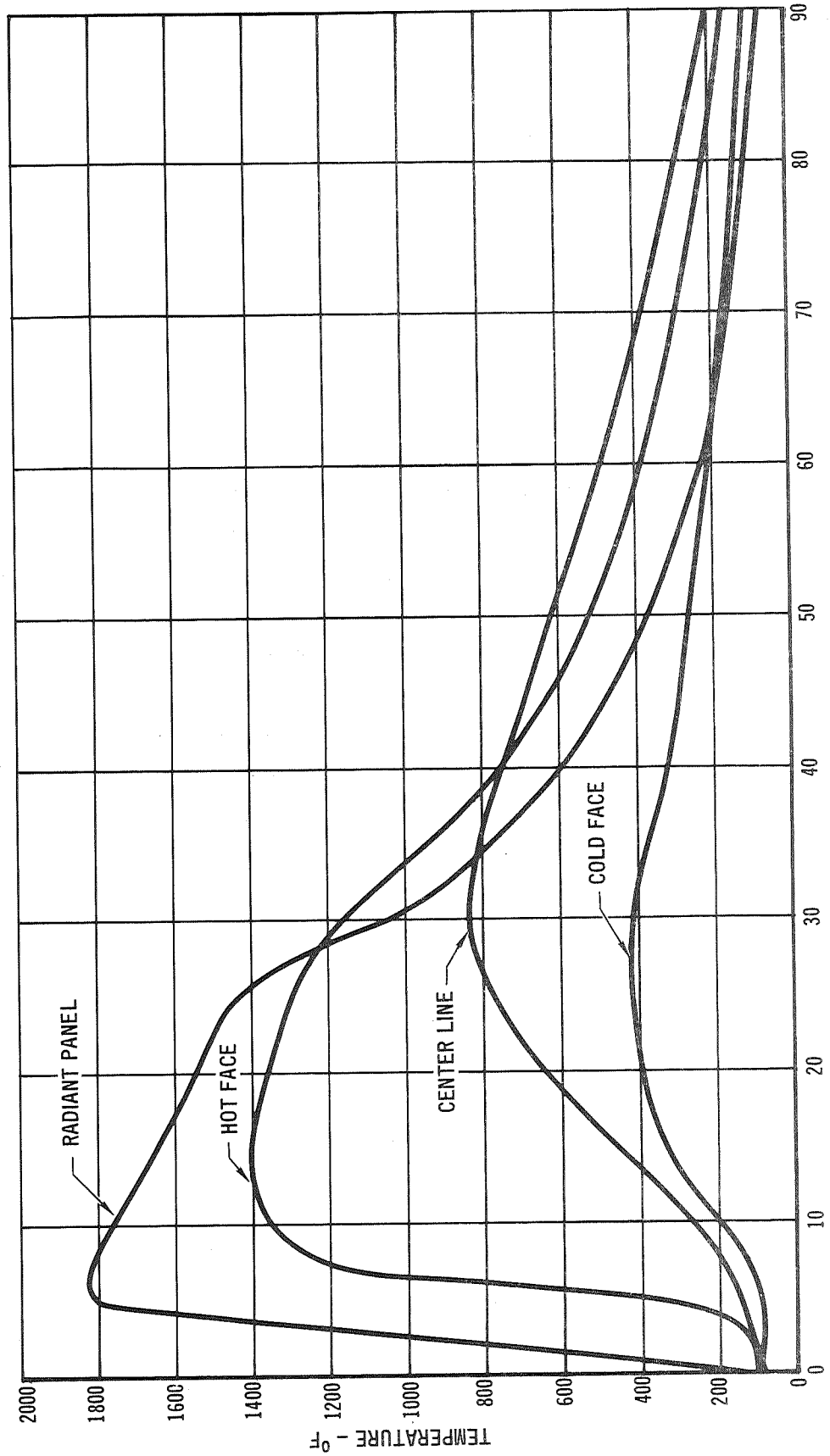
Figure 10



VIEWS OF VACUUM CHAMBER FOR THERMAL TEST WITH INSTRUMENTATION AND CONTROLS

457-1132

Figure 11



TEMPERATURE HISTORY OF FLEXIBLE MIN-K DURING FIFTH CYCLE

457-1133

Figure 12

but were held by only one set of tabs (on the cool side) in the thermal test. The test fixture, before mounting of the test specimens, is shown in Figure 13, and after mounting the specimens, in Figure 14.

3.5 Test Specimens

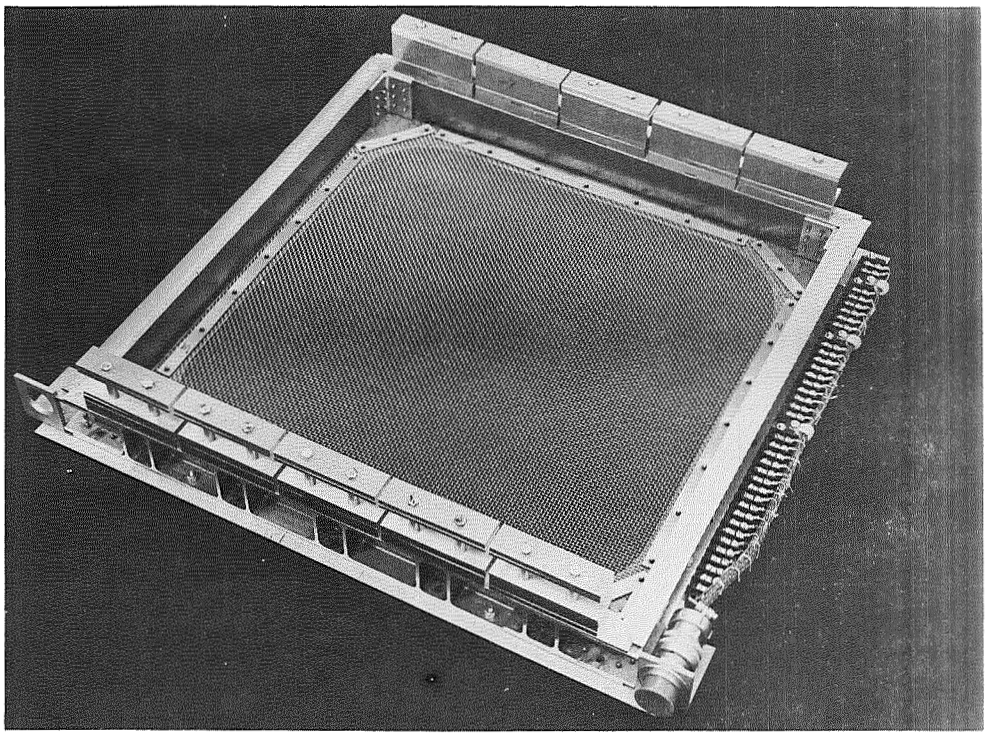
The test specimens consisted of low density felts enclosed in thin gage metal foil packages. The specimens were 3.85 inches wide, 20 inches long, and either 1.5 or 2.0 inches thick. The usual metal foil package was a simple box shape with the hot and cool skins extended to provide tabs for mounting in the test fixture; however, other package configurations were also tested, as described later. The cool face of the box and the end closures were attached by spot welding. In many cases the necessary width of flat sheet for forming the boxes was obtained by seam welding narrow strip. To permit the package to breathe during pressure changes in the vacuum chamber, holes, 1/16-1/8 inch diameter, were made in the cool face. Initially four holes were used, later changed to 16. However, even the latter number was not entirely adequate to prevent some bloating of the package during pump down of the vacuum chamber for thermal testing.

A photograph of representative packaged specimens is shown in Figure 15, and the basic configuration in Figure 16.

Three thermocouples were installed in each specimen near the center. One was about 0.1 inch from the hot surface, the second one at the center of the thickness, and the third about 0.1 inch from the cool surface. The position of the thermocouples has to be qualified because in inserting the thermocouples, there was no assurance that they would not drift to one side or the other. After assembly, the package was x-rayed to determine the final position of the junction.

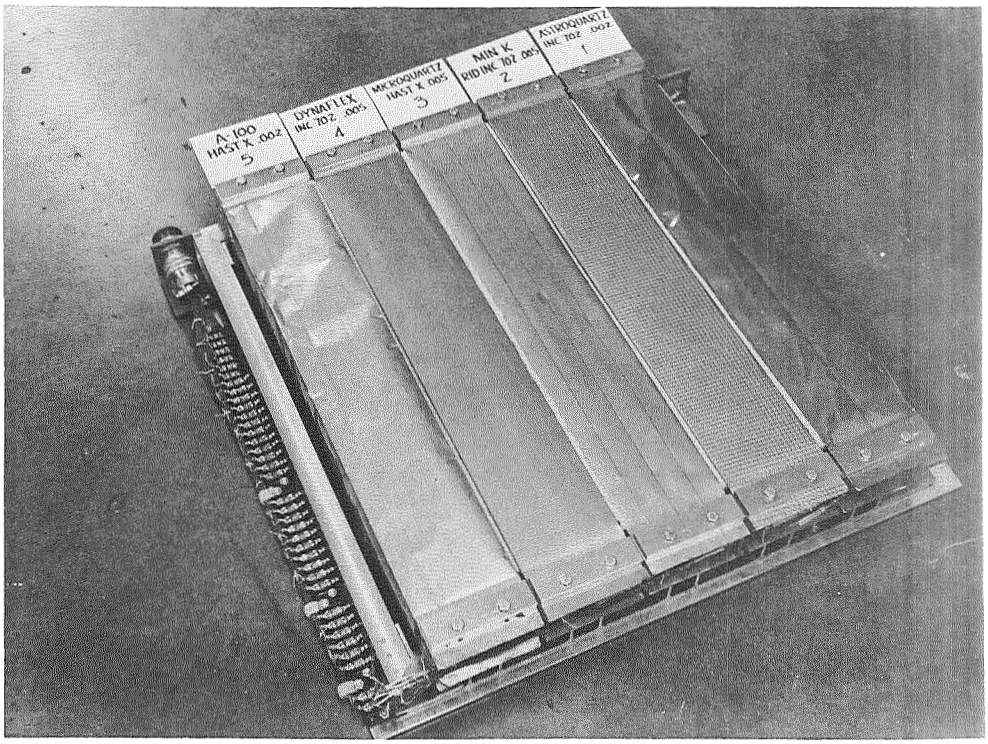
The thermocouples were metal sheathed (Inconel), type K, 0.040 inch diameter sheath with an exposed bead. During the course of the tests, the thermocouples were a continuing problem. Frequent breakage of the exposed 0.005 inch diameter wires at the bead occured, necessitating frequent removal and repair, and loss of position information. Also, x-rays at the conclusion of many cycles indicated movement of the thermocouples away from their original location, even when not disturbed by repairs. This negated much of the value of the temperature histories, at least as far as making precise thermal efficiency comparisons.

The metal foil for packaging was in the range of 0.002 to 0.005 inches thick, and was used as flat sheet, and also in texturized form for added rigidity. The texturized form was achieved by passing it through corrugating rollers in two passes, each pass at right angles to the other. The texturizing was performed by



UNIVERSAL TEST FIXTURE

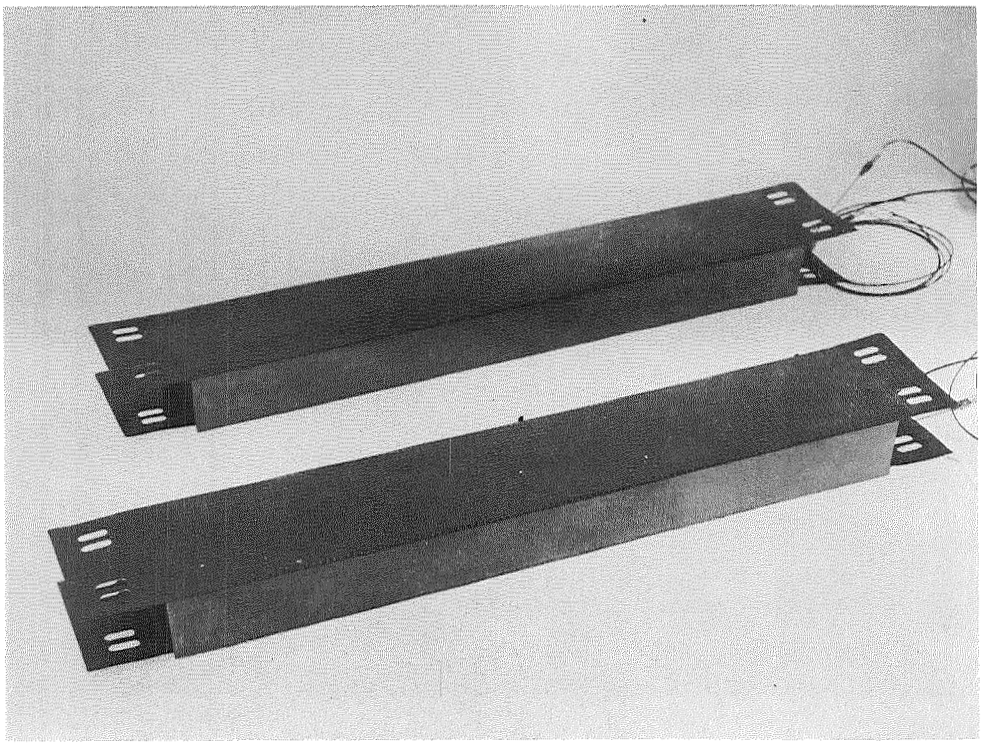
Figure 13



TEST SPECIMENS MOUNTED IN TEST FIXTURE
PRIOR TO FIRST VIBRATION TEST

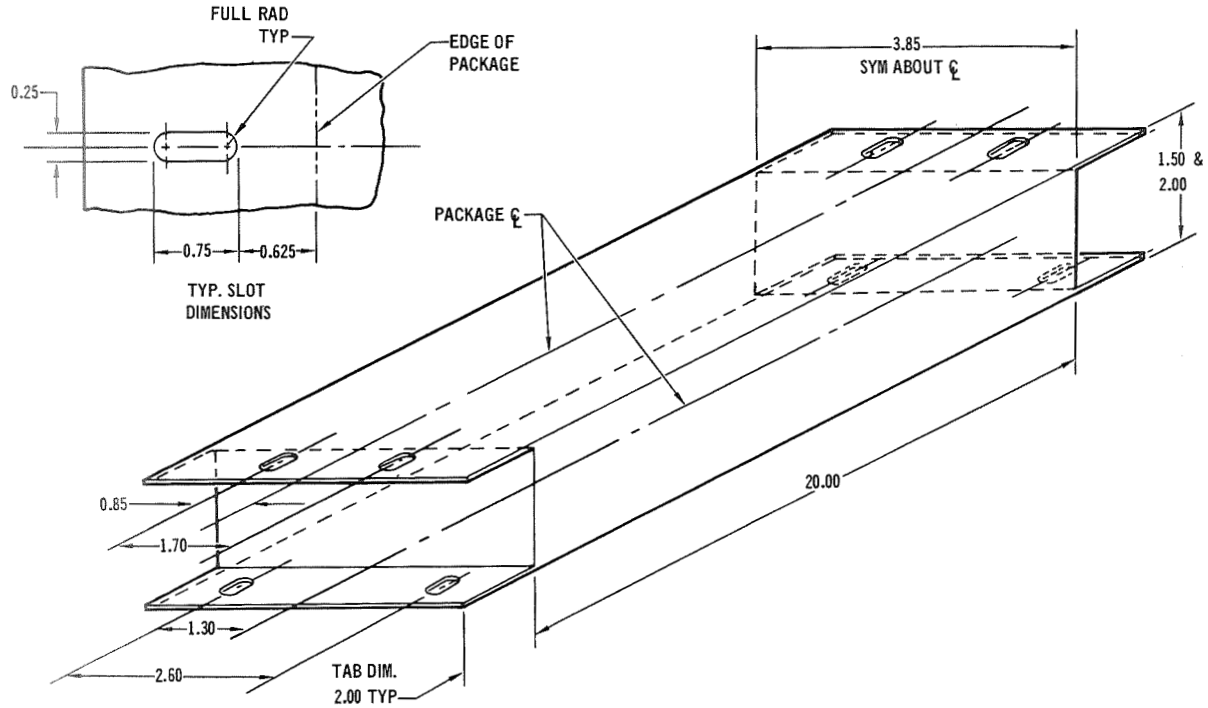
457-1134

Figure 14



METAL FOIL PACKAGED TEST SPECIMENS

Figure 15



457 1135

HIGH TEMPERATURE SPECIMEN (FOIL ENCLOSED)

Figure 16

HITCO at Atlanta, Ga. Later in the program a dimpled form of foil was also used, using a metal female mold and a rubber die.

4.0 TEST RESULTS

4.1 Material Selection

For comparative evaluation of insulations the program was divided into three temperature ranges, to evaluate those insulations and packaging materials believed capable of satisfactory performance at temperatures up to 1800°F, 2200°F, and 2500°F. This division was the result of the characteristics of the materials and of the temperatures encountered on the Shuttle vehicle. At 1800°F and below, the silica and alumino-silica fiber based materials were expected to be usable for long times without problems of devitrification. The 2200°F limit was expected to be about the upper temperature capability of this same group of materials, depending on duration of exposure, and was also expected to be the upper limit for the thin gage superalloy metal foil packaging. The 2500°F case was established by vehicle peak temperature requirements.

Both flexible and rigid materials were to be evaluated. The flexible felts had an inherent advantage, in that they were available at lower densities than the rigid blocks and consequently may be more weight efficient. Whether this advantage would continue to exist after exposure to the Shuttle environment was to be determined. However, the potential weight advantage strongly influenced our selection of materials for testing. Initial selection also considered thermal conductivity, but unfortunately, very little data was available (except for isolated examples) for conductivity at the reduced pressures and high temperatures at which Shuttle insulations would operate. A technique was developed for estimating conductivity as a function of pressure based on 1-atmosphere data and has been issued as a separate report (Ref. 3).

The insulations selected for the Initial Evaluation Tests were based on current knowledge of available materials, coupled with results from a vendor survey. Specific materials selected are listed in Table I.

The ultimate selection of insulations for Shuttle use will be based primarily on minimum weight, of those shown capable of surviving the environment. During this program, a study was conducted to determine the effects of insulation density on the weight of insulation per unit surface area. As thermal conductivity usually varies as an inverse function of insulation density (in this temperature and density range of interest), some potential tradeoffs were thought possible. This study is described in Appendix B.

TABLE I

INITIAL MATERIALS SELECTION

INSULATIONS

Fiberfrax paper	Carborundum Co.
Lo-Con Fiberfrax blanket, 6 lb/ft^3	Carborundum Co.
F-13 Fiberfrax block	Carborundum Co.
Thermoflex felt 3 lb/ft^3	Johns-Manville
Thermoflex felt 6 lb/ft^3	Johns-Manville
Dynaquartz block 4.5 lb/ft^3	Johns-Manville
Dynaquartz block 6.2 lb/ft^3	Johns-Manville
Flexible Min-K	Johns-Manville
Min-K 2000 block	Johns-Manville
Microquartz felt 3.5 lb/ft^3	Johns-Manville
Microquartz felt 6 lb/ft^3	Johns-Manville
Dynaflex felt 3 lb/ft^3	Johns-Manville
Dynaflex felt 6 lb/ft^3	Johns-Manville
Dynaflex felt 12 lb/ft^3	Johns-Manville
A-100 Refrasil Batt	Hitco
Irish Refrasil Batt	Hitco
Astroquartz Mat	J. P. Stevens
HCF Block	MDAC-EAST
Ceramic Fiber Block	Eagle-Picher

The metal foils for packaging were selected on the basis of reported oxidation resistance, and included Inconel 702, Inconel 601, Hastelloy X, and TD-NiCr. Titanium A-70 was included as a package "cool-side" material, but was later dropped due to problems associated with welding to the nickel base materials. For potential use above 2200°F, coated columbium was considered the primary (and possibly sole) candidate, but has not yet been tested.

Preliminary tests on the candidate metal foils were conducted by exposing them to cyclic temperatures to 2200°F at 5 Torr air pressure for 100 cycles. Results of this test are described in Appendix C.

A summary of all test specimens, their cyclic exposure and reason for test termination is presented in Table II.

4.2 1800°F Tests - Five specimens completed 80 cycles of simulated Shuttle missions, with peak temperatures to 1800°F. These specimens were:

TABLE II – TEST PROGRAM SUMMARY

Specimen Number*	Insulation (as Tested)			Packaging				Cumulative Cycles			Nominal Peak Temperature	Reason for Test Termination
	Material	Density (pcf)	Thickness (Inches)	Material	Thickness (Inches)	Texture	Construction	Vibration	Acoustic	Thermal		
I-1	Astro-Quartz	1.57	1.5	Inconel 702	.002	None	Box	40	40	80	1800°F	End of planned test series
II-2	Flexible Min-K	14.8	1.5	Inconel 702	.005	Medium Textured	Box	40	40	80	1800°F	End of planned test series
III-3	Micro-Quartz	3.7	1.5	Hastelloy X	.005	None	Box	40	40	80	1800°F	End of planned test series
IV-4	Dyna-Flex	2.82	1.5	Inconel 702	.005	None	Box	40	40	80	1800°F	End of planned test series
V-5	Refrasil A-100	5.46	1.5	Hastelloy X	.002	None	Box	40	40	80	1800°F	End of planned test series
VI-1	Dyna-Flex	5.61	1.5	Inconel 702	.005	None	Box	20	20	40	2200°F	Packaging deterioration
VII-2	Thermoflex	4.15	2.0	Inconel 702	.002	None	Box	0	0	5	2200°F	Fabrication error-End panels melted.
VIII-3	Irish Refrasil B-1576	4.97	1.5	Inconel 601	.004	None	Box	10	10	20	2200°F	Welded seams of packaging failed.
IX-4	Micro-Quartz	6.25	1.5	Hastelloy X	.005	None	Box	20	20	40	2200°F	Packaging deterioration
X-5	Dyna-Quartz	6.14	1.5	Inconel 601	.004	None	Box	20	20	40	2200°F	Packaging deterioration
XI-2	Dyna-Flex	9.6	1.5	Inconel 702	.002	Medium Textured	Box	20	20	35	2200°F	Packaging deterioration
XII-3	Fiberfrax F-13	17.5	2.0	Hastelloy X	.002	None	Box	10	10	20	2200°F	Packaging deterioration
XIII-1	Flexible Min-K	14.76	1.5	Hastelloy X	.002	None	Shingle	40	20	55	2200°F	Packaging deterioration
XIV-2	Micro-Quartz	3.61	1.5	Inconel 702	.005	Dimpled	Box	40	20	55	2200°F	Packaging deterioration
XV-3	Refrasil A-100	3.56	1.5	Inconel 601	.004	Deep Textured	Box	40	20	55	2200°F	Packaging deterioration
XVI-4	Astro-Quartz	1.17	2.0	Hastelloy X	.002	Medium Textured	Shingle	10	15	20	2200°F	Packaging deterioration
XVII-5	Dyna-Flex	6.8	1.5	TD NiCr	.003	None	Shingle	40	60	100	2200°F	End of planned test series
XVIII-4	Coated HCF	~15	2.0	None	-	-	-	0	0	5	2200°F	Broke into 4 pieces
XIX-4	Irish Refrasil	4.93	1.5	Inconel 601	.004	Dimpled	Box	30	5	30	2200°F	Packaging deterioration
XX-1	Coated HCF	~15	2.0	None	-	-	-	0	0	5	2200°F	Broke into 2 pieces
XXI-2	Astro-Quartz	1.13	2.0	Inconel 702	.005	None	Slide-On Lid	0	40	45	2200°F	Lid would not stay in place
XXII-3/4	Irish Refrasil	7.53	1.5	Inconel 601	.004	Dimpled	Dougle-width Box	0	40	45	2200°F	Packaging deterioration
XXIII-1	Astro-Quartz W/Hastelloy X Radiation Shield	1.69	2.0	Inconel 702	.005	Dimpled	Welded Tabs	0	35	40	2200°F	Lid tab welds failed

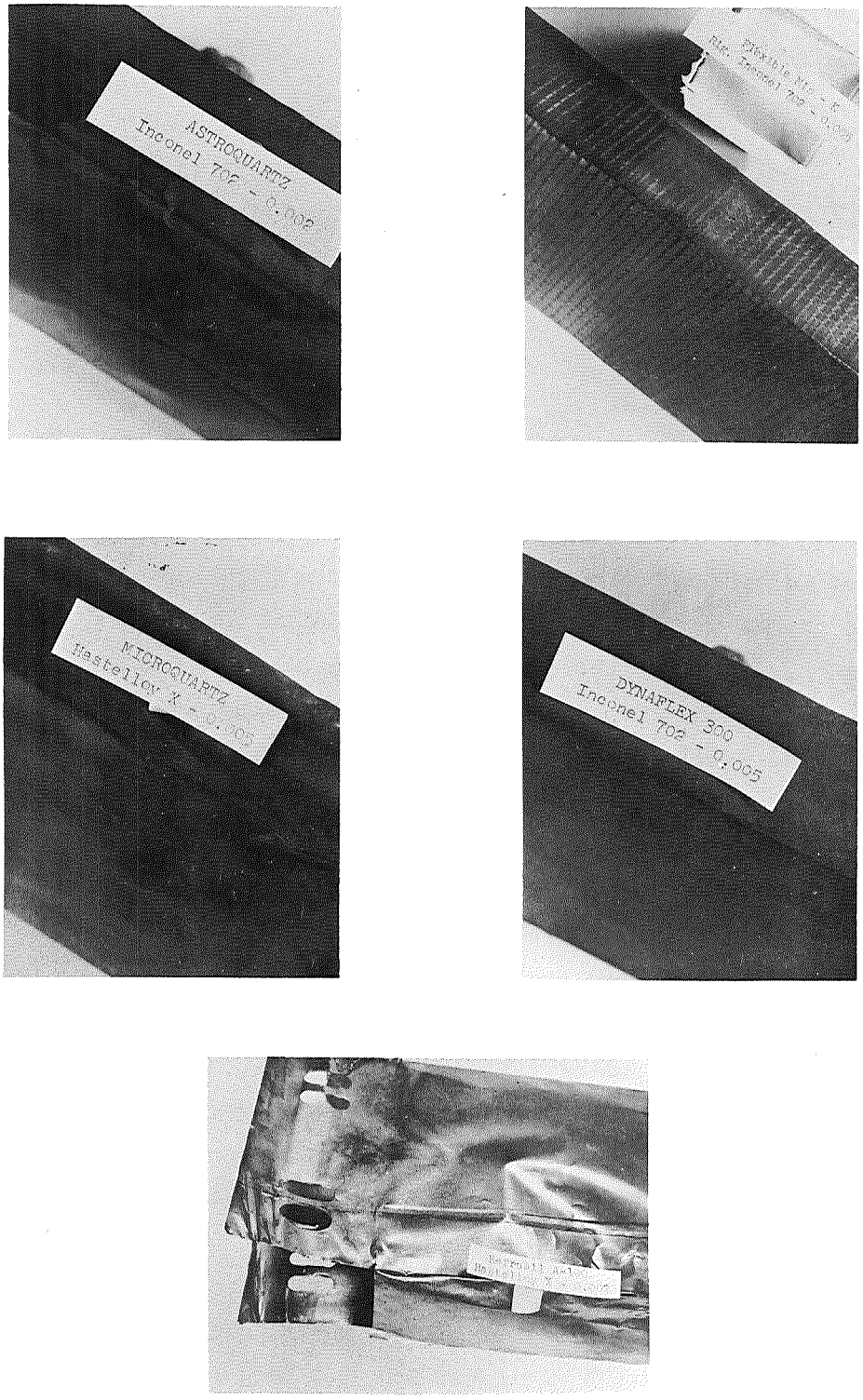
* Roman numeral is specimen identification. Arabic numeral identifies the location of the specimen in the test fixture

As Tested

Insulation	Construction @ nominal thickness	Thickness	Insulation Density	Packaging
Astroquartz 1 lb/ft^3	11 layers @ 0.2 in. ea.	1.5 in.	1.57 lb/ft^3	Inconel 702 - 0.002"
Flexible Min-K 19.2 lb/ft^3	3 layers @ 0.375 in. ea.	1.5 in.	14.8 lb/ft^3	Rigidized Inconel 702 - 0.005"
Microquartz 3.5 lb/ft^3	3 layers @ 0.5 in. ea.	1.5 in.	3.70 lb/ft^3	Hastelloy X - 0.005"
Dynaflex 3 lb/ft^3	1 layer @ 1.5 in.	1.5 in.	2.82 lb/ft^3	Inconel 702 - 0.005"
Refrasil A-100 3 lb/ft^3	12 layers @ 0.19 in. ea.	1.5 in.	5.46 lb/ft^3	Hastelloy X - 0.002"

From an external visual examination, the packages of the five 1800°F specimens survived the 80 cycles of simulated flight missions in good conditions. While there was no severe wrinkling of the top surfaces (as occurred later in 2200°F testing), there was frequent puckering at the side edges resulting in minor rupturing of the foil. Details of the external appearance and the edge puckering are shown in Figure 17. The rupturing or cracking of the foil always occurred at a "pucker" and the crack was generally at right angles to the edge. The cracks were most prevalent in Hastelloy X, especially the 2 mil thick foil. Inconel 702 had fewer cracks, and the rigidized 5 mil Inconel 702 had none at all. Many of the puckers/cracks were noted earlier in the testing, and while more occurred with subsequent testing, the existing ones did not propagate in length. The cause of these cracks is uncertain, but it is believed that they may be the result of fatigue failures where response of the foil surface to acoustic loading is restrained by the corner line of the package, combined with embrittlement due to heating and/or internal oxidation. At this level of testing these effects do not appear to be crippling defects.

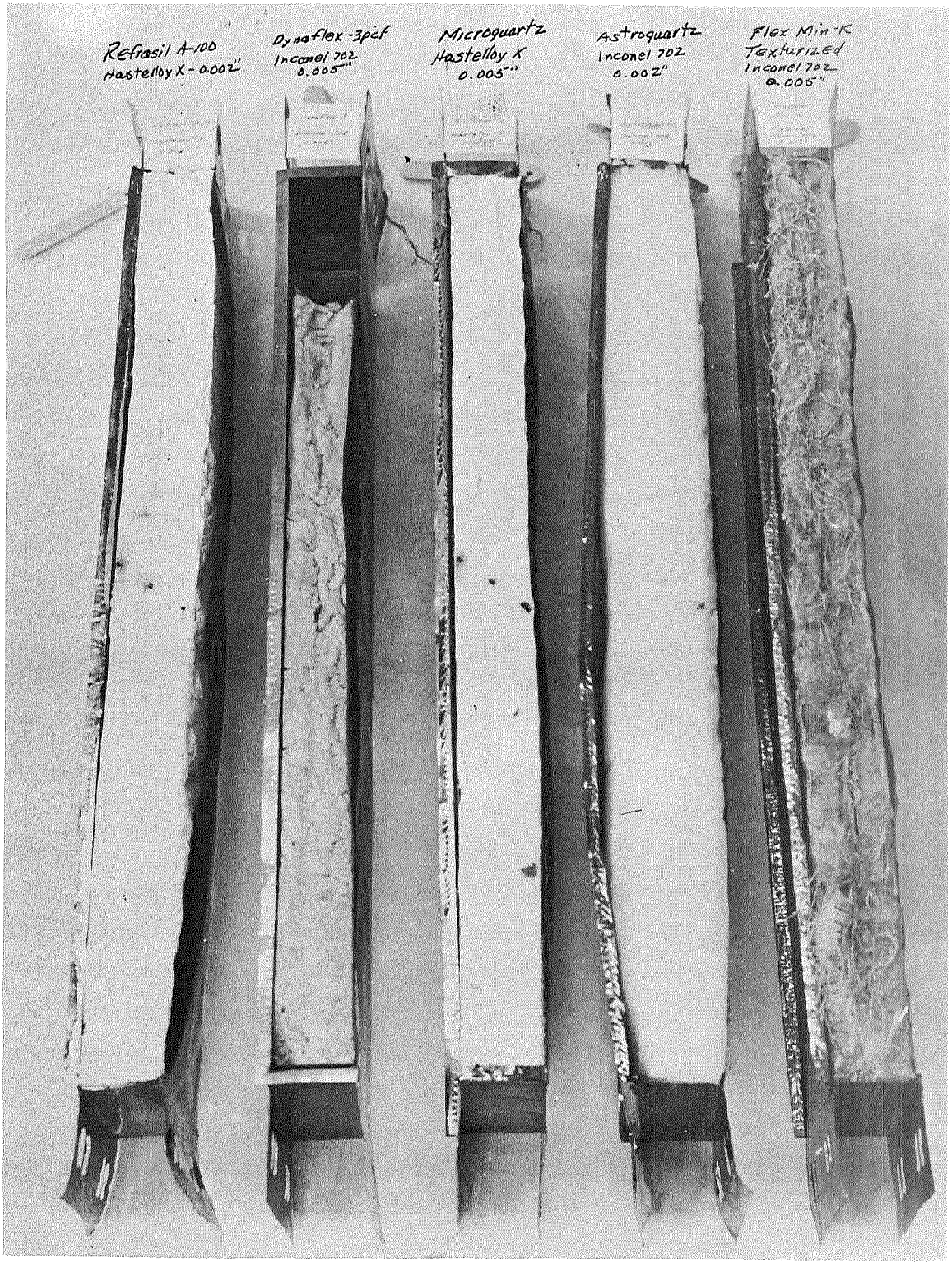
The condition of the insulation material within the packages was observed by cutting away one of the sides of the metal packages (Figure 18). The Refrasil A-100, Astroquartz, and Flexible Min-K had not been significantly affected. However, the 3 lb/ft^3 Dynaflex was found to have settled lengthwise, leaving a void of about 3 inches of its 20 inch length, (the 20-inch dimension is vertical during acoustic/vibration testing), and with an increasingly dense felt at the other end of the



SPECIMENS AFTER 80 CYCLES OF SIMULATED SHUTTLE ENVIRONMENT TO 1800°F

457-1137

Figure 17



INTERIOR OF SPECIMENS AFTER 80 CYCLES OF SIMULATED SHUTTLE SERVICE TO 1800°F

457-1138

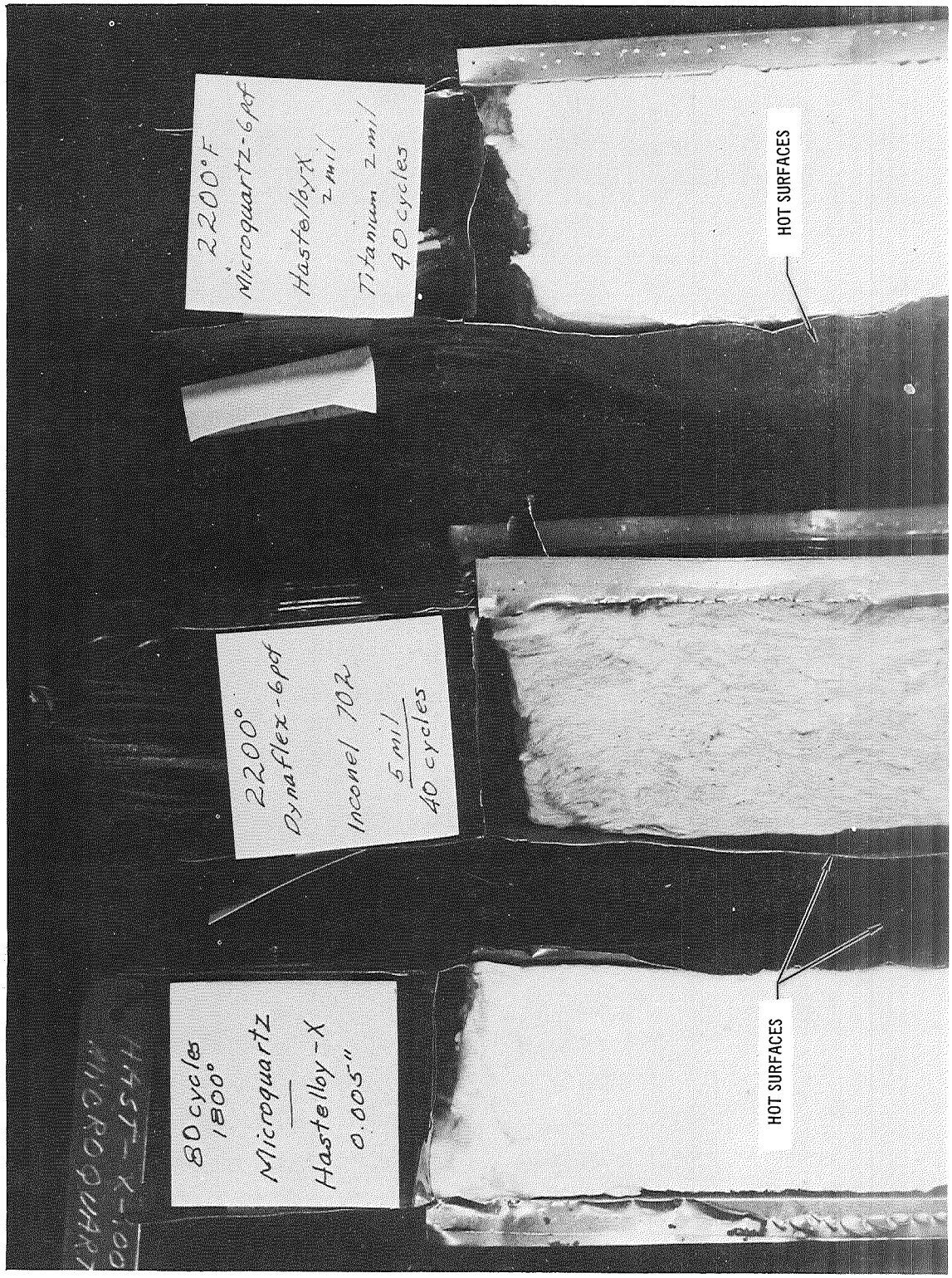
Figure 18

package. The appearance of the felt suggested that the settling of the Dynaflex was primarily the result of vibration/acoustic exposure. This assumption was supported by results with Dynaflex at densities higher than 3 lb/ft^3 in later tests at 2200°F. The settling was not detected during the course of the testing because the thermocouples remained in the same relative position within the thickness of the insulation.

The Microquartz had about a 1/4 inch void in its 20 inch length. In this case, the void space was tapered with the maximum gap at the hot side of the insulation. This would indicate shrinkage may have occurred as well as settling. A closeup of the shrinkage/settling of Microquartz is shown in Figure 19.

The excessive settling exhibited by the low density Dynaflex was somewhat disappointing as it had initially been considered a prime candidate due to its expected temperature capability (2500°F) and low weight. However, the performance of Astroquartz was encouraging in that such a low density material did not settle. A thermal analysis (Appendix B) has indicated that within a single family of materials with varying densities, the lower densities provide the most weight effective insulation. Should Astroquartz provide a density/thermal conductivity relationship similar to Dynaflex or Refrasil, it will indeed be a strong candidate for a minimum weight thermal insulation. Existing data on Astroquartz thermal conductivity was limited to 3 lb/ft^3 material, and it was comparable to 3-3.5 lb/ft^3 Microquartz.

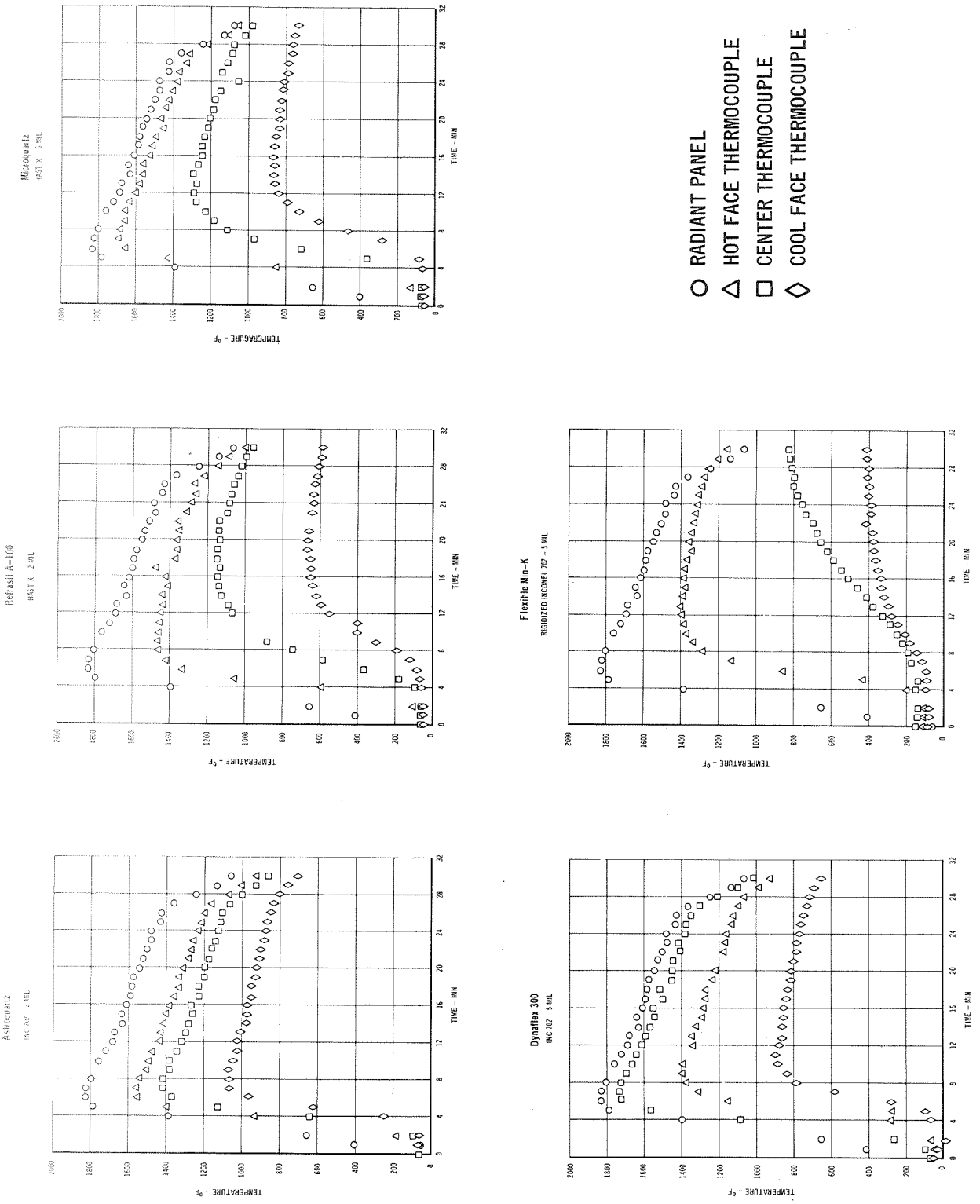
Temperature histories of the five materials at three thermocouple locations within the insulation specimens during an early cycle are shown in Figure 20. For purposes of detecting changes in thermal response, the temperatures at 15 minutes into the thermal cycle were plotted as a function of number of cycles and are shown in Figures 21, 22, 23, 24, and 25. On those occasions where a thermocouple failed due to acoustic or vibration loads (usually fracture of the 36 ga wire extending out of the metal sheath), the thermocouple was carefully extracted from the insulation, the bead repaired, and reinserted. Slight differences in locations sometimes occurred due to this procedure, as reflected by the temperature response. In those cases, detailed examination was made of the temperature history of that thermocouple during the five preceding and subsequent individual cycles to determine the temperature bias caused by removal and reinsertion of the thermocouple. All subsequent readings of that thermocouple were then corrected by adding or subtracting the bias.



HOT VS COLD SIDE SHRINKAGE OF SEVERAL INSULATIONS

457-1139

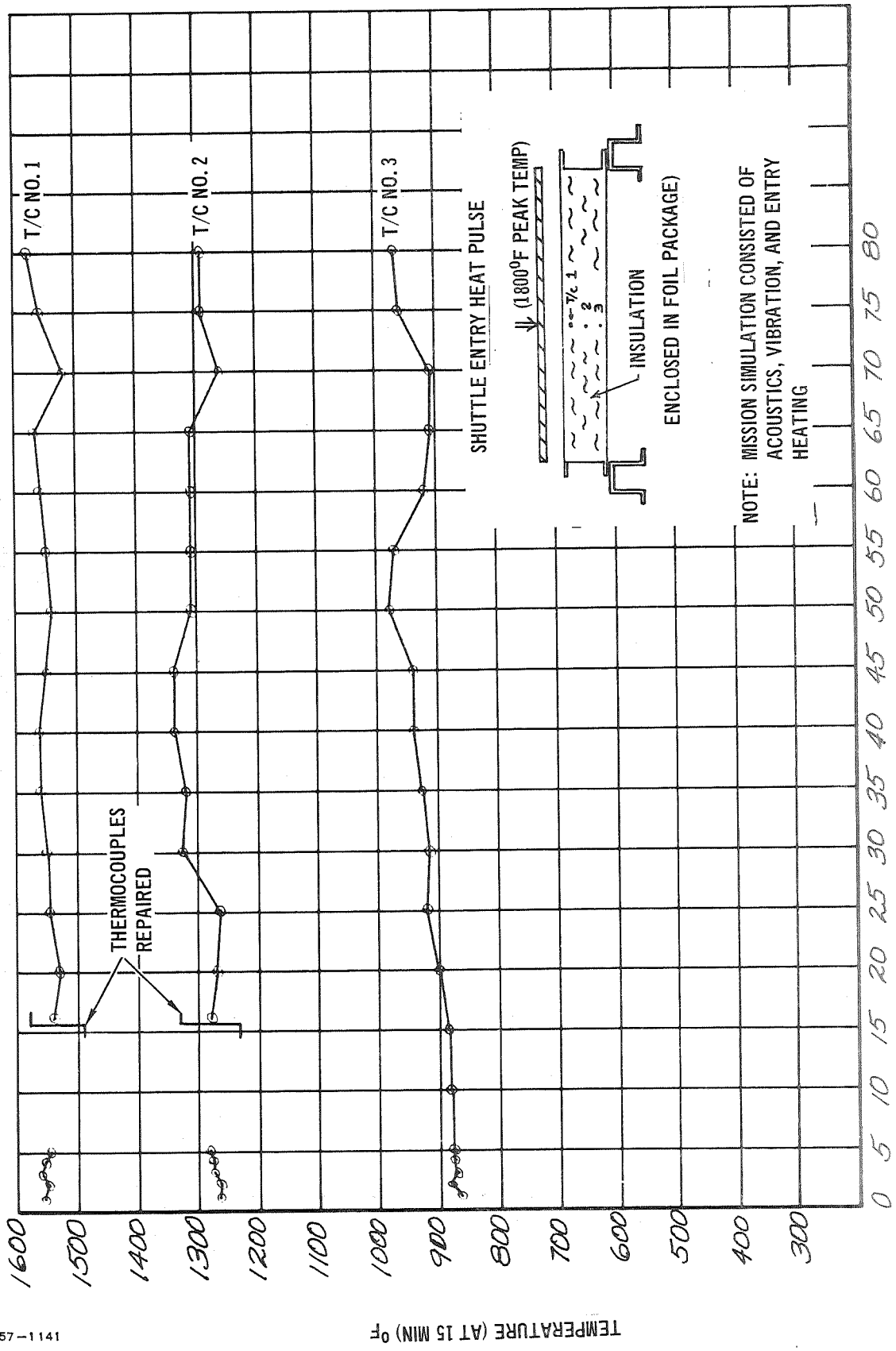
Figure 19



TEMPERATURE HISTORIES DURING THE FIFTH CYCLE

457-1140

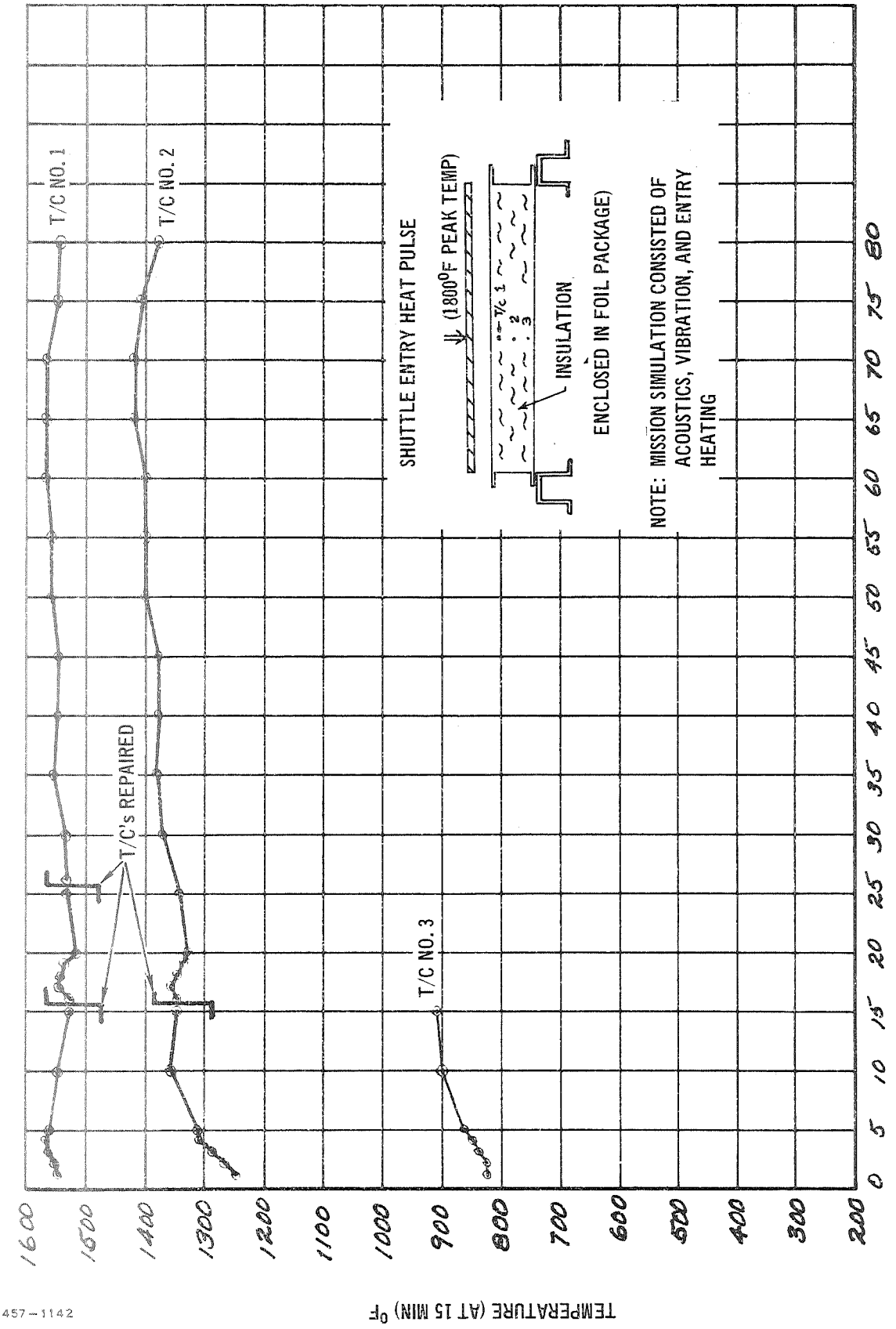
Figure 20



457-1141

TEMPERATURES IN MICROQUARTZ AS A FUNCTION OF NUMBER OF SIMULATED MISSIONS

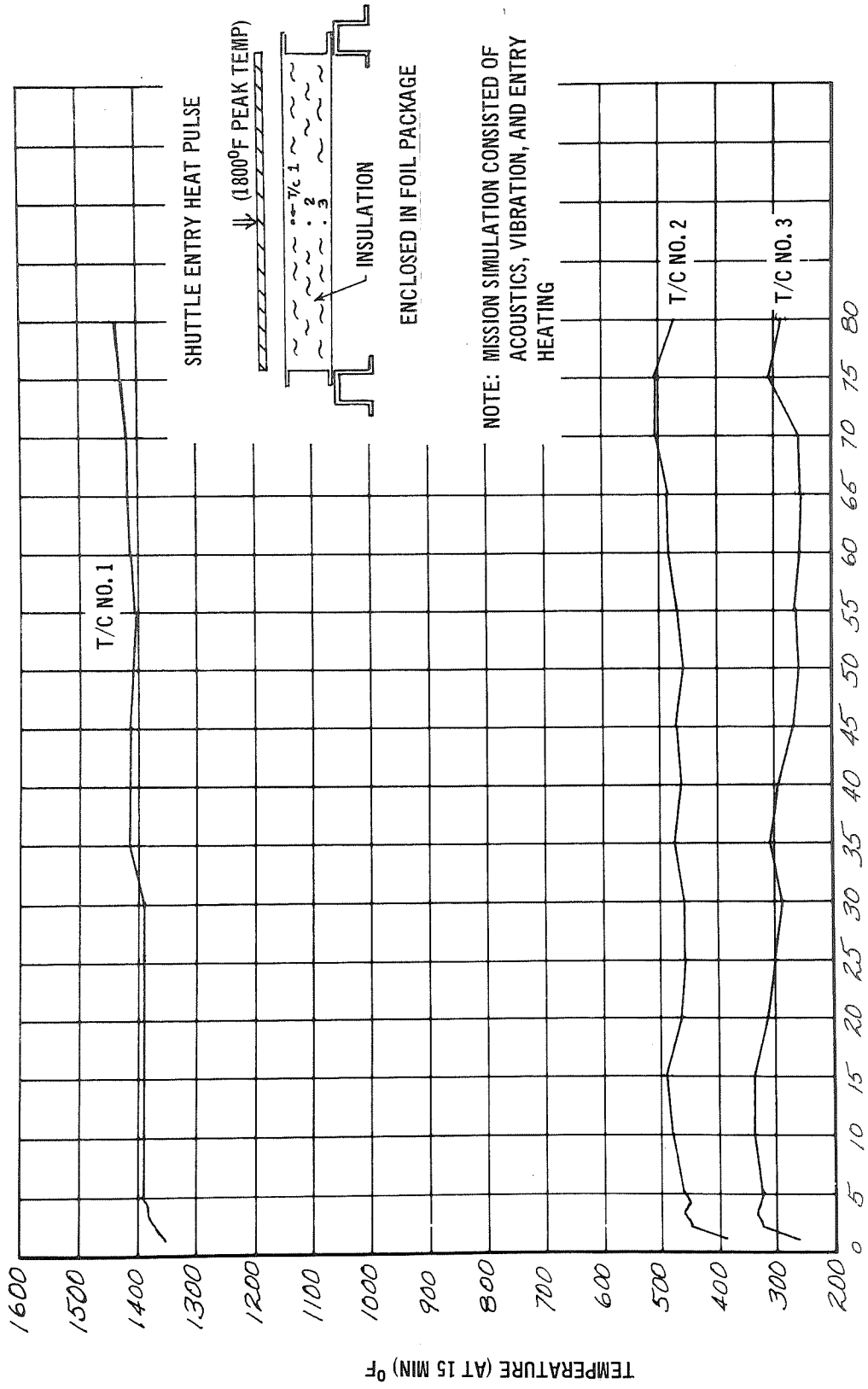
Figure 21



TEMPERATURES IN DYNAFLEX AS A FUNCTION OF NUMBER OF SIMULATED MISSIONS

457-1142

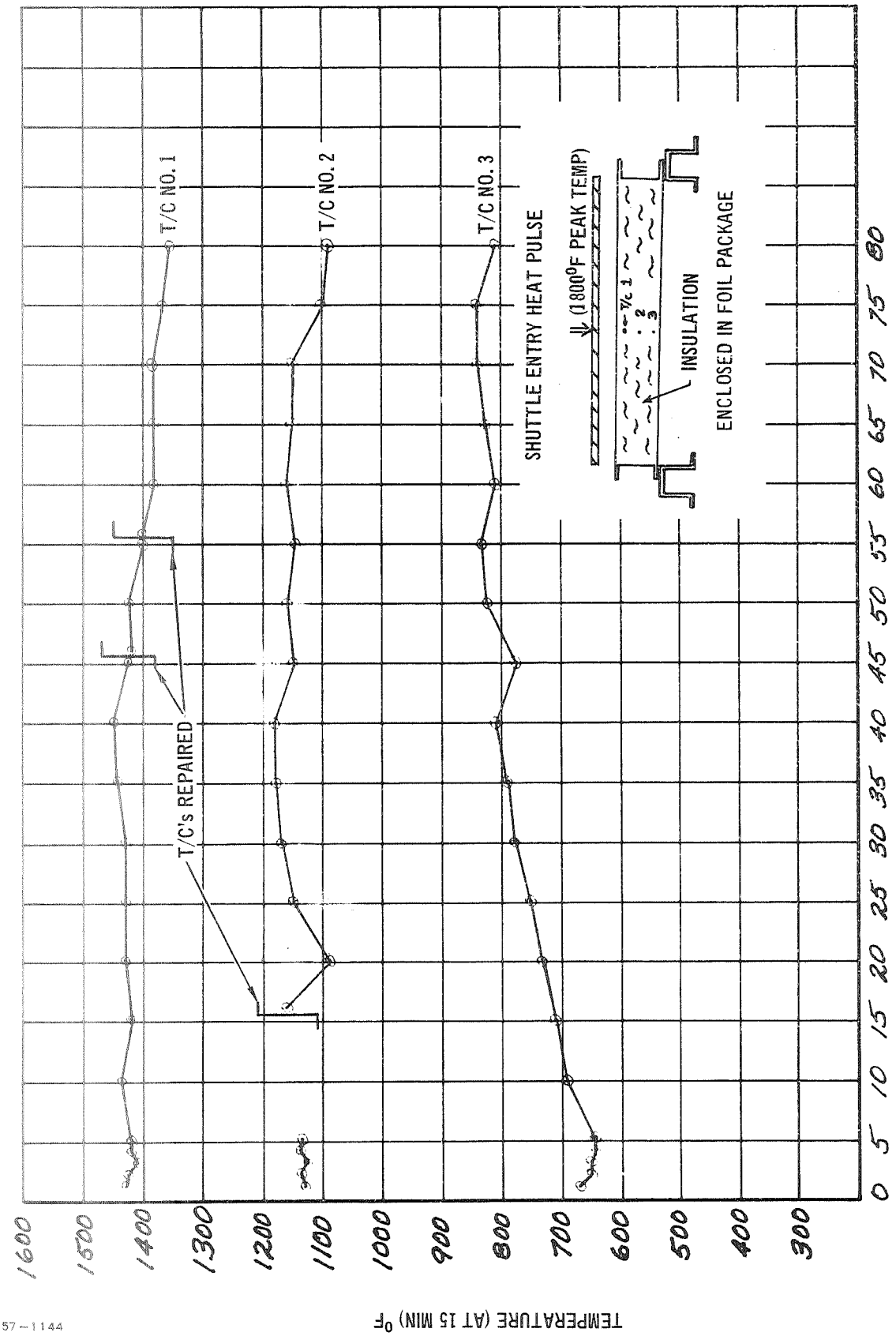
Figure 22



TEMPERATURES IN THE FLEXIBLE MIN-K SPECIMEN AS A FUNCTION OF SIMULATED SHUTTLE MISSION

457-1143

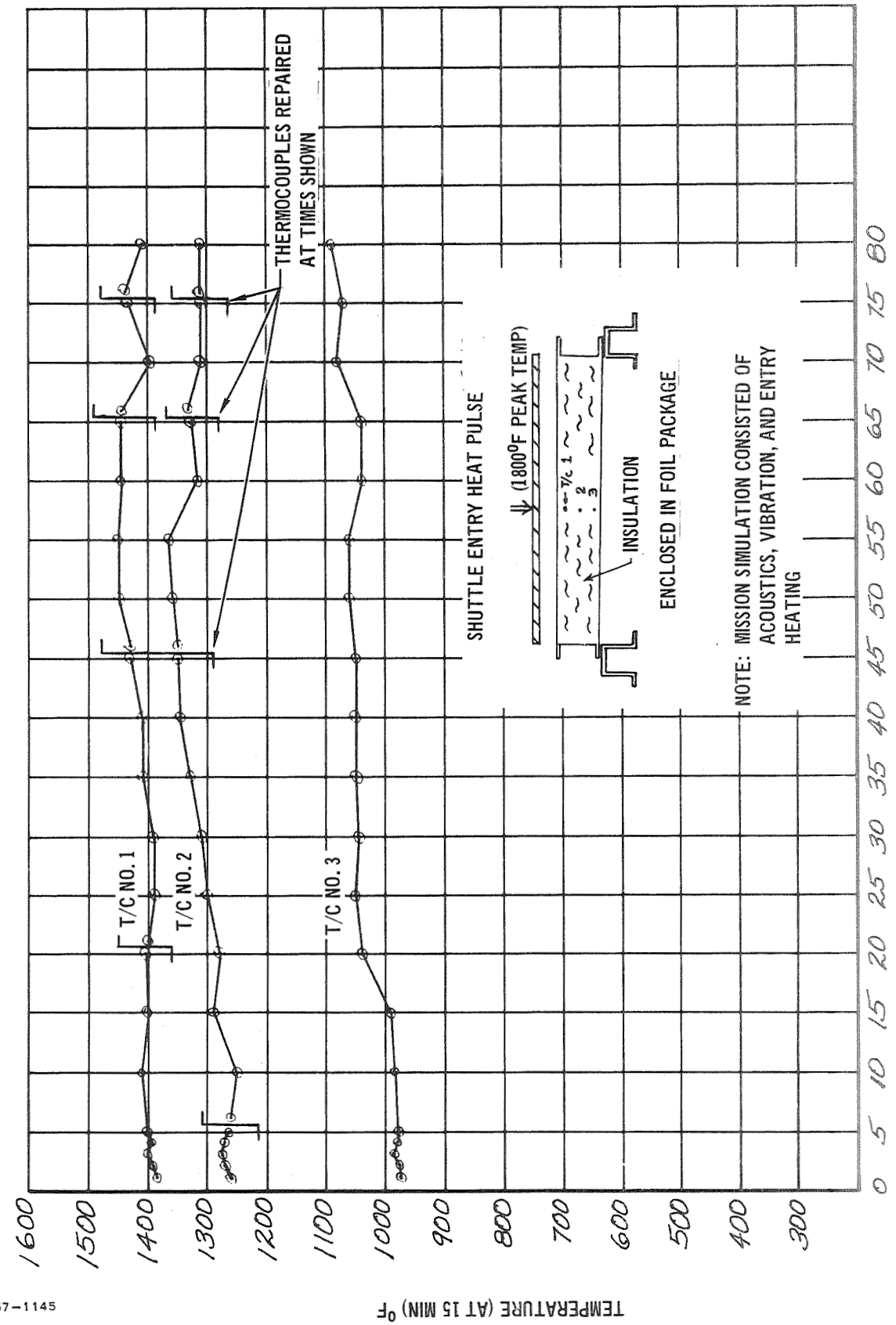
Figure 23



TEMPERATURE IN REFRASIL A-100
AS A FUNCTION OF NUMBER OF SIMULATED MISSIONS

457-1144

Figure 24



TEMPERATURES IN ASTROQUARTZ AS A FUNCTION OF NUMBER OF SIMULATED MISSIONS

457-1145

Figure 25

At the conclusion of the 80 cycles, when the specimens were disassembled from the test fixture, it was noted that the leads of the cool side thermocouple of the 3 lb/ft^3 Dynaflex had been bared by excessive heat (glass-insulated thermocouples were used for the cool side) and shorted to the metal foil package. Examination of thermocouple records indicated this occurred between the 15th and 16th cycles, and subsequent data for that thermocouple were discarded as invalid.

The net temperature variations from the 5th and 80th cycles are tabulated below.

TEMPERATURES AT 15 MINUTES INTO THERMAL CYCLE

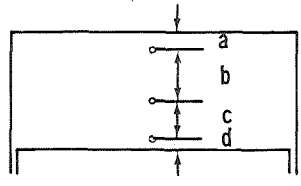
	Hot Side °F	Cool Side °F	ΔT °F
Astroquartz 5th Cycle	1400	980	420
80th Cycle	1405	1090	315
Refrasil A-100 5th Cycle	1420	640	780
80th Cycle	1355	810	545
Microquartz 5th Cycle	1545	875	670
80th Cycle	1580	970	610
Dynaflex 5th Cycle	1560	1310*	250
80th Cycle	1545	1380*	165
Flexible Min-K 5th Cycle	1390	320	1070
80th Cycle	1440	290	1150

*Center thermocouple (cool side thermocouple invalid after 15 cycles).

The location of the three thermocouples within each specimen was determined by X-ray prior to test, and after completion of the 80 cycles. However, it was not possible to dimension the location of the measuring junctions with any great precision. Thermal analysis also indicated a considerable temperature variation with changes of the order of several thousandths of an inch. The X-rays very clearly showed a shift in the location of the thermocouples which could account for changes noted above. It is for this reason that we are reluctant to ascribe the change in ΔT to a change of the thermal properties of the insulation. The positions of the thermocouples before the test and after 80 cycles, as noted from the X-rays are shown in Figure 26.

THERMOCOUPLE LOCATIONS

HOT SIDE



	PRE TEST DIMENSIONS – INCHES				POST TEST DIMENSIONS			REMARKS
	a	b	c	d	b	c	d	
DYNAFLEX	0	0.74	0.74	0.02	0.5	–	–	HOT T/C SAME POSITION
ASTROQUARTZ	0.22	0.49	0.75	0.04	0.6	0.45	–0.4	MIDDLE T/C STABLE POSITION
FLEXIBLE MIN-K	0.06	0.65	0.70	0.09	NO CHANGE IN POSITION			
MICROQUARTZ	0.02	0.65	0.58	0.25	1.0	–0.0		ALL T/C'S SHIFTED
REFRASIL A-100	0.15	0.60	0.72	0.03	0.60	0.34		HOT AND CENTER T/C SAME POSITION COOL T/C SHIFTED.

NOTE: CHANGES IN T/C POSITIONS NOTED FROM SUPERPOSITION OF X-RAYS.

457-1146

Figure 26

4.3 2200°F Tests - The flight simulation tests with maximum temperatures of 2200°F were run in three major groups of specimens, and grossed 40, 55, and 45 cycles each. Within each group, individual specimens were occasionally substituted as defects became apparent.

4.3.1 First Group - The initial five test specimens for simulation with 2200°F expsoure and two replacement specimens are listed below with pertinent details.

Insulation @ nominal thickness	As Tested Construction	Thickness	Density	Packaging Hot Side	Cold Side
Microquartz Felt 6 lb/ft^3	3 layers @ 0.5 in. ea	1.5 in.	6.25 lb/ft^3	Hastelloy X - 0.005"	Titanium 0.005"
**Irish Refrasil B-1576 - 3 lb/ft^3	3 layers @ 1.0 in. ea	1.5 in.	4.97 lb/ft^3	Inconel 601 - 0.004"	Titanium 0.005"
Dynaquartz 6.2 lb/ft^3	1 layer @ 1.5 in.	1.5 in.	6.14 lb/ft^3	Inconel 601 - 0.004"	
Dynaflex 6 lb/ft^3	1 layer @ 1.5 in.	1.5 in.	5.61 lb/ft^3	Inconel 702 - 0.005"	
*Thermoflex Felt 3 lb/ft^3	1 layer @ 2.0 in. ea.	1.5 in.	4.15 lb/ft^3	Inconel 702 - 0.002"	Titanium
Dynaflex 12 lb/ft^3	1 layer @ 1.5 in. ea.	1.5 in.	9.60 lb/ft^3	Rigidized Inconel 702 - 0.002"	Rigidized Titanium 0.002"
Fiberfrax F-13 Block, 17 lb/ft^3	2 layers @ 1.0 in. ea.	2.0 in.	17.5 lb/ft^3	Hastelloy X - 0.002"	

Note: * Removed after 5 thermal cycles, package end plate burned out, replaced with Dynaflex, 12 lb/ft^3.

** Separation of cold side (weld failure) at 20 cycles. Replaced with Fiberfrax F-13 Block.

Failure of the package that contained the Thermoflex after the initial thermal cycles was determined to be a fabrication error. Titanium was to be the cold side only of this package, but was incorrectly used for the end plate also. The end plates are spot welded to the lips of the hot side of the package where temperatures

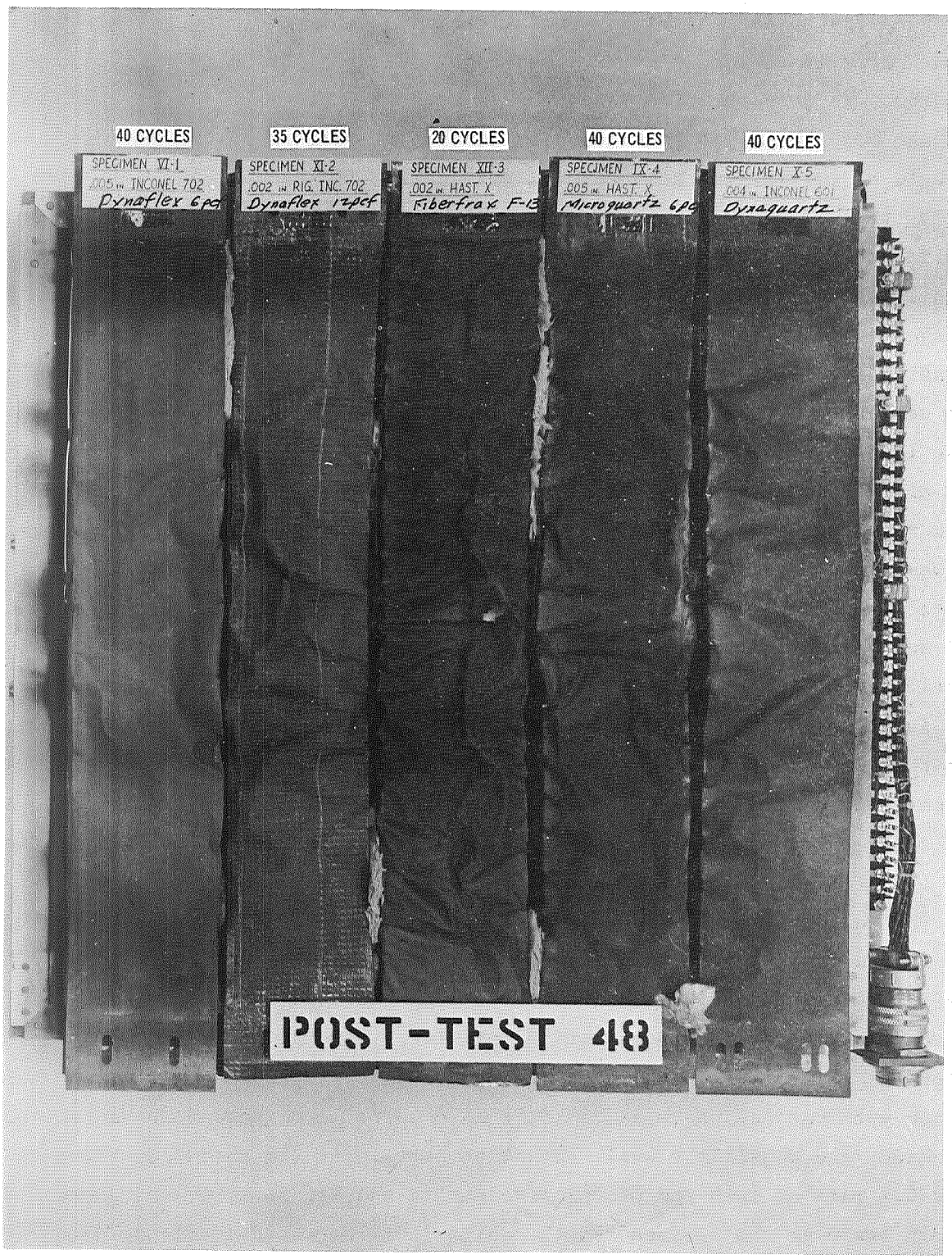
are in excess of the capabilities of titanium. Failure of the package containing Irish Refrasil was caused by very poor spot weld quality in joining Inconel to titanium. In this specific case, the greater thermal expansion at 2200°F was sufficient to bow the entire package, with subsequent failure of the weak spot welds on the cold side. Future packages will not include titanium on the cold side.

At the end of 40 cycles with thermal exposure to 2200°F, serious degradation of all the packages used in this test was apparent and testing was suspended. An overall view of the test specimens at that time is shown in Figures 27 and 28. It was thought from the condition of the specimens that the problem was the high thermal expansion of the package at 2200°F, coupled with embrittlement of the metal foil at that temperature. The interior of the specimens, with one side stripped away is shown in Figure 29.

All of the metal foils had lost much of their flexibility, though the 5 mil thick foils retained considerable toughness. The 2 mil foil, especially Hastelloy X, was weak and fragile. While the transverse cracks at the edges were not as pronounced as in the 1800°F test specimens, the foil surfaces had a very pronounced hill and valley contour and a number of surface cracks occurred on the face. Peak-to-valley depths ranged from 3/8 to 5/8 inches, and there was considerable difference in frequency of such deformation, texturized Inconel and plain Inconel having less than Hastelloy X. Based on overall condition of the metal foils used, the Inconel 702, 5 mils thick, displayed less damage than the other materials used. This might have been the result of less embrittlement from internal oxidation, or from other causes discussed in Appendix C.

The settling, previously noted on 3 lb/ft^3 Dynaflex in the 1800°F test, was much less with the higher density Dynaflex used in the 2200°F test. The 6 lb/ft^3 Dynaflex settled about 0.5 inch out of the 20-inch length, and the 12 lb/ft^3 Dynaflex had only a negligible amount of settling. Some of the settling at these densities was recovered as the materials apparently relaxed somewhat while awaiting further examination. Microquartz felt at 6 lb/ft^3 continued to exhibit lengthwise shrinkage, and possibly a small amount of settling. The shrinkage amounted to about 0.2 inch at each end of the specimen at the hot surface, and about 0.2 inch of settling over the 20-inch length. This is illustrated in Figure 19.

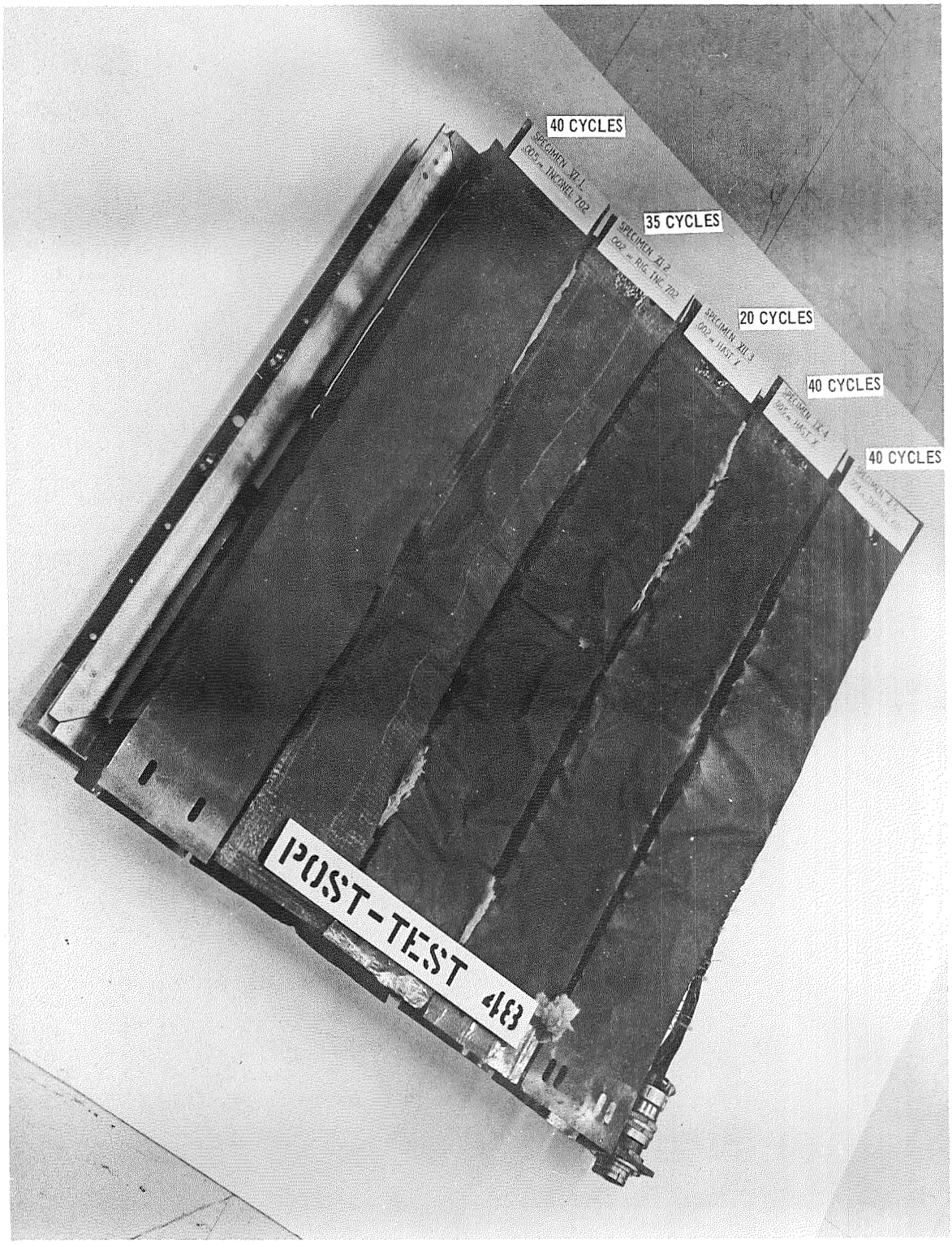
The Dynaquartz block had two major cracks completely through the block, and had the block not been enclosed by the package, the insulation would have been completely lost. This damage was undoubtedly due to acoustic/vibration loads. The Fiberfrax



CONDITION OF INSULATION PACKAGES AT SUSPENSION OF TESTING WITH THERMAL EXPOSURE TO 2200°F

457-1147

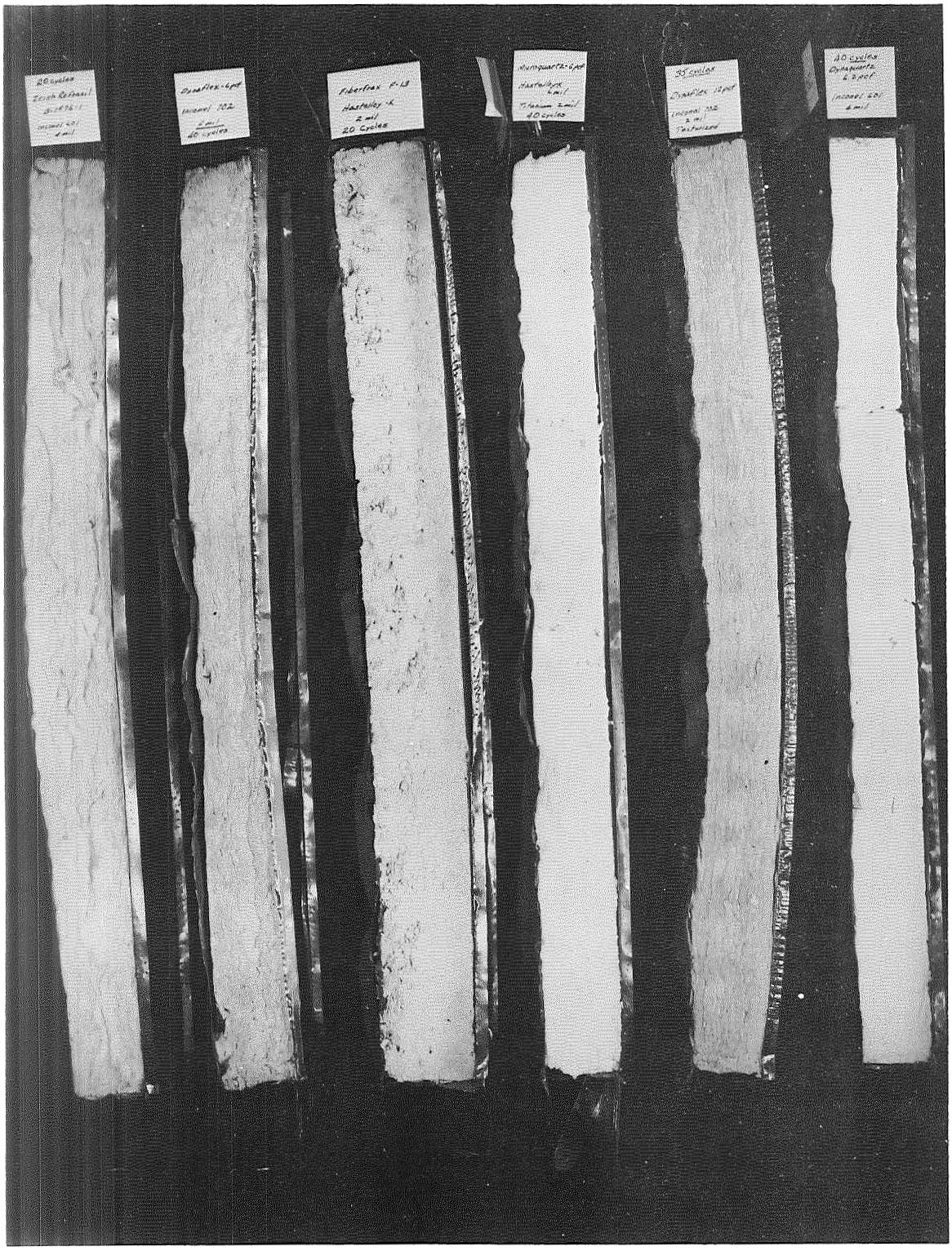
Figure 27



457-1148

INSULATION PACKAGES AFTER 2200°F EXPOSURE

Figure 28



INTERIOR OF INSULATION PACKAGES AFTER SIMULATED FLIGHTS WITH 2200°F TEMPERATURE

457-1149

Figure 29

F-13 block, which is a combination of refractory fibers and clay, appeared to lose some of the clay filler in the hotter areas of the specimen, exposing some of the fiber nodules. The Irish Refrasil was not affected by the test environment, and as a result, may become the prime candidate for 2500°F service if its reputed temperature capability is confirmed.

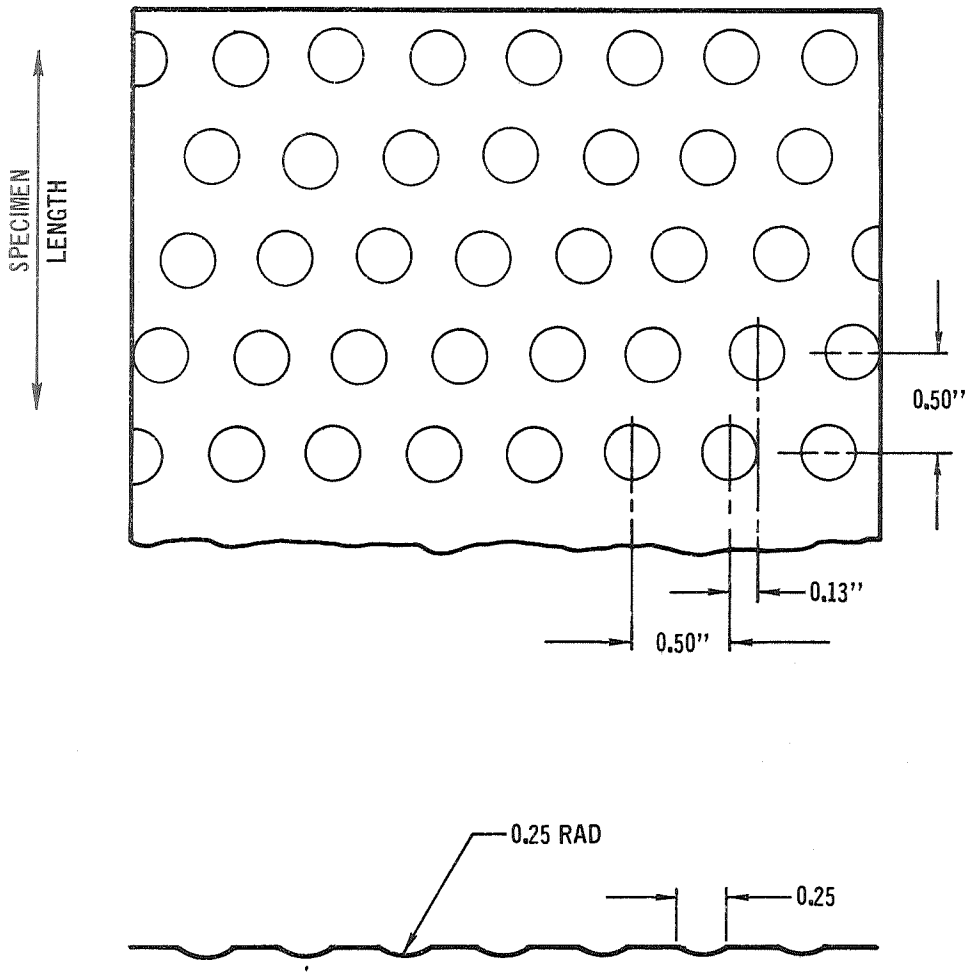
4.3.2 Second Group 2200°F - Because of the wrinkling and cracking of the metal foils experienced in the initial group of 2200°F specimens alternate design approaches were prepared for the next group of specimens. These included:

- o Heavier texturizing of the metal foil
- o Use of dimpled foil
- o Shingle construction of packages.

The texturized foil approach is similar to that previously used except the corrugations in the foil are deeper. Dimpled foil was processed in our experimental shop by milling spherical segment cavities in a metal block and using the block as a die. The foil was pressed into the die by means of a rubber sheet in a press. In indenting the foil, the metal is locally stretched and there is no reduction in the overall length or width of the foil. The pattern of the dimples is shown in Figure 30.

The third configuration was the shingle design shown in Figure 31. In this design each individual section was 4.5 inches long, with a 0.5 inch overlap of adjacent sections. The cool side panel was still a single piece, and adjacent "roof sections" were spot welded together about one-third the height from the cool side towards the hot side. Thus, the hot surface was relatively free to expand, while a strong base was provided on the cool side.

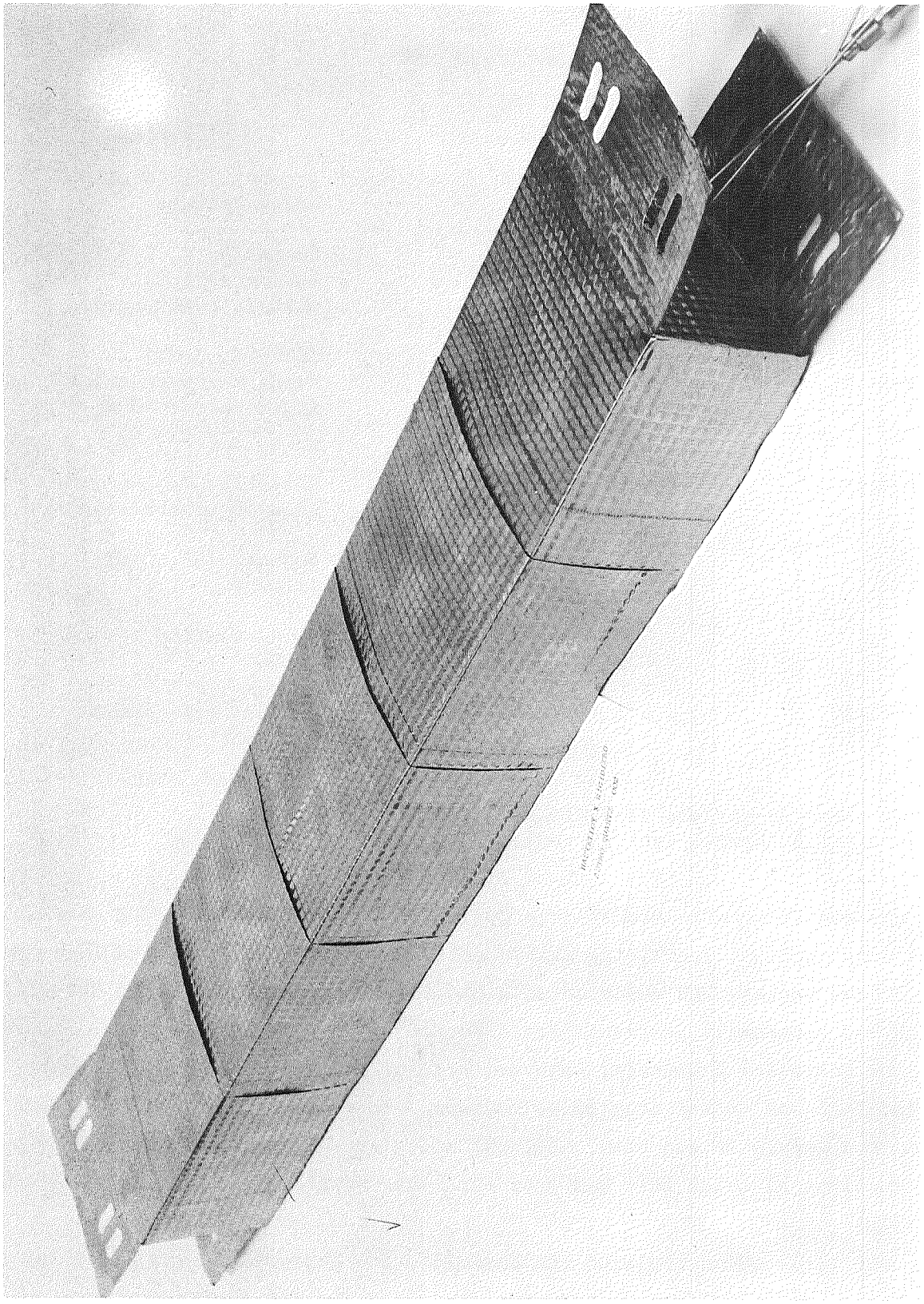
The specimens included in the second test group were:



DIMPLE PATTERN IN METAL FOIL

457-1150

Figure 30



SHINGLE CONSTRUCTION

457-1151

Figure 31

2200°F TEST SPECIMENS

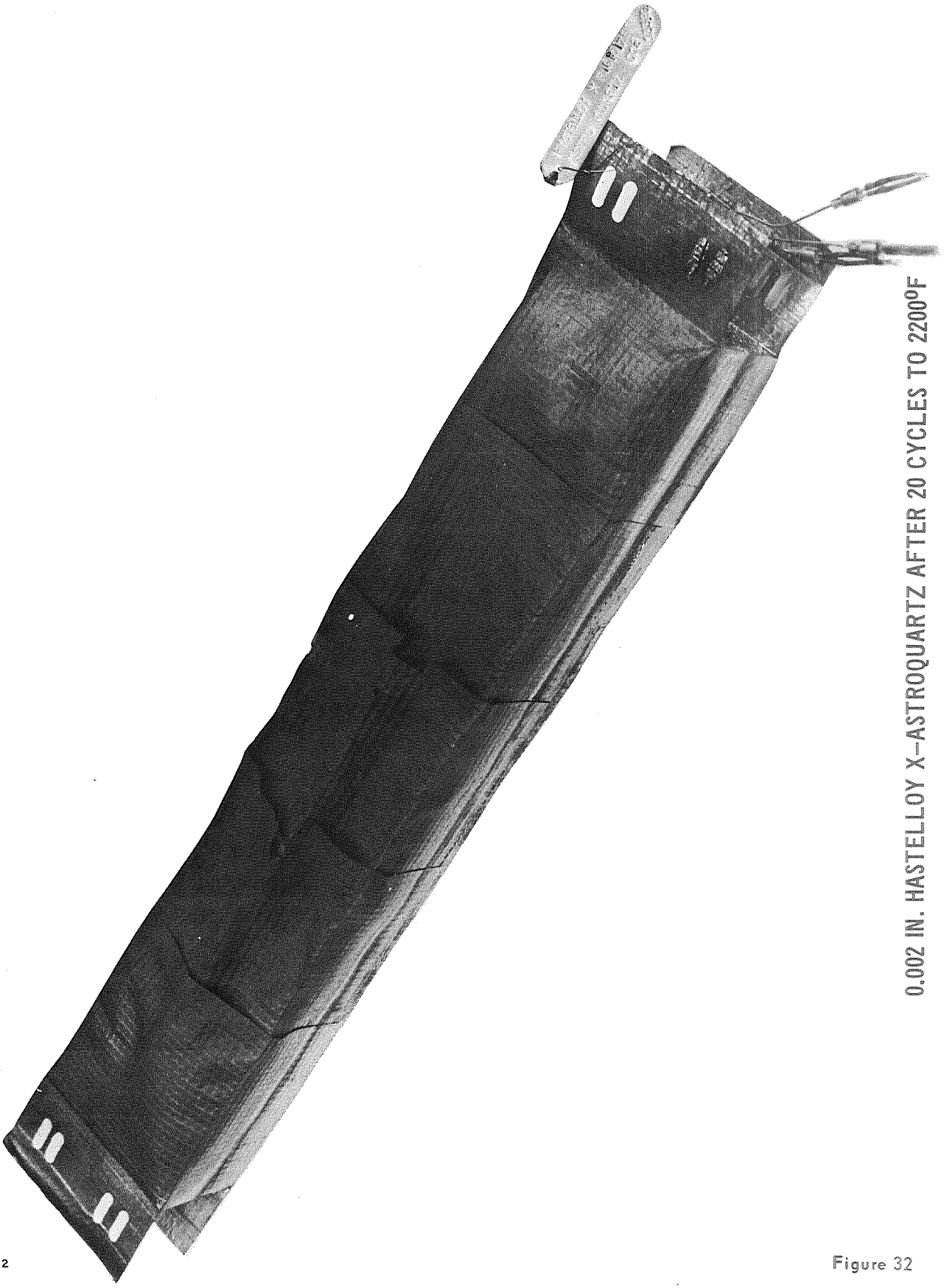
Second Series

Insulation	Installed Density	Packaging
Refrasil A-100 3 lb/ft^3	3.56 lb/ft^3	Inconel 601, 4-mil heavy texture
*Astroquartz 1 lb/ft^3	1.17 lb/ft^3	Hastelloy X, 2-mil medium texture shingle construction
Dynaflex 2-2" layers of 3 lb/ft^3 compressed to 1.5"	6.8 lb/ft^3	TD-NiCr, 3-mil shingle construction (cold face Inconel 601)
Flexible Min-K	14.76 lb/ft^3	Hastelloy X, 2-mil shingle construction
Microquartz 3.5 lb/ft^3	3.61 lb/ft^3	Inconel 702, 5-mil dimpled
**HCF 14.7 lb/ft^3	17.7 lb/ft^3 with coating	M25A7 Coating
Irish Refrasil A-100	4.93 lb/ft^3	Inconel 601, 4-mil dimpled

* Removed after 20 cycles, replaced by HCF block
**Removed after 5 thermal cycles, replaced by Irish Refrasil A-100

At the end of 20 simulated flight cycles, the two mil Hastelloy X package (shingle construction) containing Astroquartz, was removed from test due to deterioration of the package and replaced with the coated HCF specimen. The shingle construction had apparently performed its function in presenting lengthwise deformation of the Hastelloy X package; however, lateral expansion had occurred with the texturized foil and formed lengthwise creases. This also caused the open ends of the shingle segments to gap open. Several holes appeared in the center roof segment, and two sections of metal foil had been torn out, apparently by acoustic exposure (Figure 32).

The HCF block which replaced the Hastelloy X - Astroquartz was installed prior to the thermal test, and was removed immediately following that test due to three



0.002 IN. HASTELLOY X–ASTROQUARTZ AFTER 20 CYCLES TO 2200°F

457–1152

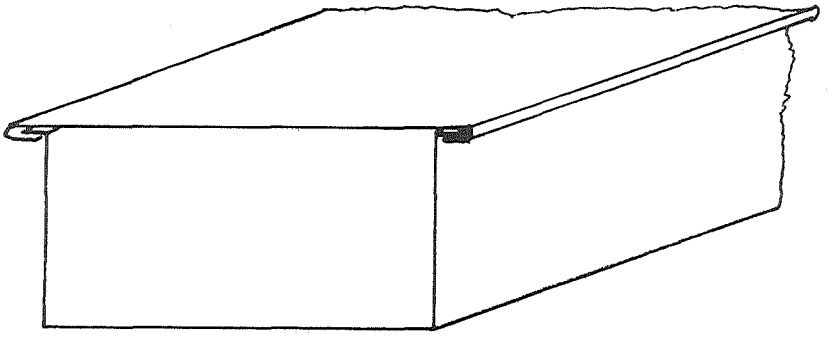
Figure 32

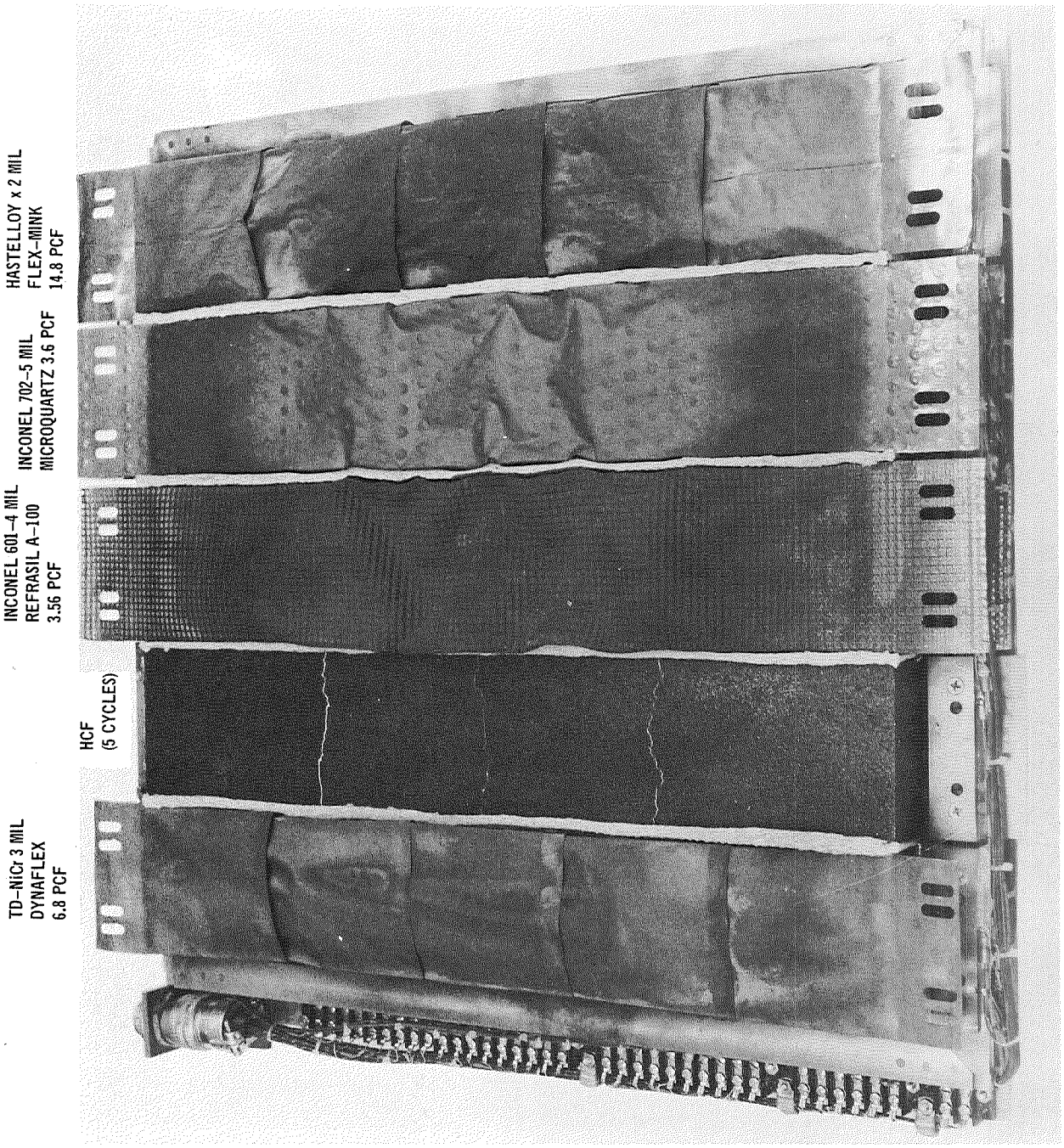
cracks completely through the block, from hot to cold side (Figure 33). Review of the thermocouple data indicated that the failure occurred in the first thermal cycle. It was also determined that the HCF had been improperly installed which may have contributed to its failure. For mounting on the test fixture, 0.030 inch thick stainless steel tabs had been bonded to the cool side of the block with a silicone adhesive. To accommodate thermal expansion, the screws through the slotted holes in the tab were to be loosened for thermal cycling. However, only the screws at one end were loosened and there were indications that the expansion exceeded the movement available.

The HCF block was replaced with the Irish Refrasil A-100 packaged in dimpled Inconel 601 (4 mil), and testing continued. At 55 cycles on this group, testing was halted due to general deterioration of the packages (Figure 34), with one significant exception. The exception was the 3 mil TD-Ni-Cr package containing Dynaflex, and which was retained for additional cycling with the next group. The Inconel 601 was badly wrinkled, and in one specimen, a small section had been torn out. The Hastelloy X was extremely weak and easy to tear.

The condition of the insulation within the packages is shown in Figure 35. The Flexible Min-K, Refrasil A-100, Irish Refrasil A-100, and Astroquartz showed no appreciable degradation. However, Microquartz at 3.5 lb/ft^3 nominal density had shrunk 0.5 inch of its 20-inch length.

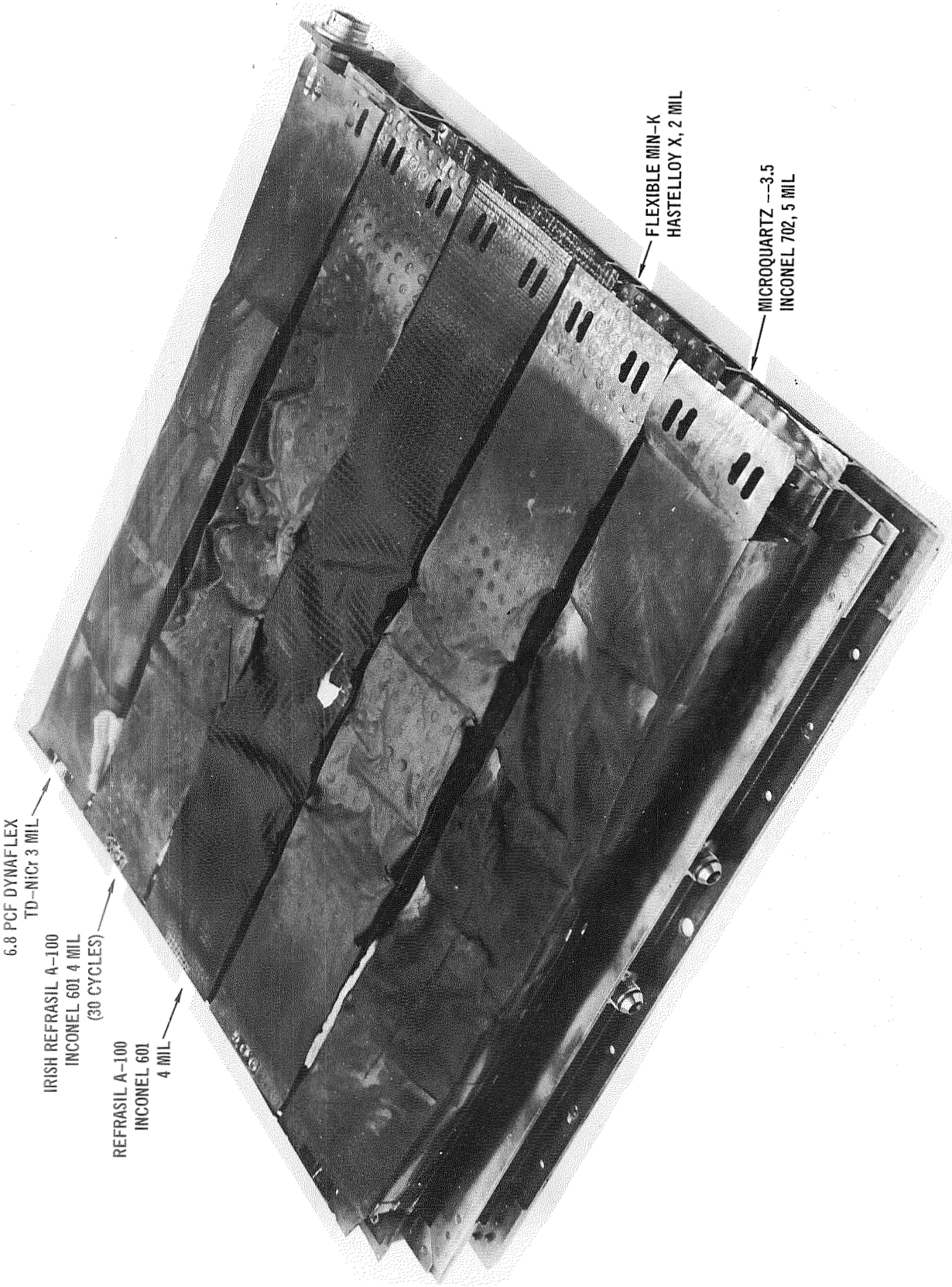
4.3.3 Third Group - 2200°F - Because restraint of the hot side of the package by the sides appeared to be contributing to the wrinkling and deformation of the packages, two alternative designs were assembled for testing with the third group of test specimens. These new designs incorporated a "floating" top which would be relatively free to expand and contract with minimum restraint. Sketches of these designs are shown below:





457-1153

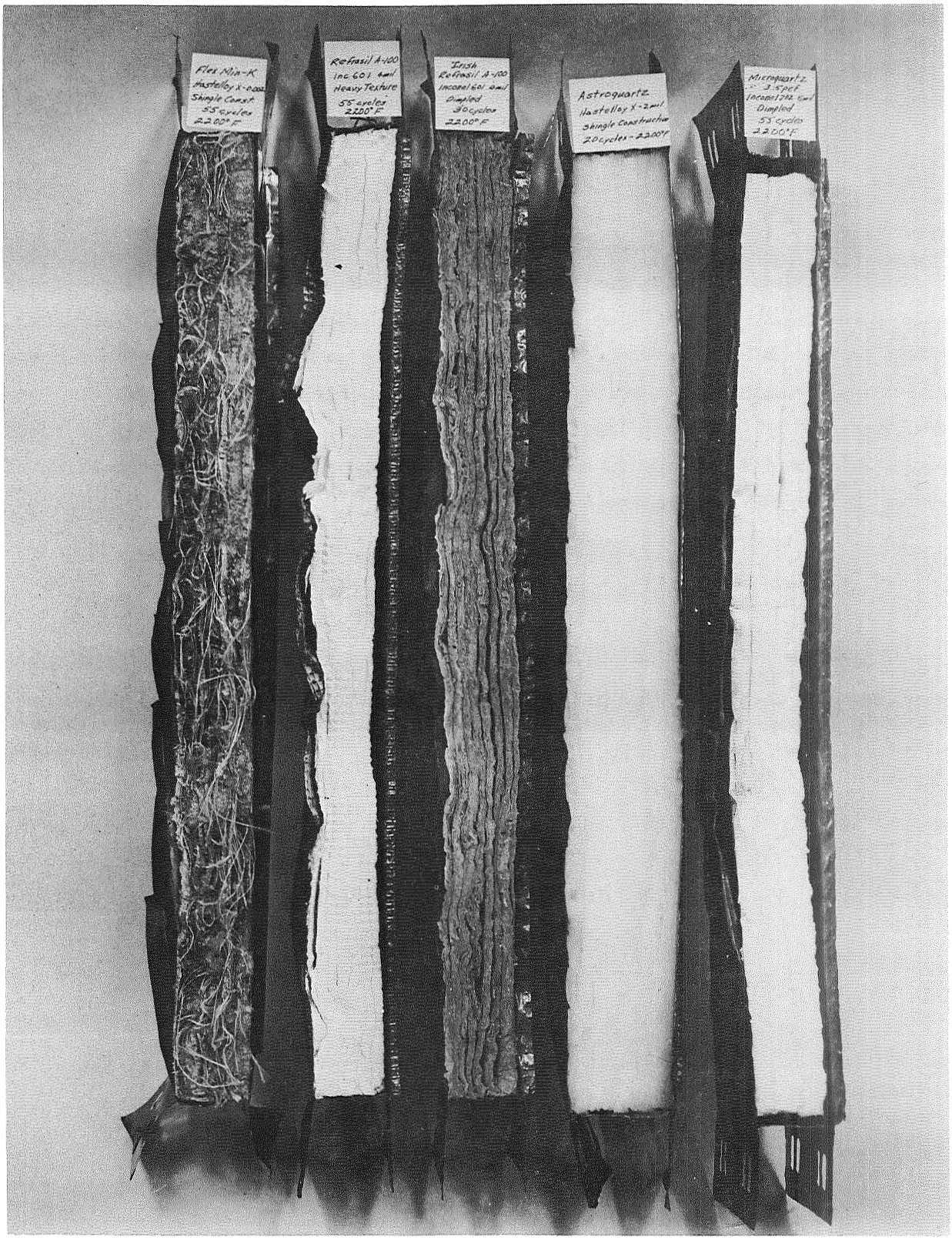
Figure 33



TEST SPECIMENS AFTER 55 CYCLES (EXCEPT WHERE NOTED)
SIMULATED SERVICE 2200°F – SECOND SERIES

Figure 34

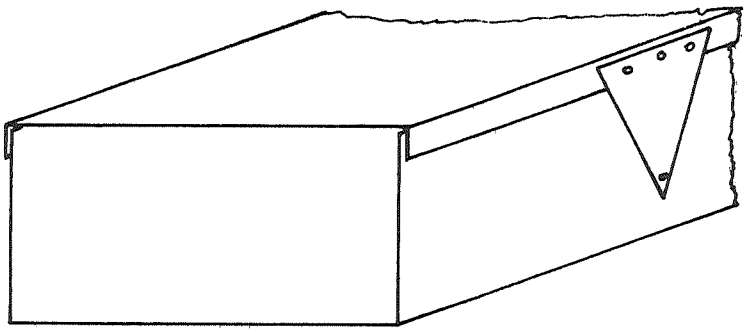
457 – 1154



SECOND GROUP OF SPECIMENS EXPOSED TO PEAK TEMPERATURE OF 2200°F DURING MISSION CYCLING. 55 CYCLES EXCEPT WHERE NOTED

457-1155

Figure 35



Both of these packages contained Astroquartz Mat; however, one also included a single sheet of 2 mil Hastelloy X about 0.3 inch from the hot side, sandwiched between layers of Astroquartz. The purpose was to determine if a radiation barrier would sharply reduce the conductance of this very lightweight insulation. Other specimens (see table below) included: a double width specimen to gain an early indication of width effects in evaluation; an HCF specimen; and continuation of testing of the TD-NiCr package.

2200°F SERIES

THIRD GROUP

Insulation	Thickness	Density	Packaging
*Dynaflex 2 - 2 inch layers of 3 lb/ft^3 compressed to 1.5 in.	1.5 in.	6.8 lb/ft^3	TD-Ni-Cr, 3 mil shingle construction (cold face Inconel 601)
**Coated HCF 14.9 lb/ft^3	2.0 in.	18.3 lb/ft^3 with Coating	M25A7 Coating
Astroquartz 1.0 lb/ft^3	2.0 in.	1.13 lb/ft^3	Inconel 702, 5 mil slide-on lid
Irish Refrasil A-100	1.5 in.	7.53 lb/ft^3	Inconel 601, 4 mil dimpled double width specimen
Astroquartz 1.0 lb/ft^3 with Hastelloy X Radiation Barrier	2.0 in.	1.69 lb/ft^3	Inconel 702, 5 mil dimpled free box-lid

*Continued in test from second group.
**Cracked into two pieces in first five thermal cycles. Replaced with Astroquartz with radiation barrier.

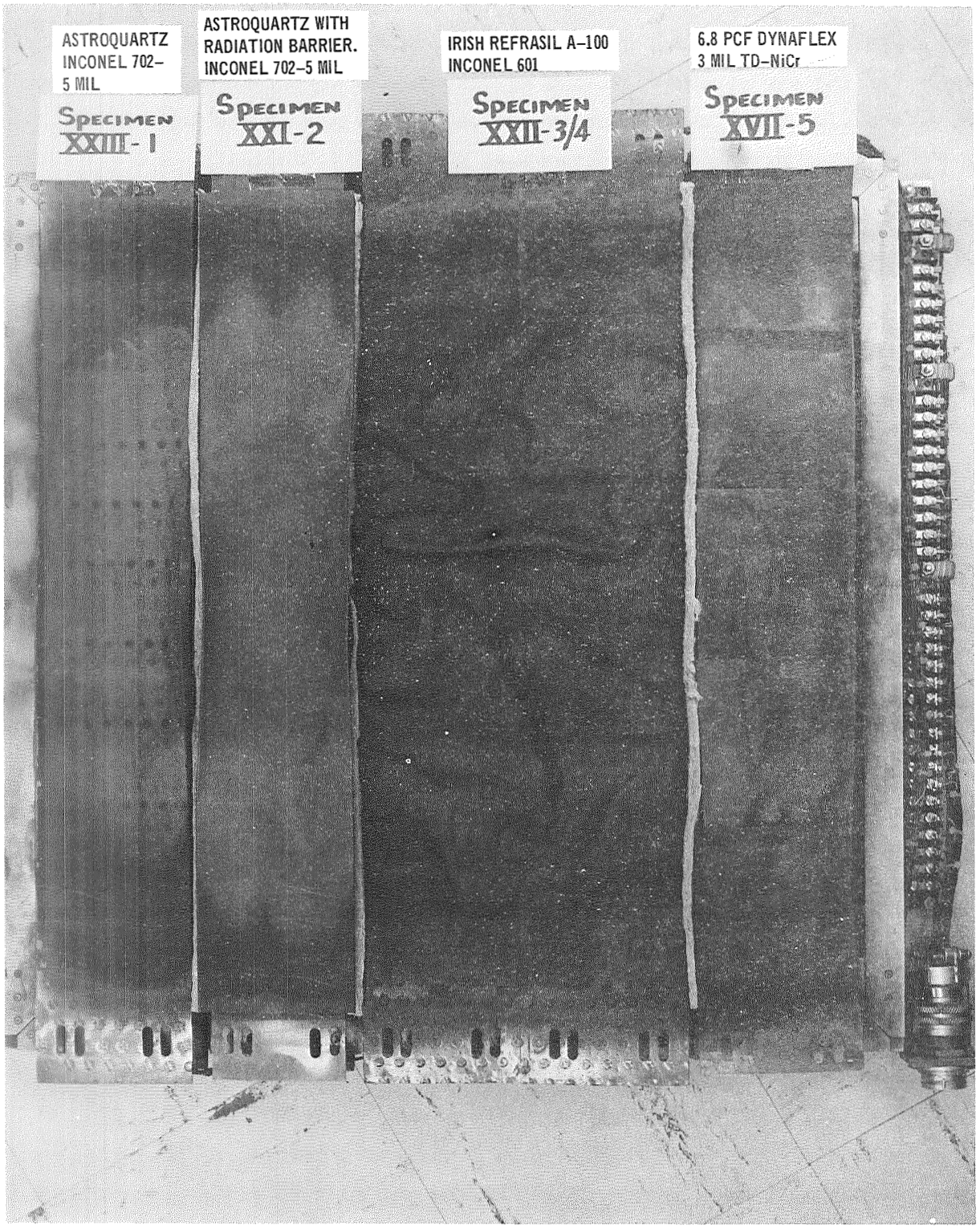
In previous testing groups, vibration testing had been alternated with acoustic testing. In the third group at 2200°F, due to a planned shut-down of the air supply for the air stream modulator it was desired to obtain multiple acoustic tests early, and vibration tests later in the sequences. As events turned out, the tests were terminated prior to the shutdown of the acoustic facility, and all cycles were with acoustics only.

A total of 45 cycles were completed on this group when it was deemed unproductive to continue testing (Figure 36). The TD-NiCr package at this time had accumulated a total of 100 cycles and was still in excellent condition (Figure 37). It did not have the severe wrinkling and deformation of the hot surface which was characteristic of the Inconels and Hastelloy X at this temperature. The metal foil also remained flexible after exposure. On one roof section there were two compression scallops, the cause of which is uncertain. The packages with "free-floating" tops successfully eliminated the severe creasing that had normally occurred with the particular metal foil in 2200°F testing. However, package integrity suffered. The slide-on lid permitted the sides of the box to be deformed inwardly at the top during the thermal test as much as 3/8 inch on a side. This was believed caused by repressurization of the vacuum chamber after each thermal cycle. The box type lid on the other specimen, however, did not exhibit a similar characteristic. Its problem was frequent failure of the spot welds that joined the bottom of the hold-down tabs to the box.

The double-width specimens had the characteristic creases and folds that Inconel 601 had displayed in earlier tests of this temperature. There appeared to be no aggravation of the problem by the larger size, nor any relief.

The Dynaflex used in the TD-NiCr package was 3 lb/ft^3 material compressed to 6.8 lb/ft^3 (it had been intended to provide an 8-9 lb/ft^3 insulation - as an intermediate range between the previously tested 6 lb/ft^3 and 12 lb/ft^3), and which was found to have compacted about 0.75 inch (of the 20-inch length) at one end. As in previous cases with Dynaflex, this was due to vibration/acoustics. The Irish Refrasil A-100, and Astroquartz insulations were not affected.

The effectiveness of the Hastelloy X radiation barrier in the Astroquartz specimens was evaluated by comparison of the temperature difference between the hot and cold thermocouples at the time the respective hot thermocouples reached their peak, and again when the cool thermocouples peaked out. For both specimens (one with the radiation barrier, one without), these times were identical. Because the thermocouples were in the same relative positions within the specimens and



THIRD GROUP OF 2200°F MISSION SIMULATION AFTER 45 CYCLES
(100 CYCLES FOR TD–NiCr)

457–11456

Figure 36



TD-NiCr PACKAGE AFTER 100 CYCLES OF SIMULATED MISSION CYCLING WITH PEAK TEMPERATURES OF 2200°F

457-1157

Figure 37

identical distances apart, a reasonable assessment can be made. Data were taken at the fifth cycle of the first thermal exposure of each specimen. Because neither specimen had been exposed to acoustic or vibration exposure at this time there was good assurance that the thermocouples had not shifted position since original measurement by X-ray. The data from this comparison are:

	Hot-Side Peak	Cool-Side Peak
Astroquartz without Shield		
Hot T/C	1952°F	1941°F
Cool T/C	1357°F	1366°F
Temperature Difference	595°F	575°F
Astroquarts with Shield		
Hot T/C	1974°F	1965°F
Cool T/C	1311°F	1334°F
Temperature Difference	633°F	631°F

The Astroquartz with the radiation shield showed an average of 62°F greater temperature drop at these two times, demonstrating that the radiation shield was effective. However, it is questionable whether the weight penalty justifies the difference. A single sheet of Hastelloy X, 2 mil thick, is essentially equivalent in weight to an additional thickness of 1.0 inch of Astroquartz.

5.0 RIGIDIZING OF FELTED INSULATIONS

An exploratory development was conducted on the rigidizing of prefelted fibrous insulations as an alternative approach to rigid blocks. The development of block insulation by wet mixing loose fibers and binders (such as the HCF process) was covered by a separate contract (NAS 9-11221), and duplication of that effort was intentionally avoided.

The process studied here was to impregnate a felted insulation with a refractory binder, and dry to a rigid block. For convenience, the felt used was Dynaflex, partly because of the high temperature capabilities of its fibers, and also because it was available in a wide range of densities.

The following binder systems were studied:

Ludox - Colloidal silica sol

Syton - Colloidal silica sol

Ethyl silicate P-40

Ethyl silicate P-20 (alcohol stabilized)

Positive Sol - colloidal silica, Al_2O_3 stabilized

Alon - colloidal Al_2O_3

Aluminum phosphate

Lithium polysilicate

In order for the binders to wet the felt it was necessary to add a small amount of wetting agent to the binder. Triton X-100 was used for this purpose. The wetting agent was necessary whether or not the original binder in the Dynaflex had been burned out.

Felts of 3 lb/ft^3 density, after soaking in binder collapsed on removal. Blocks formed from felts of 8 - 12 lb/ft^3 density, allowed to gravity drain and oven dried, were more substantial. However, difficulty was encountered in securing uniform blocks; binder gradients and nonwetted areas were persistent problems.

Vacuum-assisted drainage of binder (from bottom side) was unsuccessful with low density felts (3 lb/ft^3) as the pressure gradient collapsed the felt. Felts of 8 lb/ft^3 were slightly compressed, and 12 lb/ft^3 was dimensionally stable. The latter could be dried to provide final densities of 15 $\pm$2 lb/ft^3. However, uniformity of impregnation was poor, resulting in highly variable properties through the thickness of the felt.

All of the silica binders produced fairly strong felts. The Ludox, Syton and Positive Sol were easy to process and could be recycled. The ethyl silicate required more complicated processing and was not reuseable. Positive Sol provided good strength and powdered less than the other binders when dried. The colloidal alumina (Alon) provided no significant strength, and blocks impregnated with Alon were very soft and friable. Both aluminum phosphate and lithium polysilicate attacked the fibers chemically.

To the extent that the process was studied here, this approach to make rigid blocks from prefelted blankets or matts, does not appear promising, and at this point in development, is several years behind the development of HCF. Because of the more advanced state of development of HCF, the approach described herein to make rigid blocks was suspended. The development of HCF, however, is continuing under separate contracts.

6.0 FOLLOW-ON PROGRAM

The basic program has been extended for an additional 12 months study. Principal subjects to be investigated are:

Vent requirements for packaged insulations;

Moisture accumulation and means of preventing it in packaged insulations;

Evaluation of insulations for 1000°F peak temperatures;

Testing of large flight configuration specimens;

Limited development on HCF block insulations as an internal insulation.

In addition, further preliminary evaluation tests (such as those described in this report) will be conducted at 2200°F and 2500°F.

7.0 CONCLUSIONS

Based on the tests conducted to date, the following observations can be made as to the utility of these materials in Shuttle service.

7.1 Metal Foil Packaging

For service to 1800°F, the Inconel 702, Inconel 601, or Hastelloy X may be used, with a slight preference for Inconel 702. The 2 mil foil appears adequate and is desirable from a weight standpoint. Small cracks and puckers at edges of the hot side occurred for all alloys; however, there was no compromise of structural integrity and only waterproofing was affected.

For service to 2200°F, TD-Ni-Cr is the only metal of those tested which provided adequate service beyond 10 reuses. All the other superalloys tested exhibited excessive wrinkling and oxidation embrittlement.

7.2 Insulations

Astroquartz - Capable of 2200°F service. Very lightweight, may require excessive thickness. Data not available on conductivity at high temperatures at 1 lb/ft^3.

Microquartz - At 1800°F a small amount of shrinkage occurred which is probably tolerable. At 2200°F, the shrinkage/settling increased to what may be a critical amount.

Dynaflex - Disappointing performance, as it was expected to be a prime candidata due to its temperature capabilities. Unsatisfactory at 3 lb/ft^3 due to excessive settling; 6 lb/ft^3 is borderline; 12 lb/ft^3, satisfactory. Latter could possibly be used at 2500°F with only a slight weight penalty.

Dynaquartz - Unable to withstand mechanical loads without cracking.

Refrasil A-100 - Satisfactory for use to 2200°F. However, difficult to achieve nominal density in practical use. Could lead to problems in estimating total weight.

Irish Refrasil A-100, Irish Refrasil B-1576 - Satisfactory for use to 2200°F. May become principal candidates for low density 2500°F service.

Flexible Min-K - Satisfactory for use to 2200°F. Low conductivity, excellent for volume-limited applications.

Coated HCF - Failure of coated HCF specimens was due to high thermal gradients through the thickness. Thermal stresses in the coating on the specimen sides were analytically determined to be on the order of four times allowable strength. Coating failure appeared to induce cracks in the HCF which resulted in complete failure

of the specimens. The existing coating (M25A7) has an allowable tensile strain of approximately 144 μ in/in. A major objective of current HCF programs is to reduce the modulus and increase the allowable strain of the coating.

Use of HCF as an internal insulation would most logically be in areas seeing peak temperatures of 2200-2500°F, where its conductivity is competitive to soft felts, and where its integral waterproof coating (when successfully modified) may be more advantageous than the projected coated columbium packaging for soft felts.

7.3 Rigidizing of Felted Insulations - Rigidizing of prefelted insulation by impregnation with a ceramic binder is not a satisfactory process at present. Non-uniformity of wetting and distribution of binder in the final dried product are the principal problems. The slurry method of forming blocks (such as HCF) is at a more advanced state of development and is preferred.

7.4 Test Procedures - The test procedures employed in this program are effective, economical means of evaluating insulations for Shuttle service. Areas of possible improvement are: thermocouple measuring junctions which are less susceptible to failure, and means to measure more accurately the position of the thermocouples within the insulation, as well as to prevent their movement. Future work will use sheathed thermocouples with measuring junctions enclosed within the sheath.

8.0 REFERENCES

1. ASSET, Aeroelastic and Dynamic Experiments, Flight Results and Correlation (U) McDonnell Aircraft Co., AFFDL TR-65-31, Vol. 13, Contract AF 33(616)8106 (Conf.)
2. Coe, Chas. F., Buffet and Aerodynamic Noise, NASA-Ames. Presented at Space Transportation System Technology Symposium, NASA-Lewis Research Center, 15-17 July 1970, NASA TM-X-52876, Vol. 2.
3. Hughes, T. A., A Technique for Estimating the Thermal Conductivity of Insulations at Low Pressures, MDAC-EAST Report MDC-E0285, 8 January 1971.
4. Pettyjohn, R. R., Thermal Conductivity Measurements on a Fibrous Insulation Material, General Dynamics Corp., Convair Div., Proceedings of the Seventh Conference on Thermal Conductivity, NBS Special Publication No. 302 (1967).

Appendix A

Entry Thermal Environment for
Shuttle TPS High Temperature Insulations

Entry Thermal Environment for Shuttle TPS High Temperature Insulations

1. Summary

The thermal environments for eight Shuttle Orbiter entries have been analyzed, and simplified temperature-time histories derived for the purpose of environmental testing of high temperature insulations. The procedure used to obtain this data is contained herein.

2. Thermal Environment

Analysis of entry trajectories investigated in previous Shuttle studies, and in our current Phase B study, reveals that many different types of heat pulses are possible with approximately the same peak radiation equilibrium temperature. Not only do variations in vehicle flight parameters and cross-range maneuver capabilities affect heat pulse shape, but also vehicle angle of attack, flow field divergence, vehicle station, and boundary layer turbulence. Figure A-1 summarizes the entry trajectories currently probable for Shuttle Orbiters. Trajectory cross range is the dominant characteristic which distinguishes the trajectories and is related directly to duration of entry. The higher cross range missions are more severe on the insulation due to higher total heat and longer time at temperature. Also listed in Figure A-1 are aerodynamic heating parameters and heat pulse characteristics which are discussed in succeeding paragraphs. Because trajectory evolution will continue throughout the various phases of Shuttle development, it appears extremely practical to deduce a simplified temperature-time curve which is not unique to a specific entry trajectory, but encompasses the severe elements of any reasonable trajectory. The degree of simplification should be minimal so as to retain as much correspondence as possible with actual Thermal Protection System requirements. With this as an objective, representative temperature-time curves are examined for shape, time at maximum temperature, and total heat.

3. Heat Pulse Characteristics

The three entry trajectories selected from our current Phase B study produce radiation equilibrium temperatures which illustrate the various shapes of temperature-time curves. These temperature-time histories (Figures A-2, -3, and -4) were determined in such a way that all local aerodynamic heating is rejected at each instant during entry from the vehicle outer mold line by thermal radiation. All temperatures were obtained considering 0.8 surface emittance and radiating to a

SHUTTLE ENTRY TRAJECTORY PARAMETERS

	PHASE A		PRE-PHASE B (ORBITER "B" MOD 1)			PHASE B (DEVELOPED BY MDAC AS OF 8/1/70)		
	LOW CROSS RANGE MSC-ILRV	HIGH CROSS RANGE (SAMSO)	LOW CROSS RANGE *	MEDIUM CROSS RANGE *	HIGH CROSS RANGE *	HIGH CROSS RANGE MARK 1 SHAPED → 2000°F INCL. DES. MAR.	HIGH CROSS RANGE DRAWBRIDGE LOW ALT DISP. INCLUDES DES. MAR.	LOW CROSS RANGE LOW ALT. DISPERSED 60° BANK NO DESIGN MARGINS
CROSS RANGE (NM)	231	2000	350	1260	1700	1500	2180	140
DOWN RANGE (NM)	2000	9800	2800	5400	6500	6300	6500	2100
W/C_LS (W/S)	(30)	(53)	73	108	156	118	216	60
L/D	.54	2.2	.7	1.45	1.75	1.75	2.0	.52
VEHICLE LENGTH (FT)		160	170	170	170	156	148	148
ENTRY ANGLE (DEG.)	-1.6	-1.5	-1.6	-1.6	-1.6	-1.6	-1.6	-1.6
ENTRY TIME (SEC)	1260	3100	1138	2079	2523	2590	2755	720
ANGLE OF ATTACK (DEG.)	60	43-20	53	31	23	14-20	18	60
MAXIMUM DYNAMIC PRESSURE (LBF/FT^2)	35-40		75	125	182	112	272	56
MAXIMUM SURFACE TEMP. (°F)	2200	2200	2100	2100	2100	2000	2200	2200
TOTAL HEAT (A) (BTU/FT^2)	7600	44400	-	-	-	15989	22275	5340
TOTAL HEAT (B) (BTU/FT^2)	-	-	-	-	-	17623	31950	5315
TOTAL HEAT (C) (BTU/FT^2)	-	-	6116	14699	16994	15055	18305	4892
TIME @ MAX. TEMP($\pm 20°$)(A) (SEC)	60	60	-	-	-	140	100	75
TIME @ MAX. TEMP($\pm 20°$)(B) (SEC)	-	-	-	-	-	250	230	100
TIME @ MAX. TEMP($\pm 20°$)(C) (SEC)	-	-	20	250	70	50	60	35

* $\frac{X}{L}$ = 0.25 with X = 42.5 ft.

HEAT PULSE SHAPE
(A) EARLY TEMPERATURE PEAK
(B) DOUBLE TEMPERATURE PEAK
(C) LATE TEMPERATURE PEAK

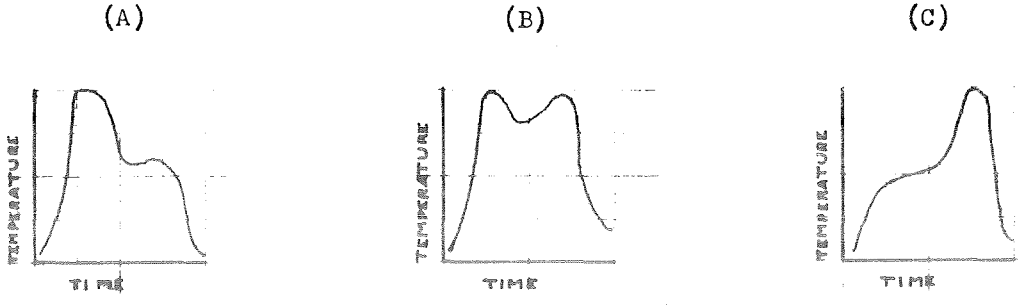
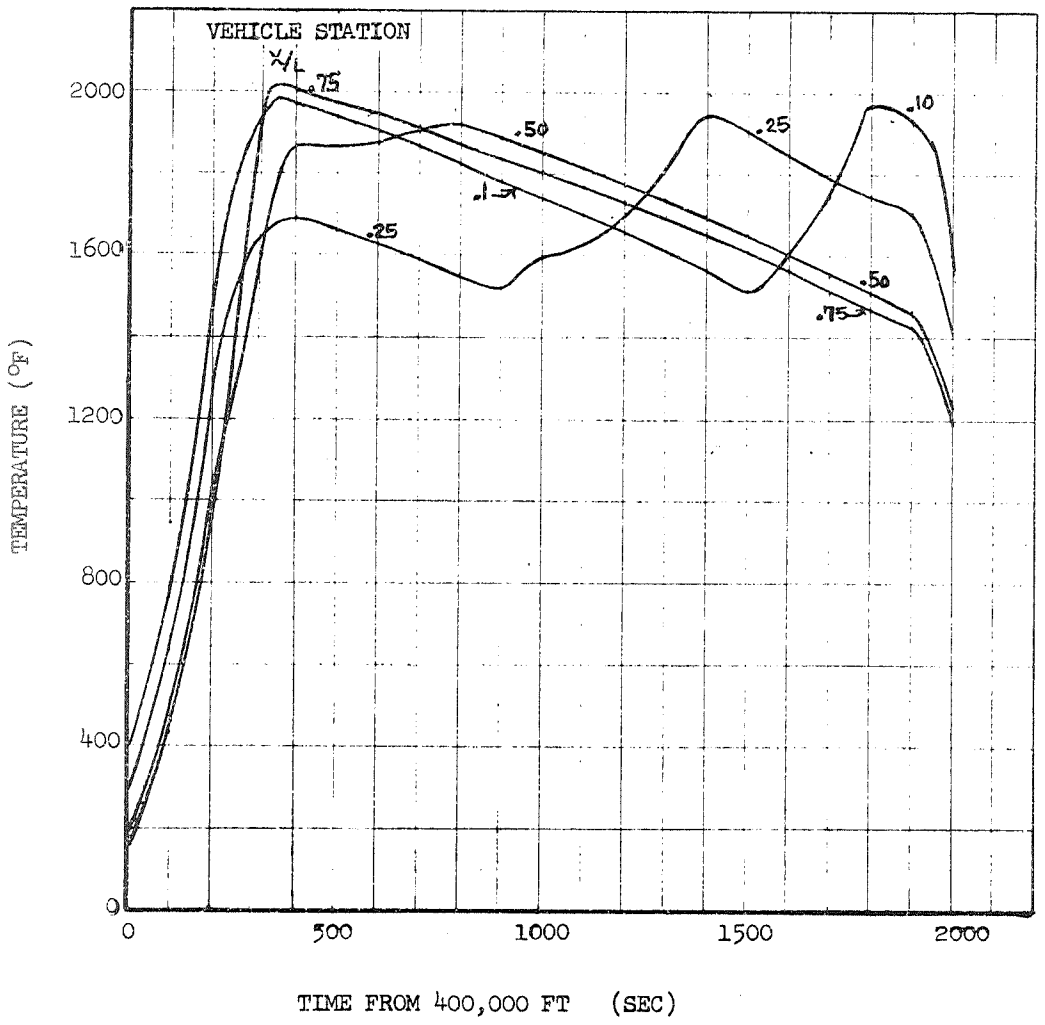


Figure A-1

- RADIATION EQUILIBRIUM (0.8 EMISSIVITY)
- ANGLE OF ATTACK (14° TO 20°)
- HEATING FACTOR (1.1)

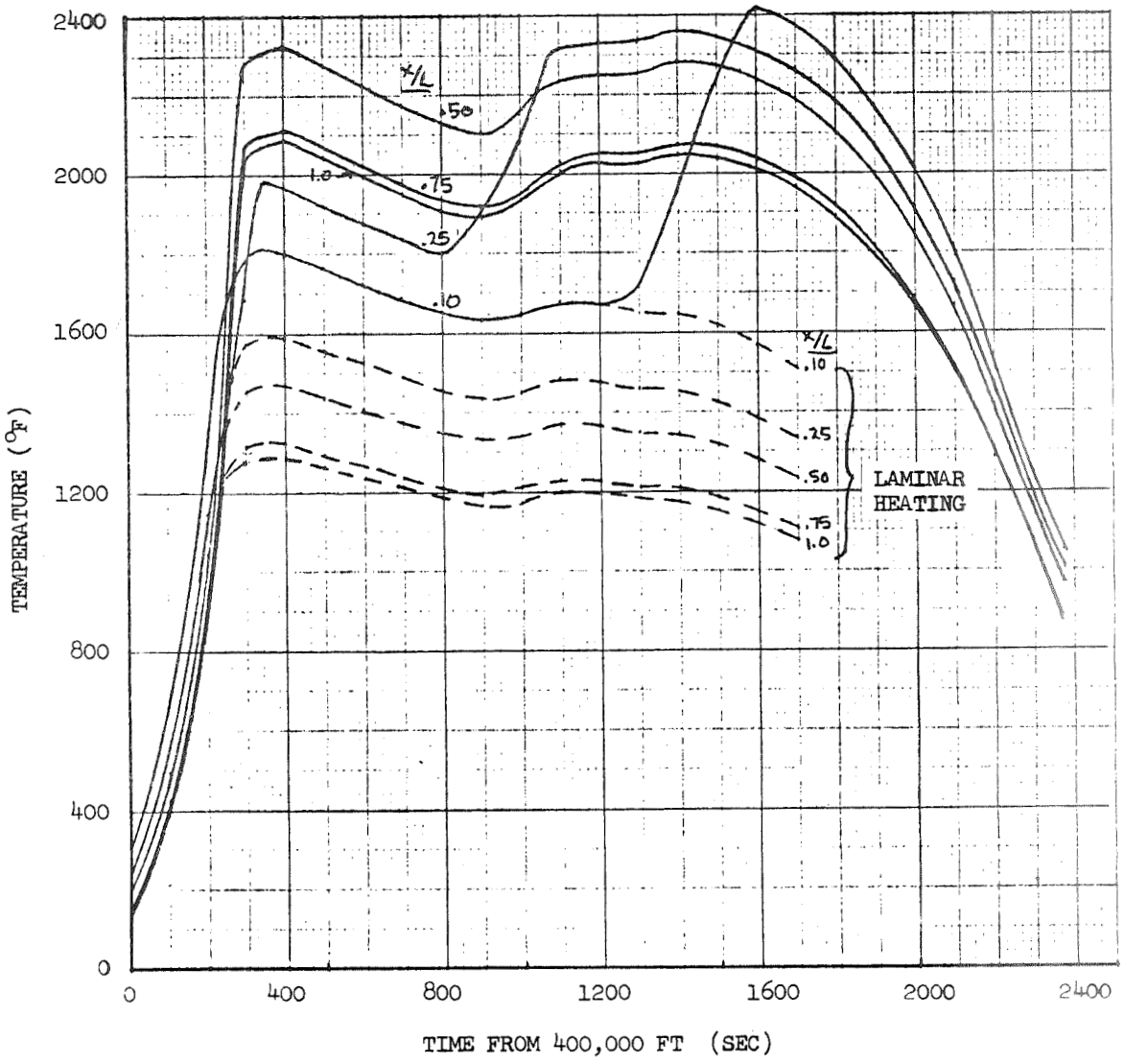


TEMPERATURES ALONG BOTTOM ℄ OF HIGH CROSS RANGE - MARK 1 DELTA ORBITER

457--1159

Figure A-2

- LOW ALTITUDE DISPERSED SHUTTLE TRAJECTORY
- RADIATION EQUILIBRIUM
- ANGLE OF ATTACK = 18°



TEMPERATURE ALONG BOTTOM ℄ OF HIGH CROSS RANGE-DRAWBRIDGE ORBITER

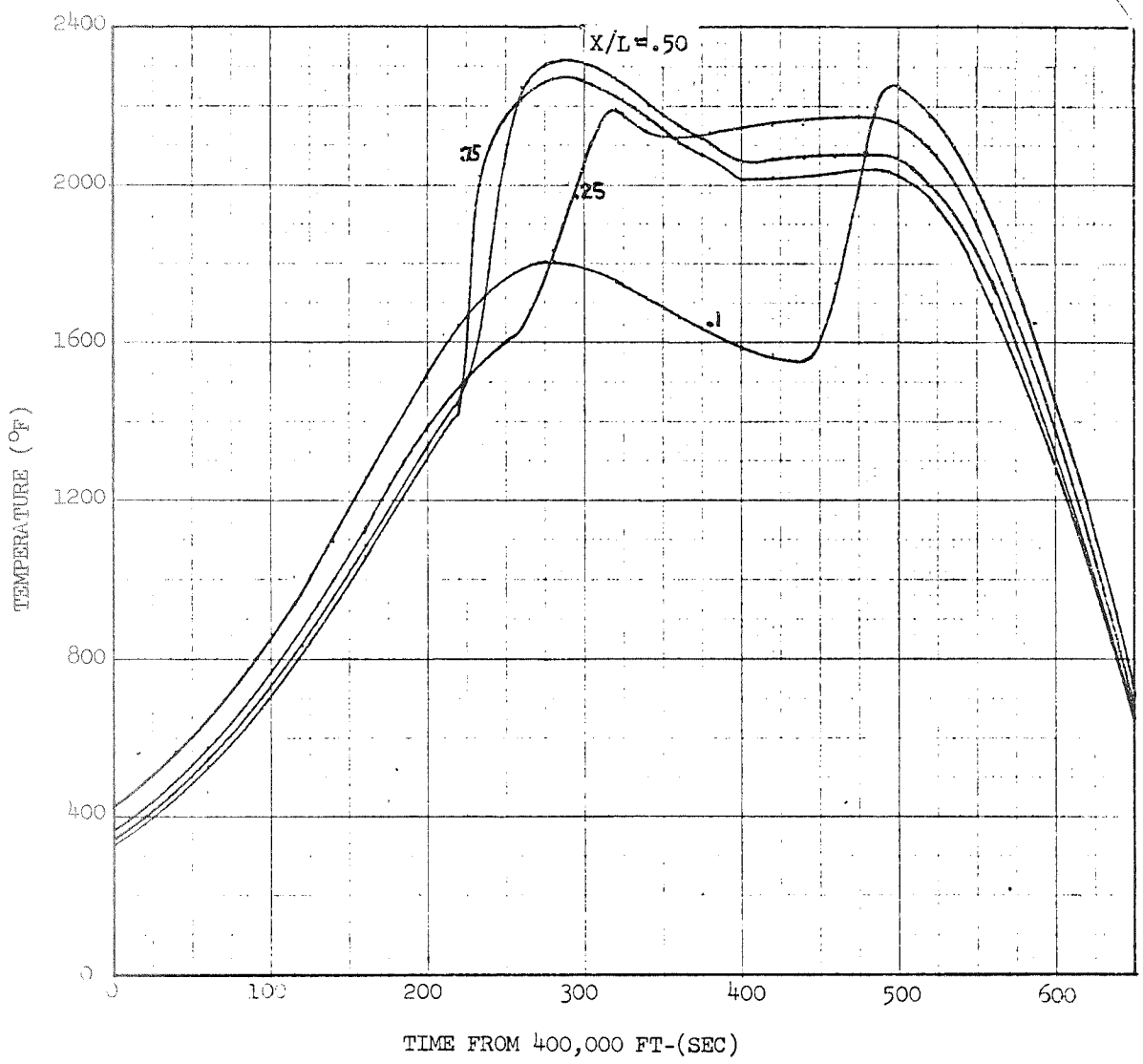
457-1160

Figure A-3

- LOW ALTITUDE DISPERSED SHUTTLE TRAJECTORY
- RADIATION EQUILIBRIUM (0.8 EMISSIVITY)
- ANGLE OF ATTACK (60°)

L = 145 FT





TEMPERATURES ALONG BOTTOM ℄ OF LOW CROSS RANGE ORBITER

457-1161

Figure A-4

cold sink. Trajectory "tailoring or shaping" was employed to restrict vehicle surface temperatures below a design temperature of 2000°F and 2400°F. This "tailoring" is accomplished by banking the vehicle's lift vector. All of these temperature-time curves consist of an initial heat-up followed by an interval of modulating heating prior to heating drop-off during latter stages of entry. The degree of heating modulation distinguishes the thermal histories. As can be seen from Figures A-2, -3, and -4, these histories fall into three categories:

(a) Surface temperature which peaks early during entry.

(b) Surface temperature with two peaks - early and late.

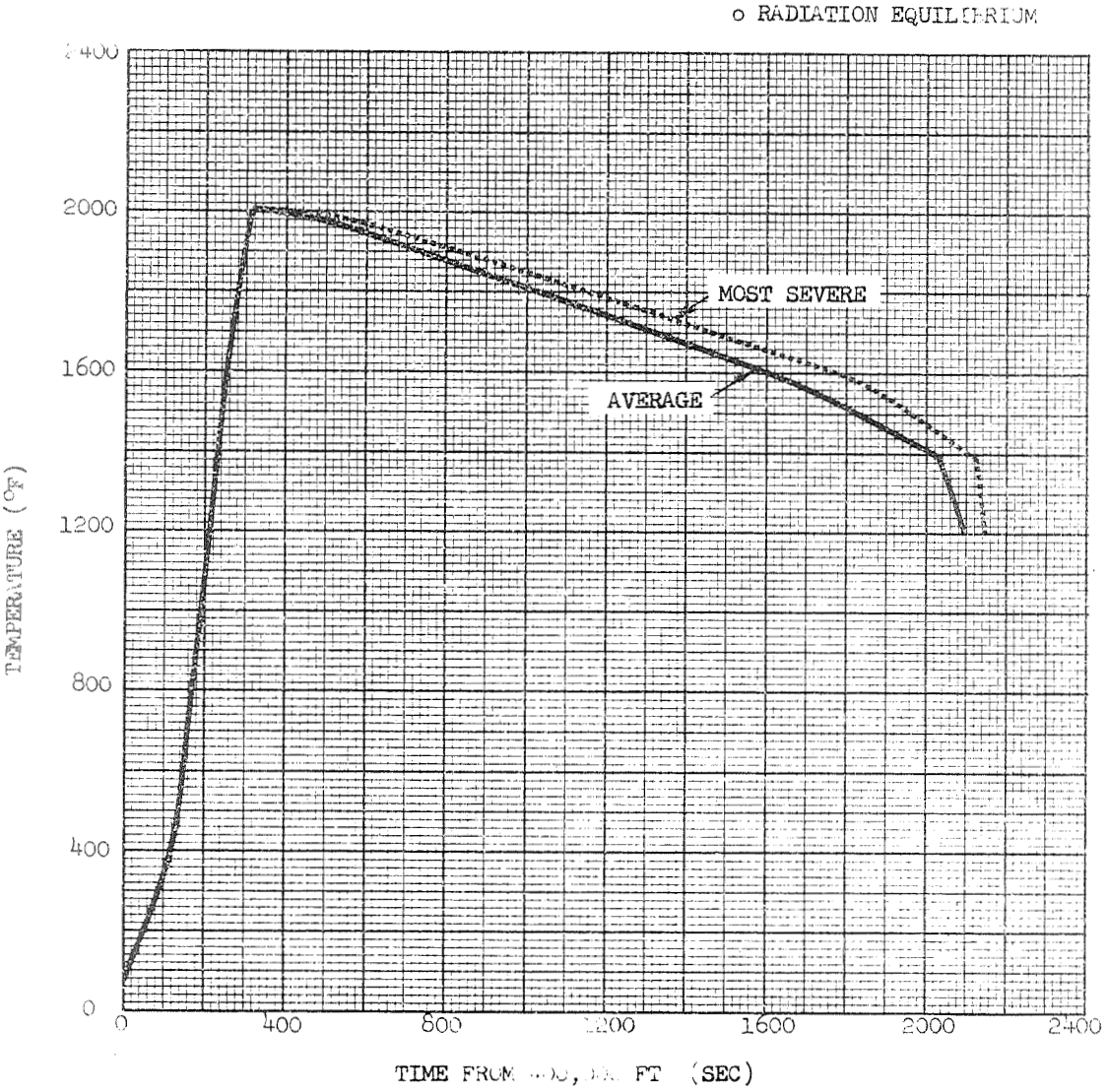
(c) Surface temperature which peaks late in flight.

The double peak has the greatest time at elevated temperature and correspondingly, the greatest total heat for the same maximum temperature.

4. Method for Simplifying Heat Pulse

The "heat-up" for these three trajectories nominally takes 300 to 350 seconds. In order to evaluate materials for thermal shock, the shorter "heat-up" time was selected. This may be a little more severe thermal shock than may be flown; however, the high cross-range trajectory (Figure A-1, column 1) has a 270 second heat-up. First, the high cross-range entry (Figure A-1, column 6) was analyzed for a characteristic 2000°F thermal history. The "time after heat-up" was tabulated from Figure A-2 for the four vehicle stations (X/L = 0.1, 0.25, 0.5, and 0.75). The times at, or above, a temperature were averaged for the four (X/L) stations to derive the simplified temperature-time curve (Figure A-5). The heating rate corresponding to this simplified temperature time integrated over the entry is 17000 Btu/ft^2, which compares favorably with the average of 16000 Btu/ft^2 for Figure A-3. Also shown in Figure A-5 is the envelope of most severe time at temperature (which would be at most an additional 100 seconds).

The general aptness of Figure A-5 was tested by a comparison with the high cross-range drawbridge entry. This is accomplished by working at a 2200°F maximum surface temperature by adjusting aerodynamic heating factors for the Drawbridge Orbiter. In addition, an all-laminar heating condition was imposed on the X/L = 0.75 vehicle station which produced a category (a) shape heat pulse necessary for the comparison. The modified temperature-time curves for the "Drawbridge" Orbiter are shown in Figure A-6, and the corresponding times at temperature are shown in Figure A-7. The data points in Figure A-7 suggest that the variation in time-at-temperature diminishes at lower temperatures. The "average" simplified thermal

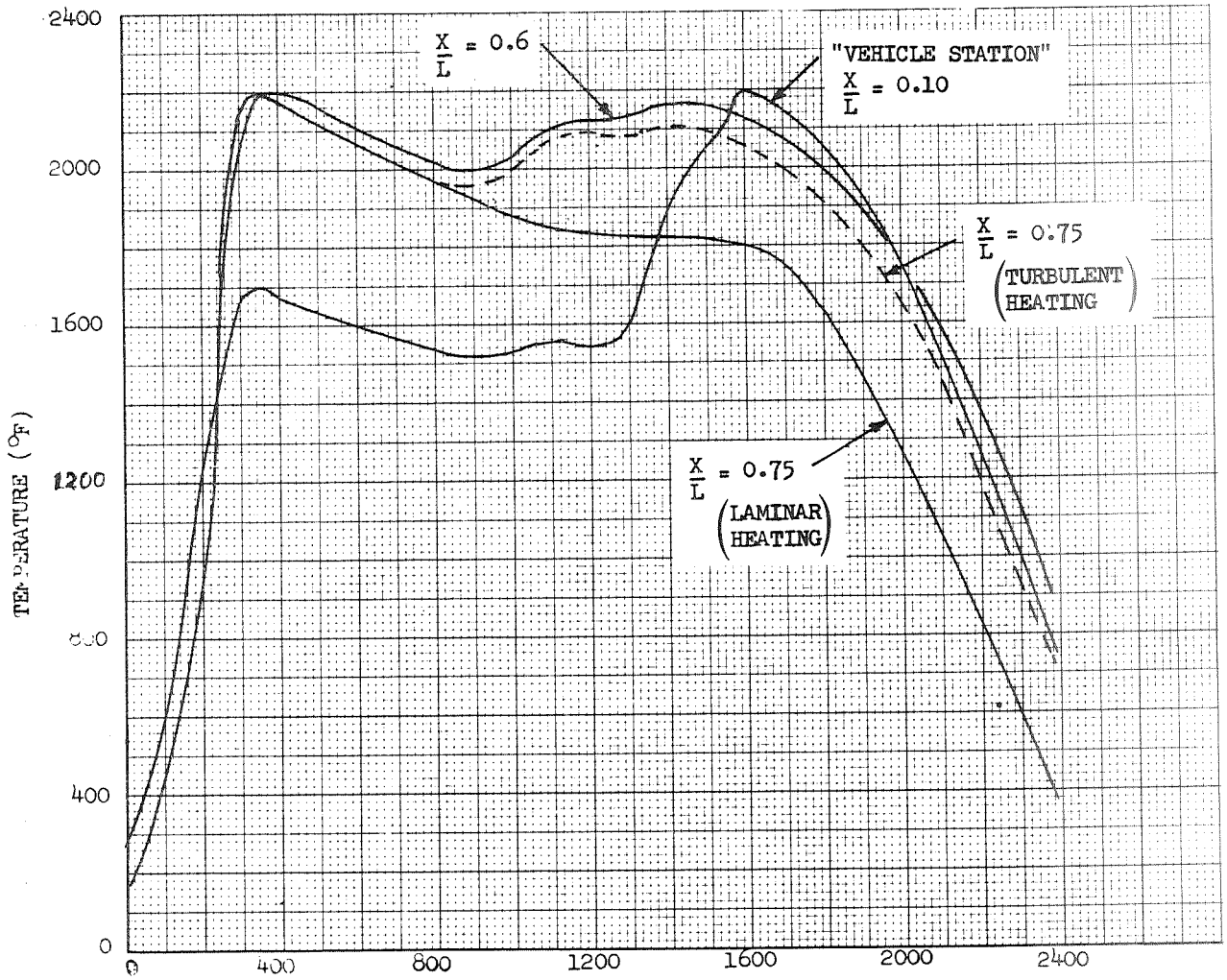


SIMPLIFIED TEMPERATURE-TIME HISTORY FROM BOTTOM ℄
OF MARK-1 DELTA ORBITER

457-1162

Figure A-5

- o LOW ALTITUDE DISPERSED SHUTTLE TRAJECTORY
- o RADIATION EQUILIBRIUM (.8 EMISSIVITY)
- o ANGLE OF ATTACK = 18°
- o HEATING FACTOR FOR 2200°F PEAK SURFACE TEMPERATURE



TIME FROM 400,000 FT ~(SEC.)

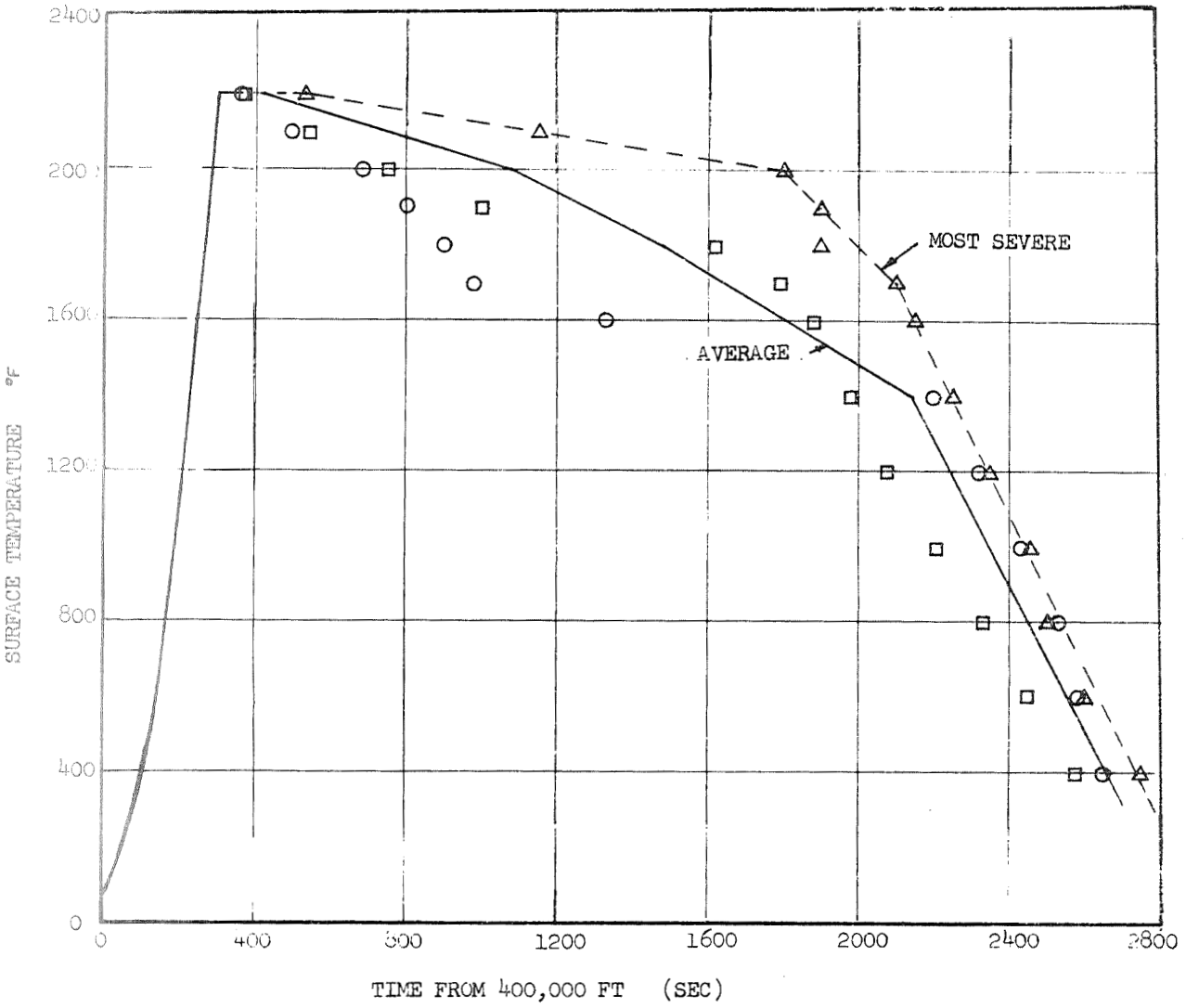
MODIFIED TEMPERATURES ALONG BOTTOM ℄ OF HIGH CROSS RANGE - DRAWBRIDGE ORBITER

457-1163

Figure A-6

o LOW ALTITUDE DISPERSED ENTRY

VEHICLE STATION
○ X/L = 0.1
△ X/L = 0.6
□ X/L = 0.75



TEMPERATURE HISTORY (SIMPLIFIED) FOR BOTTOM ℄ OF HIGH CROSS RANGE DRAWBRIDGE ORBITER

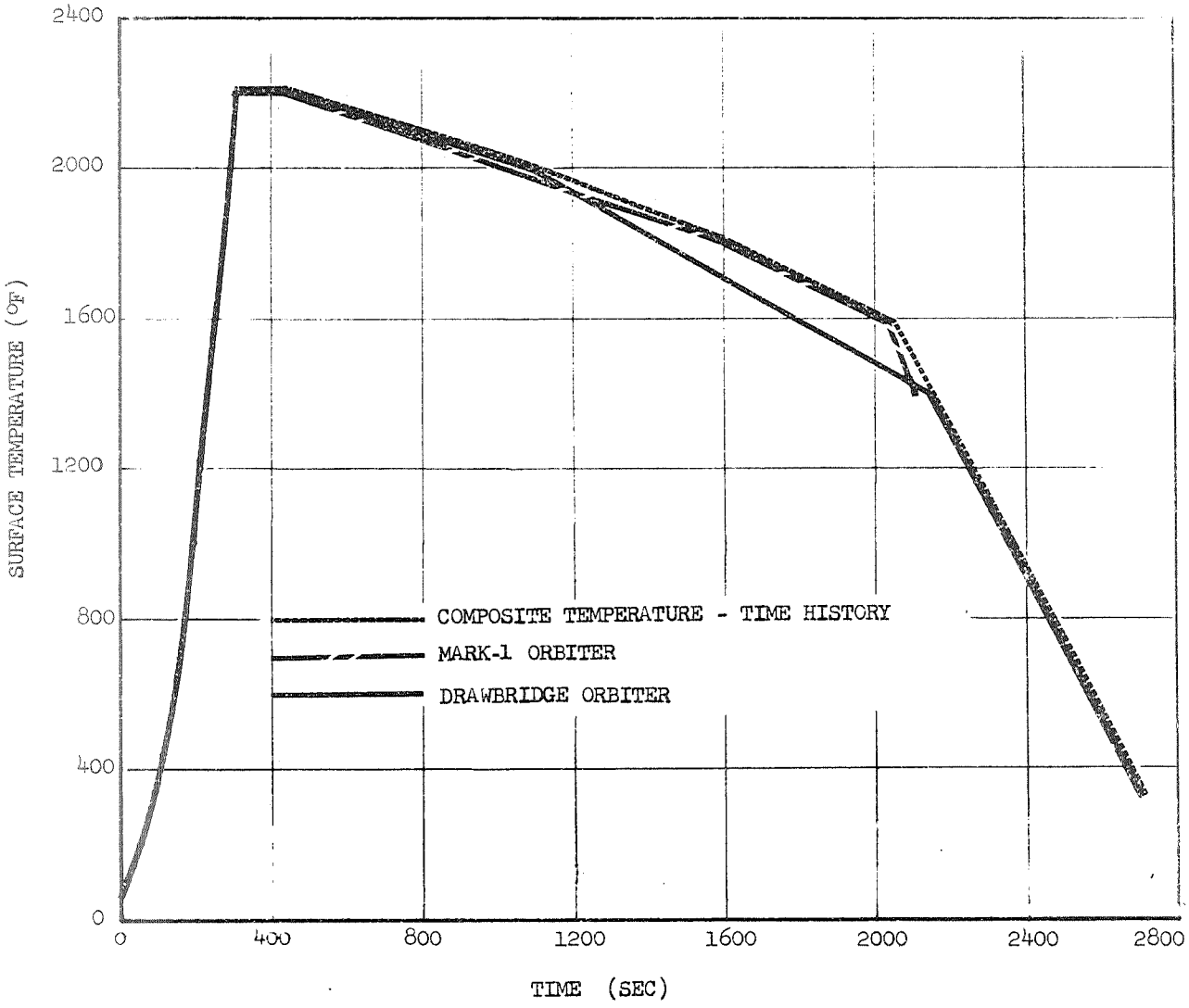
457-1164

Figure A-7

histories for the Mark 1 and Drawbridge as shown in Figure A-8 are in close proximity to one another. The heating factor for Mark 1 was increased to obtain 2200°F necessary for the comparison. The close proximity of these two curves further suggests that adjusting the heating factor can describe thermal conditions for similar entries. This is most likely restricted to entries of approximately the same duration.

An interesting point, seen in Figure A-1, is a spread in total heat from 5340 to 44,400 Btu/ft^2 for the entries investigated. This factor of (8+) in total heat correspondingly imposes a large variation in vehicle insulation weight requirements. Also tabulated in Figure A-1 are the time at maximum temperature, which shows that high cross-range vehicles used to obtain the composite heat pulse have more time at temperature during entry.

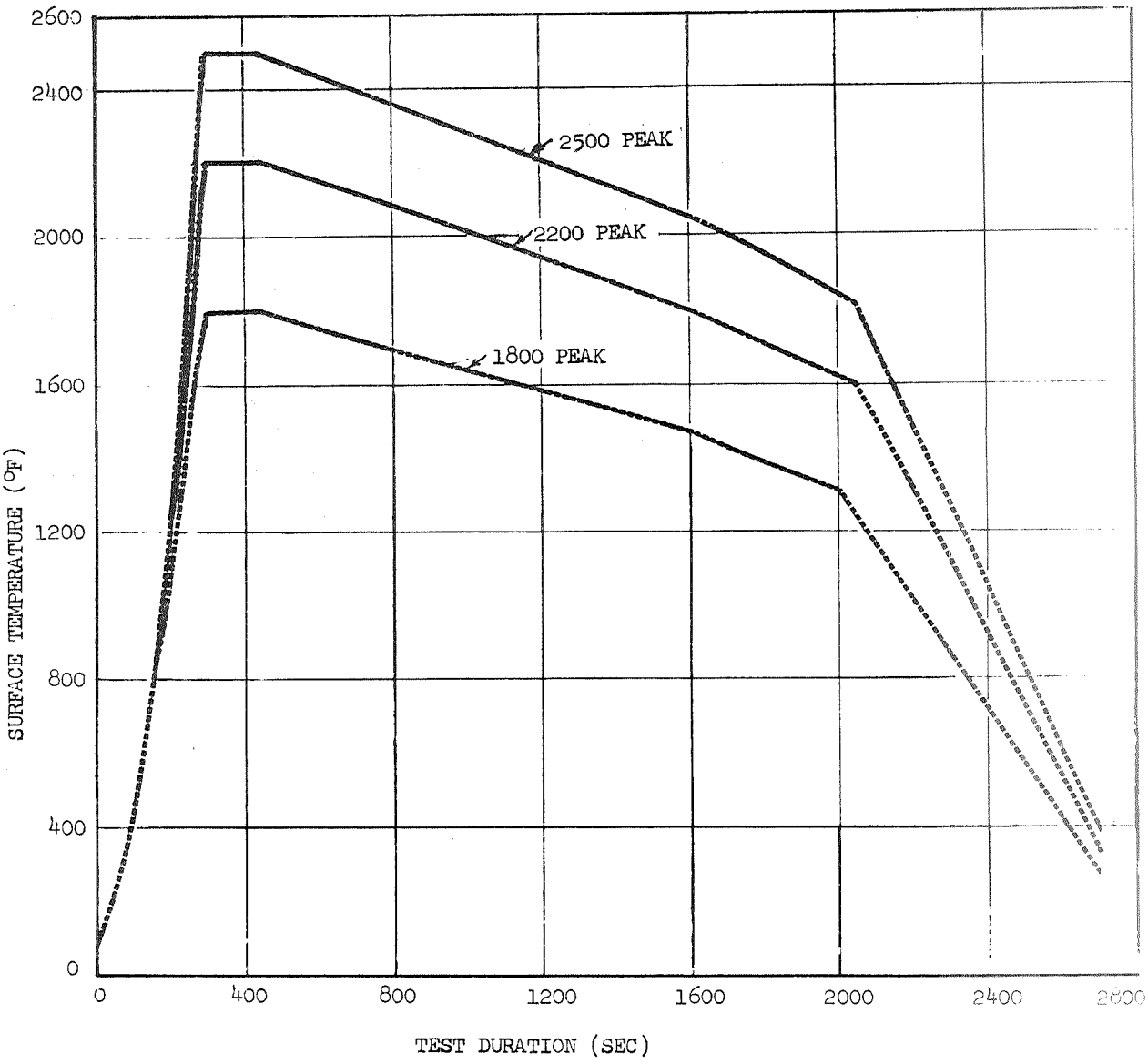
The net result from this comparison is a "composite temperature-time history," which is suitable for testing and general analysis. Figure A-9 is the culmination of this heating pulse modeling and employs the composite curve with appropriate design heating factors to achieve peak temperature of 2500°F, 2200°F, and 1800°F which are suitable for evaluating performance of high temperature insulations. Figure A-10 shows an expanded graph of the initial 300 seconds of heating. These curves have the actual entry durations and simulate the time at temperature along the lower surfaces of two Orbiters during entry. As additional Shuttle entries are evolved, it would be advantageous to compare the time at temperature with the composite curves. If significant changes are evident, the composite curves should be updated.



TEMPERATURE HISTORY FOR HIGH TEMPERATURE INSULATION
(2200°F MAXIMUM TEMPERATURE)

457-1165

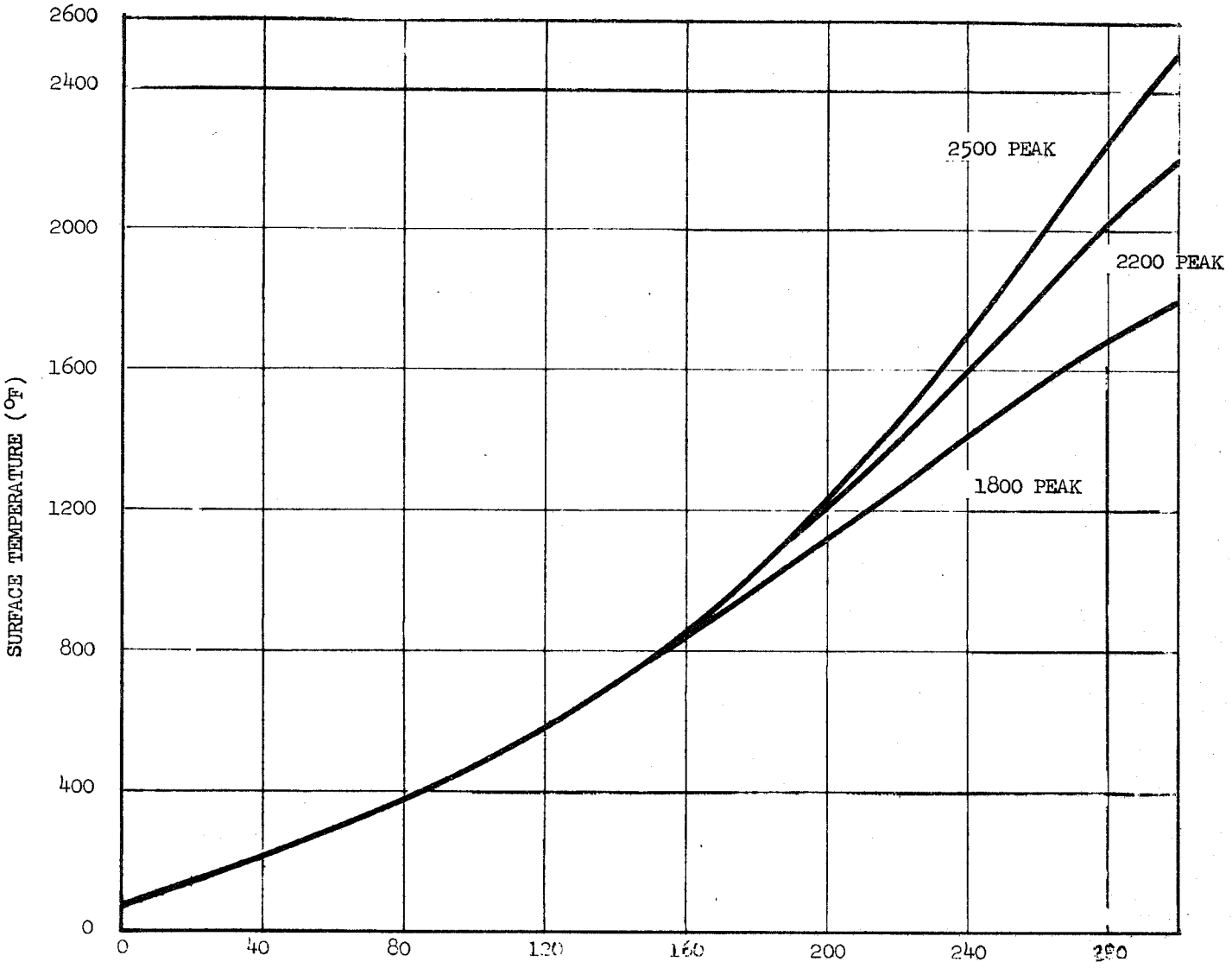
Figure A-8



COMPOSITE TEMPERATURE-TIME CURVES FOR TESTING HIGH TEMPERATURE INSULATIONS

457-1166

Figure A-9



HEAT UP PORTION OF TEMPERATURE TIME CURVE FOR EVALUATING
HIGH TEMPERATURE INSULATION

457-1167

Figure A-10

Appendix B

Density-Conductivity Tradeoff Study

Density-Conductivity Tradeoff Study

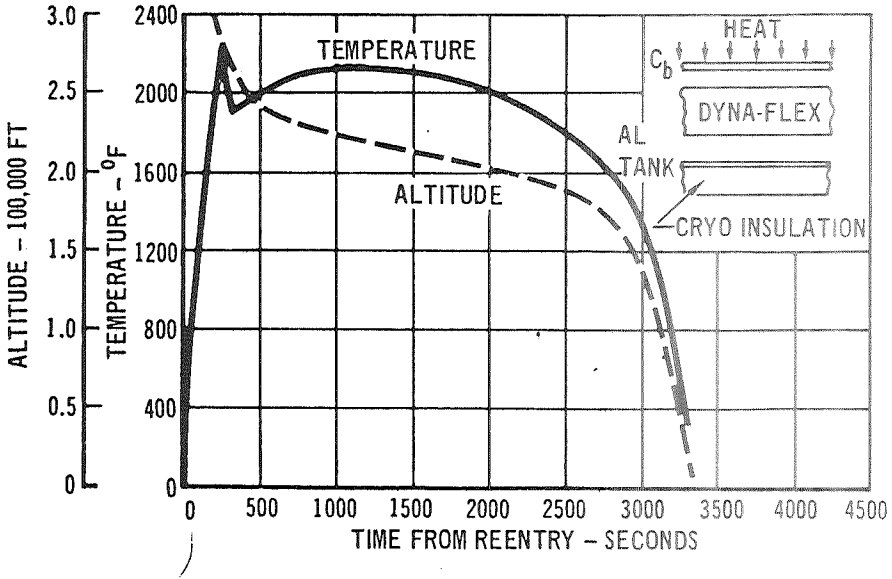
In a steady-state heat flow case, minimum weight occurs at minimum $k\rho$. For most insulations that are available in a range of densities, while the conductivity decreases with increase in density (in the temperature range of interest), the minimum $k\rho$ occurs at minimum available densities using atmospheric pressure data. It has been shown, however, (Reference 4) that when determining $k\rho$ as a function of ambient air pressure, the curves approach each other in value, and in some cases, cross. This would indicate that higher densities might have more favorable $k\rho$ values under vacuum conditions than low density materials. This could also be advantageous in that higher density products usually have more desirable physical properties.

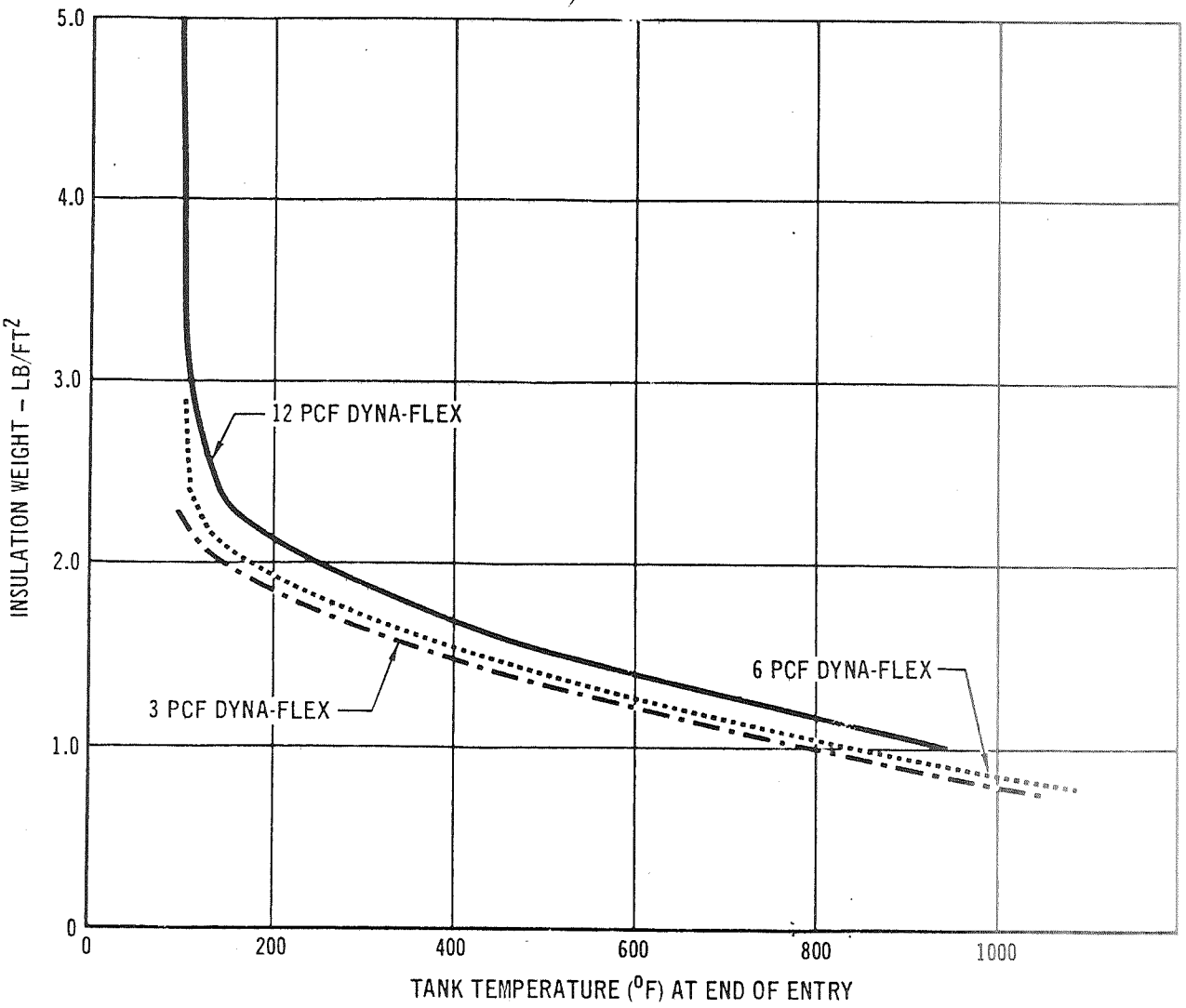
Because of the general lack of thermal conductivity data as a function of ambient pressure for most products of interest, we have developed a technique for calculating such data. In comparing calculated results with the limited experimental data available, agreement is excellent. This has also provided a valuable tool to calculate the net heat transfer in Shuttle vehicle insulations with much greater accuracy than previously, in that we can now include conductivity as a function of altitude (pressure) as well as of temperature. It was the purpose of this calculation to provide better guidance in the selection of insulations for test purposes, and to determine whether emphasis should be placed on low density or high density insulations.

In modeling the Shuttle heat transfer, a long cross-range delta Orbiter trajectory was assumed, with a temperature peak of 2200°F. For calculation purposes, Dynaflex felt was assumed to be the insulation, with densities of 3, 6, and 12 lbs/ft^3. The limiting factor was the resultant temperature of the cryogenic propellant tank, and the data are plotted as weight of insulation per unit area for various tank temperatures.

It is apparent from Figure B-1 that low density insulations will provide the lowest weight insulation, though the density effect is not great.

- MAX CROSS RANGE ENTRY
- 2200°F MAX TEMPERATURE
- TANK TEMPERATURES ARE AT END OF ENTRY (3100 SEC)
- DYNA-FLEX THERMAL CONDUCTIVITY SENSITIVE TO ALTITUDE (PRESSURE)





457–1168

LIGHTER INSULATIONS REDUCE TPS WEIGHT

Figure B–1

Appendix C

Oxidation Resistance of Metal Foils

Oxidation Resistance of Metal Foils

Candidate metal foils were examined for oxidation resistance under the reduced pressure they would experience in Shuttle reentries. The evaluation was performed by cycling specimens 1.5 inches wide by 4 inches long in an Astro Industries Model 60-280 furnace at 5 Torr air pressure. Variable temperature as a function of time was obtained by positioning of the specimens within the furnace and was provided by a programmed controller. The thermal profile used was that of the short cross range Orbiter with a peak temperature of 2200°F. At the time of this test, the short cross range Orbiter was the vehicle of primary interest.

At the conclusion of 10, 25, 50, and 100 cycles, the specimens were removed and examined as follows:

(a) Photographs made of each specimen;

(b) Each specimen weighed to $\pm$0.1 mg;

(c) Each specimen was bent 180° around a 1.0 inch diameter mandrel to evaluate ductility and note cracking or flaking of surface oxide film;

(d) A 1/4 x 1/2 inch specimen was cut from each specimen for metallographic examination.

(e) Specimens reweighed.

The alloys examined were:

Inconel 601 - 4 mil

Inconel 702 - 5 mil

Hastelloy X - 2 mil

TD-NiCr - 11 mil

Data from these examinations are presented in Table C-1.

Each of the specimens experienced weight gains as surface oxide films formed during the reentry cycling. The TD-NiCr exhibited the lowest total weight gain and the thinnest oxide film buildup of the four alloys. Substrate thickness remained nearly constant through 100 cycles on the TD-NiCr and Hastelloy X, but receded in excess of 1 mil on the Inconel 702 specimens. The latter also had the thickest oxide film buildup. Internal oxidation was present in all the specimens except Inconel 702, and was most severe in the Inconel 601.

Photomicrographs of these specimens are shown in Figures C-1, -2, -3, and -4.

All of these superalloys, with the exception of the TD-NiCr, displayed various amounts of curling during the 100 cycles. However, as long as they remained

ductile they were readily straightened and continued in test. In retrospect, this may have been a key to their later unsatisfactory performance as packaging materials for 2200°F service. The cause of the curling in the astro furnace tests could have been due to: grain growth, residual stresses, preferential oxidation on one side, alloy depletion, incipient melting, or even thermal stresses.

The curling of the flat specimens was not restrained by specimen configuration. However, when shaped into packages later, the restraint imposed by the specimen geometry might have caused the considerable deformation that occurred in the packages in the 2200°F evaluation tests.

Photographs of the furnace coupon specimens at the four stages at which they were examined are shown in Figures C-5, -6, -7, and -8. It is interesting to note that curling was first noted in the following sequence:

Hastelloy X	after 10 cycles
Inconel 601	after 25 cycles
Inconel 702	after 50 cycles
TD-NiCr	No curling occurred

The notches in the specimens shown in Figures C-5, -6, -7, and -8 were sections removed for metallographic examination.

TABLE C-1 RESULTS OF REENTRY CYCLING ON METAL FOILS

Alloy	No. of Cycles	Initial Weight (grams)	Cumulative Weight Gain (grams)	Flexibility Evaluation	Substrate Thickness (inches) Micrometer	Substrate Thickness (inches) Metallograph	Max. Thickness of Surface Oxide Film (mils)	Internal Oxidation
Hastelloy X	0	1.5473	-	-	0.0020	-	-	Oxidation occurred in the grain boundaries.
Hastelloy X	10	-	0.0415	Passed (1)	-	0.0019	0.12	
Hastelloy X	25	-	0.0552	Passed	-	0.0019	0.18	
Hastelloy X	50	-	0.0764	Passed	-	0.0018	0.28	
Hastelloy X	100	-	0.1044	Passed	-	0.0018	0.35	
Inconel 601	0	3.2569	-	-	0.0043	-	-	Oxidation occurred mainly in the grain boundaries.
Inconel 601	10	-	0.0506	Passed	-	0.0048	0.16	
Inconel 601	25	-	0.0735	Passed	-	0.0042	0.22	
Inconel 601	50	-	0.1045	Passed (2)	-	0.0040	0.28	
Inconel 601	100	-	0.1633	(3)	-	0.0036	0.36	
Inconel 702	0	4.1977	-	-	0.0053	-	-	Apparently no internal oxidation occurred.
Inconel 702	10	-	0.0242	Passed (4)	-	0.0056	0.36	
Inconel 702	25	-	0.0431	Passed	-	0.0054	0.50	
Inconel 702	50	-	0.0472	Passed	-	0.0056	0.78	
Inconel 702	100	-	0.0437	Passed (5)	-	0.0042	0.70	
TD Nickel-Chrome	0	9.1255	-	-	0.0113	-	-	Some internal oxidation was present which occurred throughout the material, not just at the grain boundaries.
TD Nickel-Chrome	10	-	0.0209	Passed (6)	-	0.012	-	
TD Nickel-Chrome	25	-	0.0247	Passed	-	0.012	0.02	
TD Nickel-Chrome	50	-	0.0284	Passed	-	0.012	0.03	
TD Nickel-Chrome	100	-	0.0252	Passed	-	0.012	0.04	

NOTES:

(1) Passed means no visible cracking of oxide layer or foil.

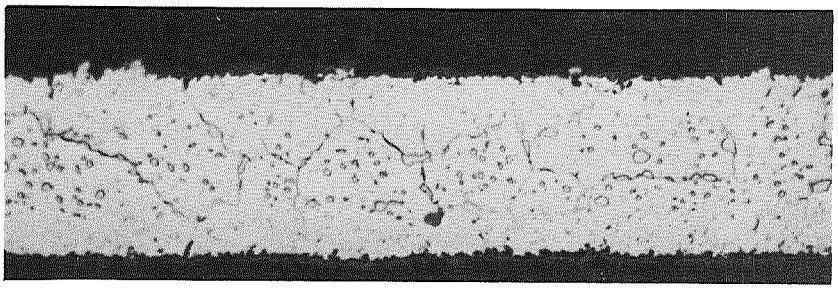
(2) Creased when straightened.

(3) Small fracture at edge (0.125" in length).

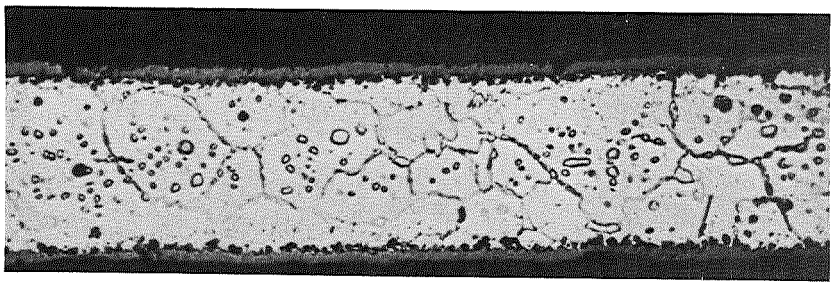
(4) Small quantity of gray dust.

(5) Creased when straightened.

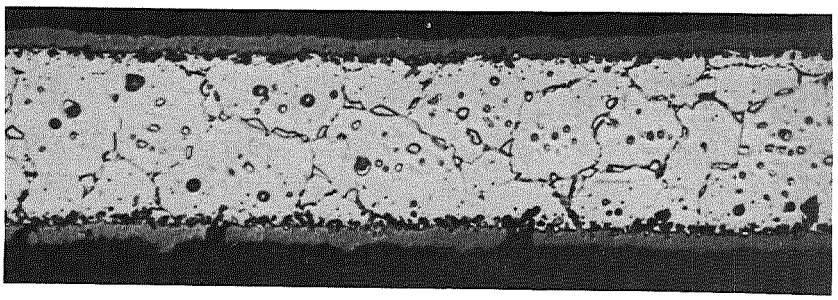
(6) Small quantity of green dust.



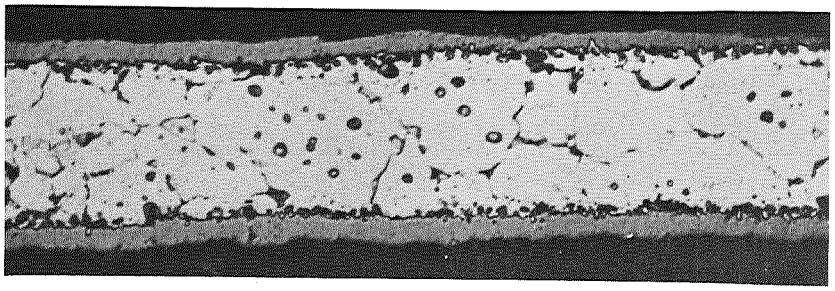
10 CYCLES



25 CYCLES



50 CYCLES



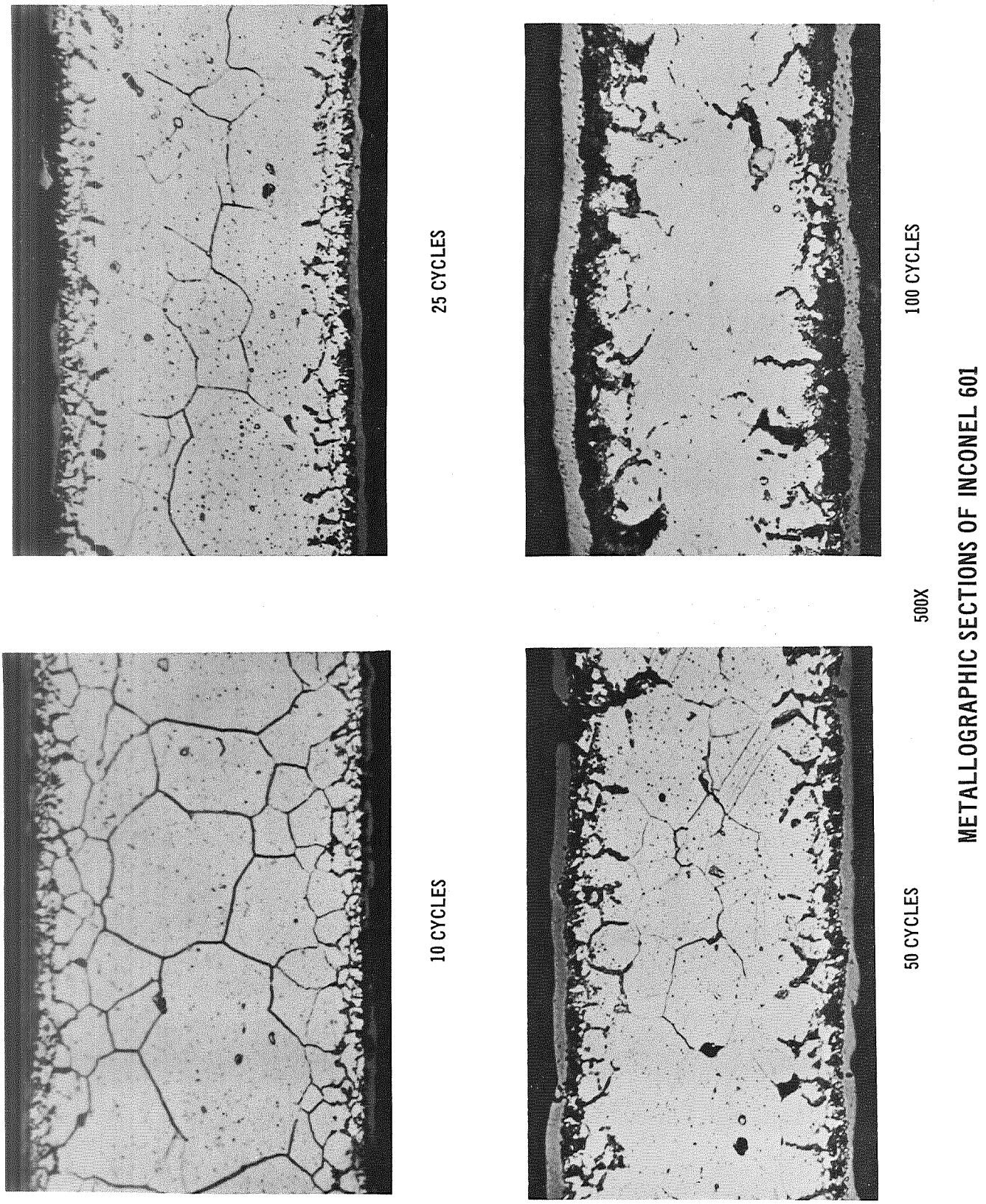
100 CYCLES

500X

METALLOGRAPHIC SECTIONS OF HASTELLOY X

457-1170

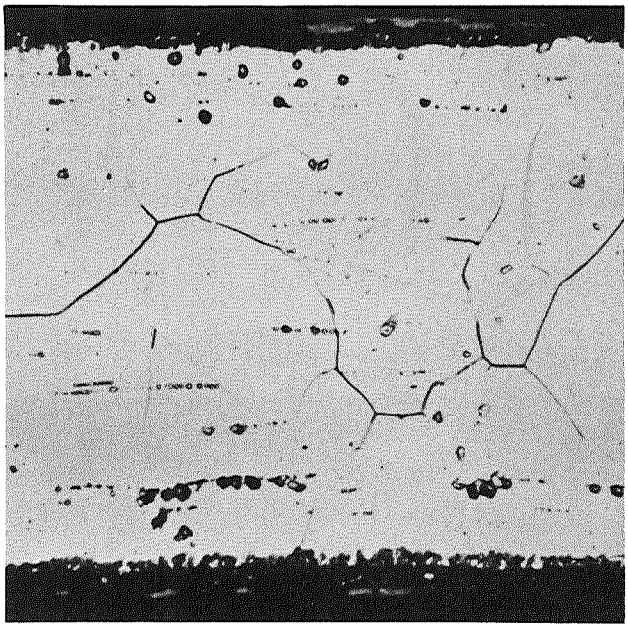
Figure C-1



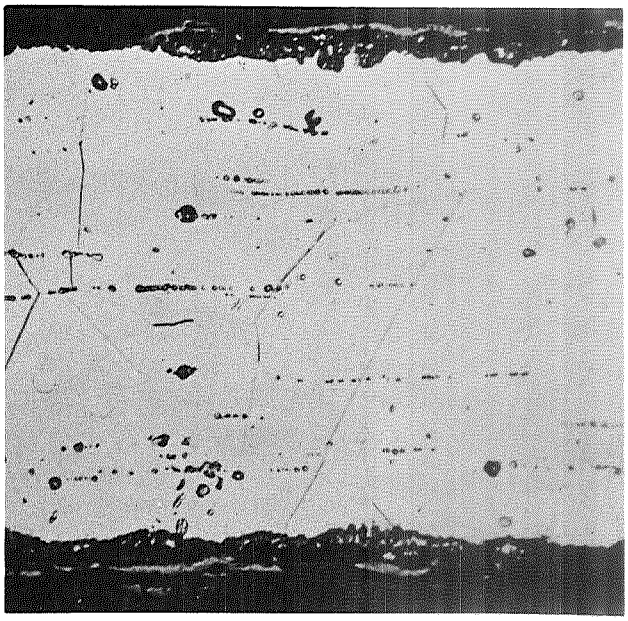
METALLOGRAPHIC SECTIONS OF INCONEL 601

457-1171

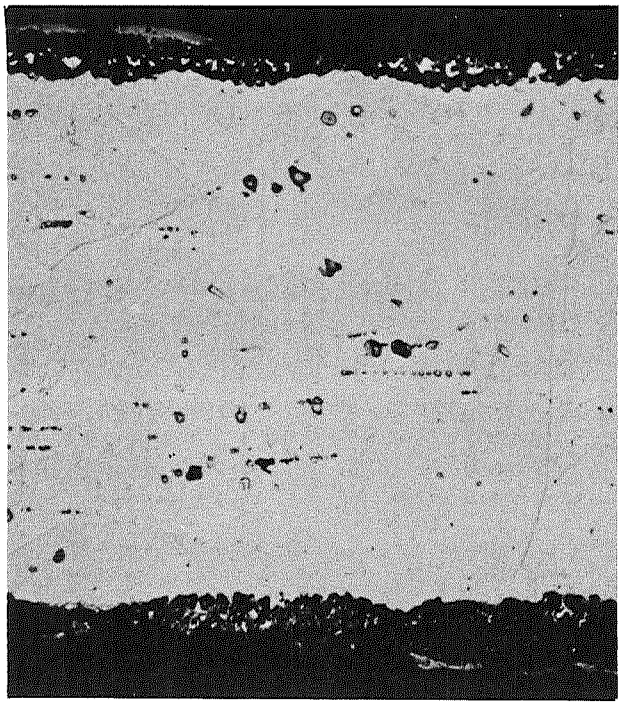
Figure C-2



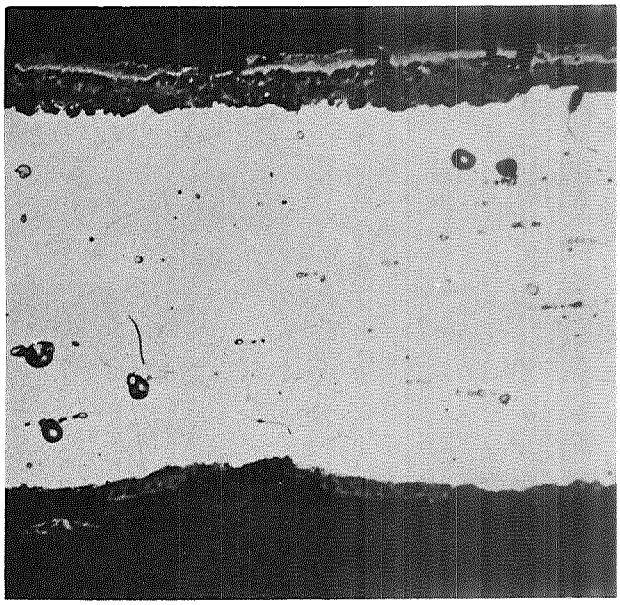
10 CYCLES



25 CYCLES



50 CYCLES



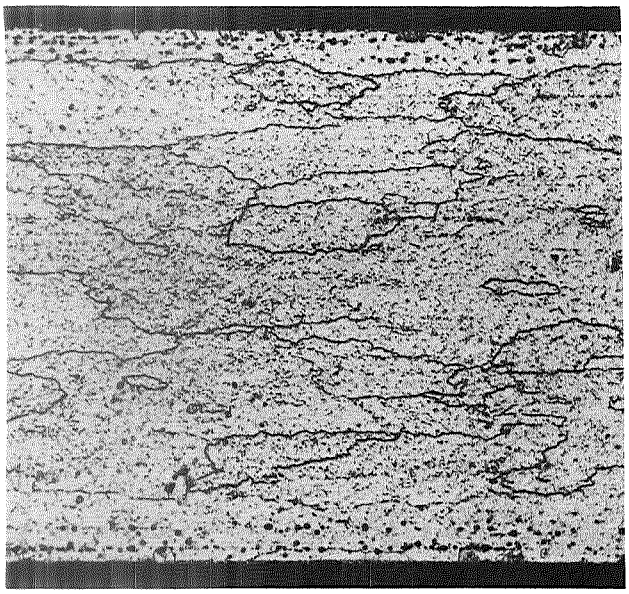
100 CYCLES

500X

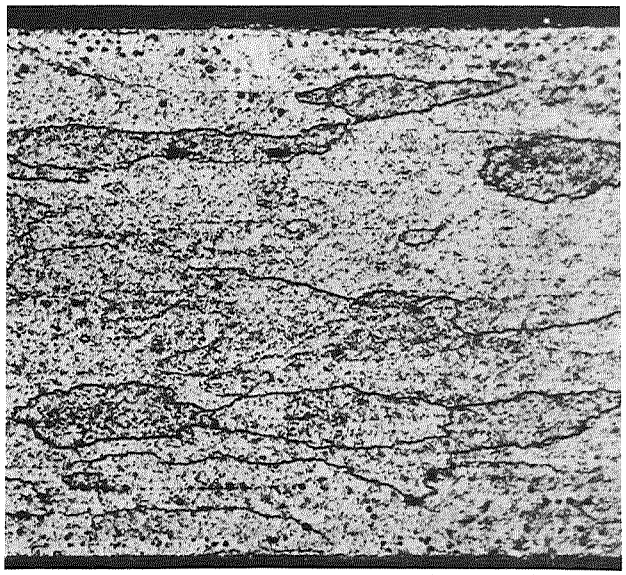
METALLOGRAPHIC SECTIONS OF INCONEL 702

Figure C–3

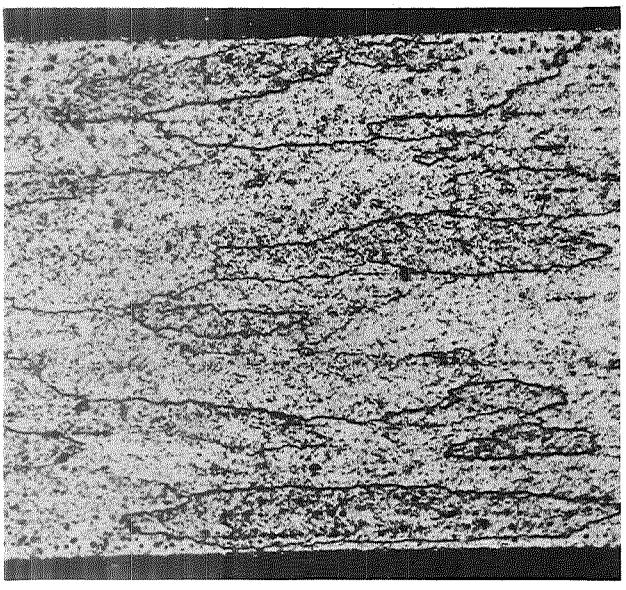
457–1172



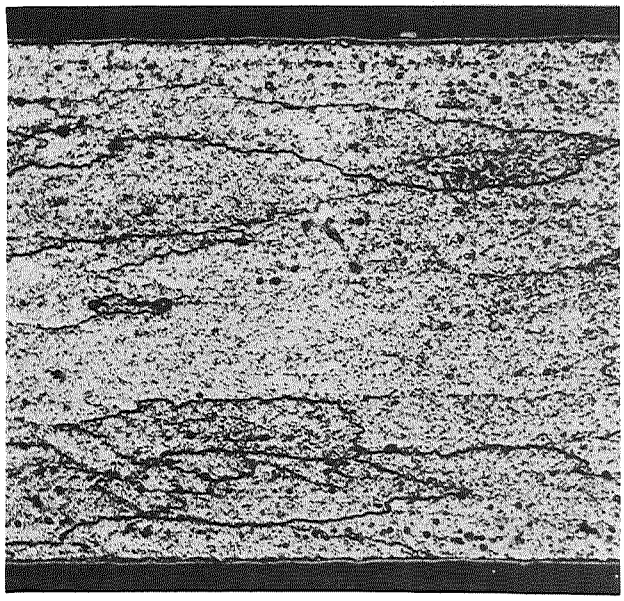
10 CYCLES



25 CYCLES



50 CYCLES



100 CYCLES

250X

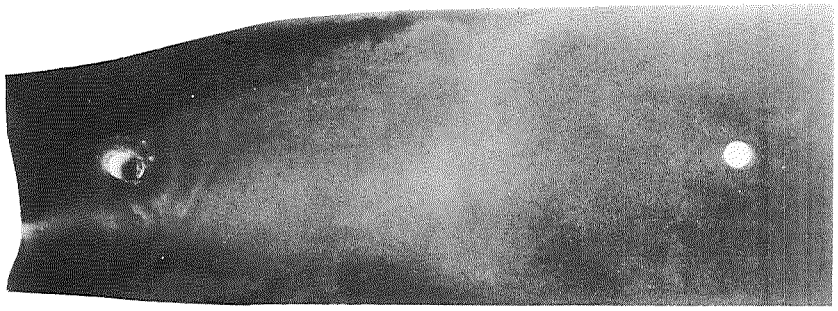
METALLOGRAPHIC SECTIONS OF TD NICKEL–CHROME

Figure C–4

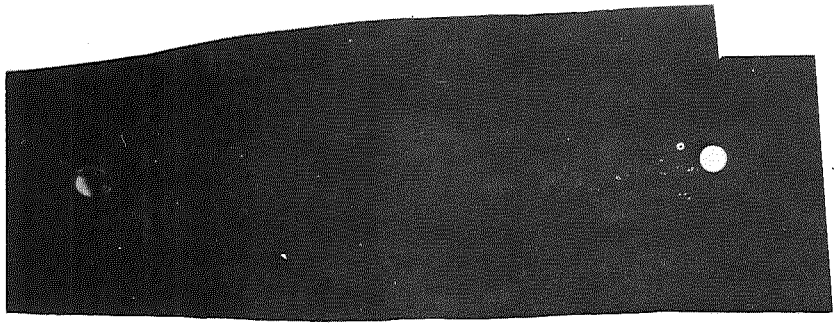
457–1173



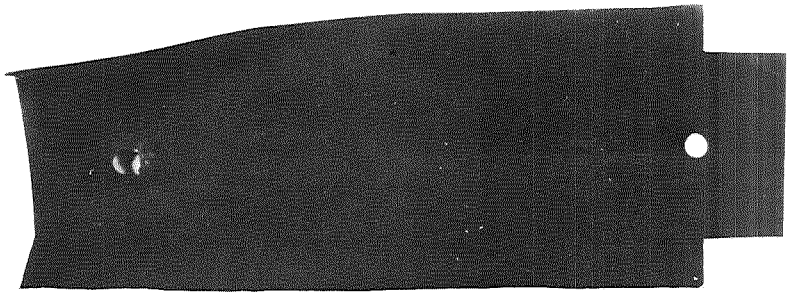
BEFORE TEST



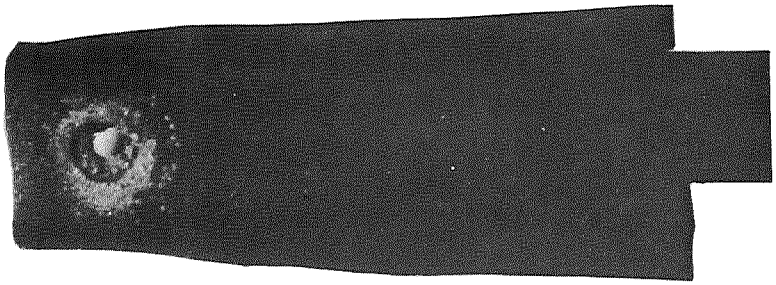
10 CYCLES



25 CYCLES



50 CYCLES

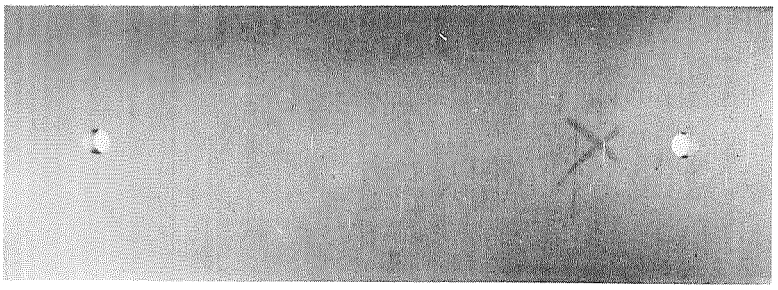


100 CYCLES

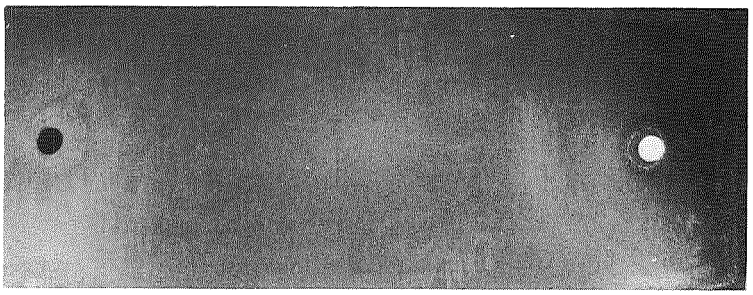
HASTELLOY X SPECIMEN

457-1174

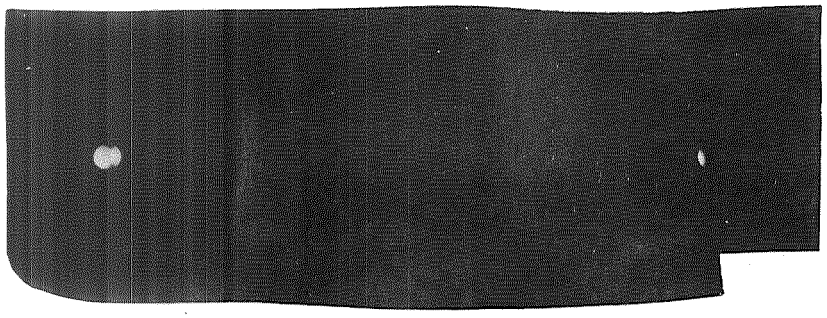
Figure C-5



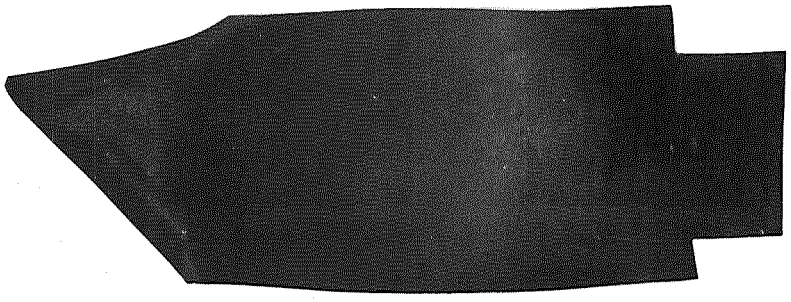
BEFORE TEST



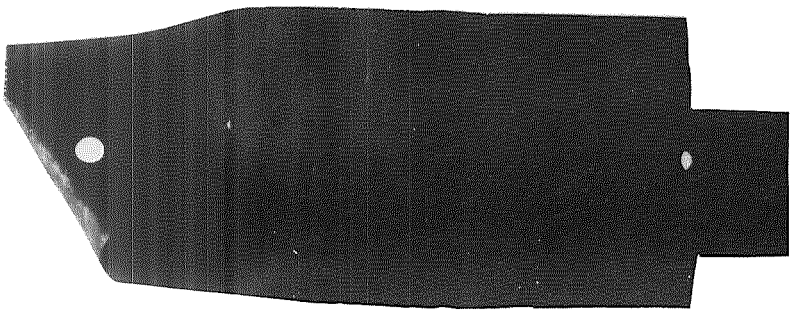
10 CYCLES



25 CYCLES



50 CYCLES

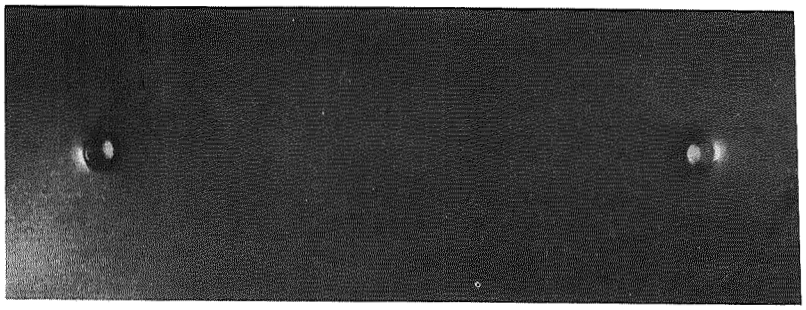


100 CYCLES

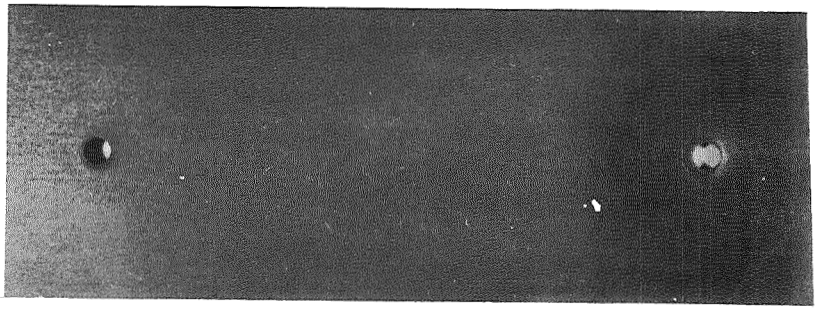
457-1175

INCONEL 601 SPECIMEN FURNACE TEST

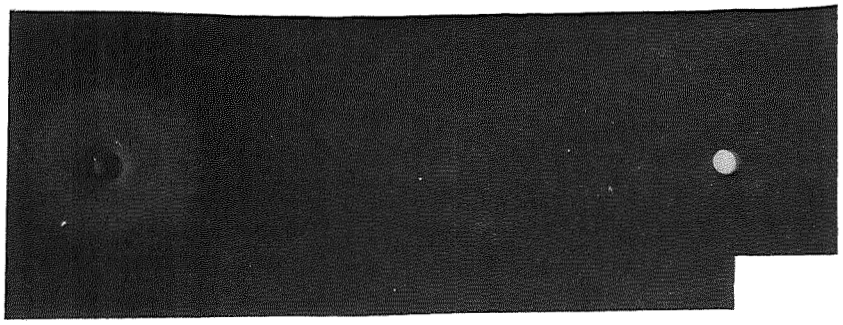
Figure C-6



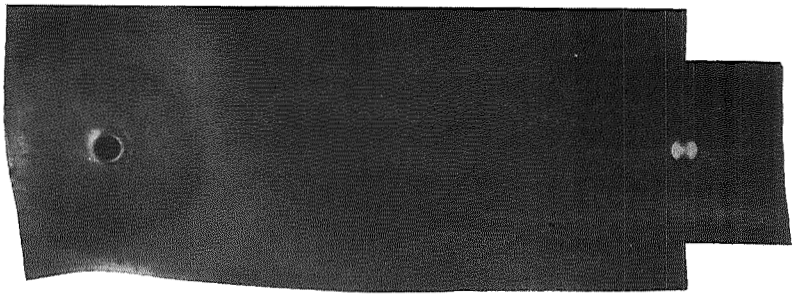
BEFORE TEST



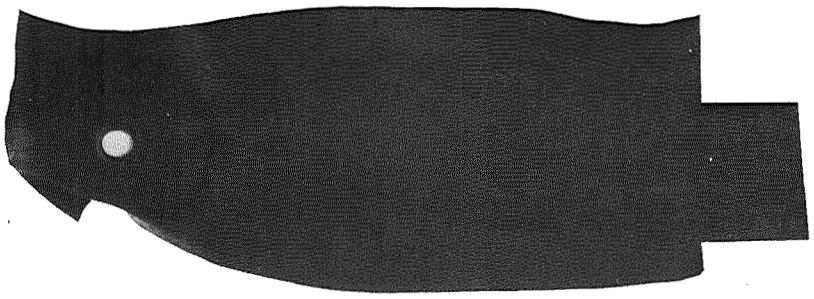
10 CYCLES



25 CYCLES



50 CYCLES

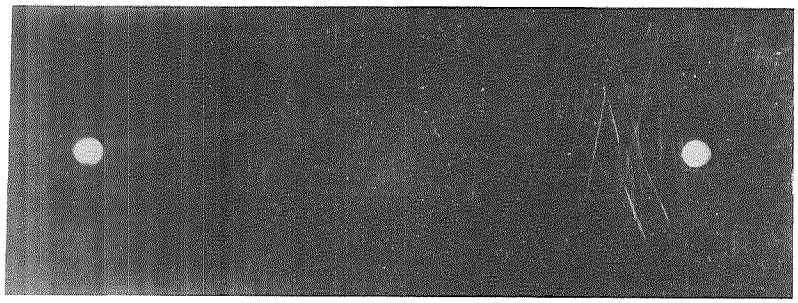


100 CYCLES

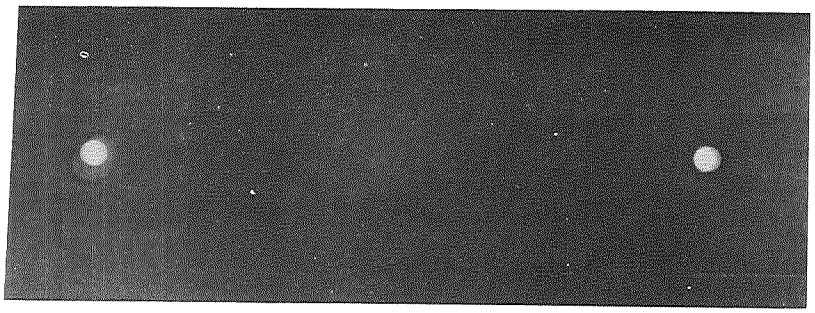
457–1176

INCONEL 702 FURNACE TEST

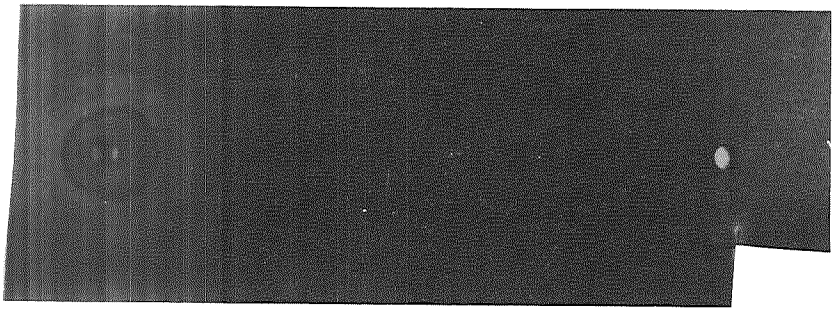
Figure C–7



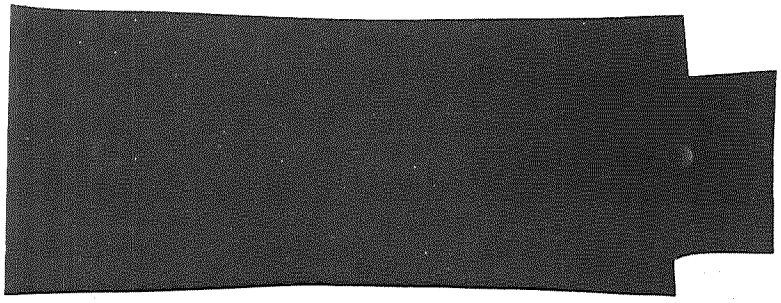
BEFORE TEST



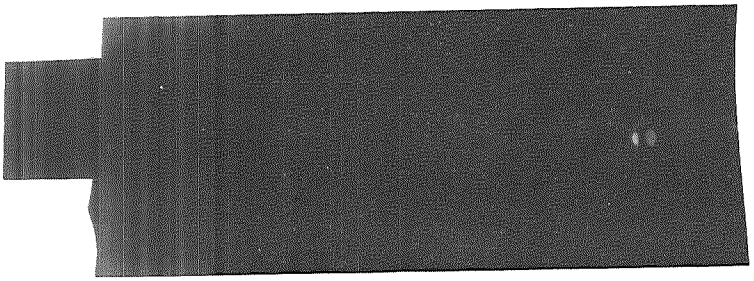
10 CYCLES



25 CYCLES



50 CYCLES



100 CYCLES

457-1177

TD NICKEL-CHROME SPECIMEN FURNACE TEST

Figure C-8

APPENDIX D
TRADE NAMES

The trade names for many of the products referred to in this report are identified below with their respective owners.

Dynaflex
Dynaquartz
Microquartz
Min-K
Thermoflex
    Johns-Manville Corp.
    New York, N.Y.

Astroquartz
    J. P. Stevens
    New York, N.Y.

Refrasil
Irish Refrasil
    HITCO
    Gardena, California

Fiberfrax
    Carborumdum Co.
    Niagra Falls, N.Y.

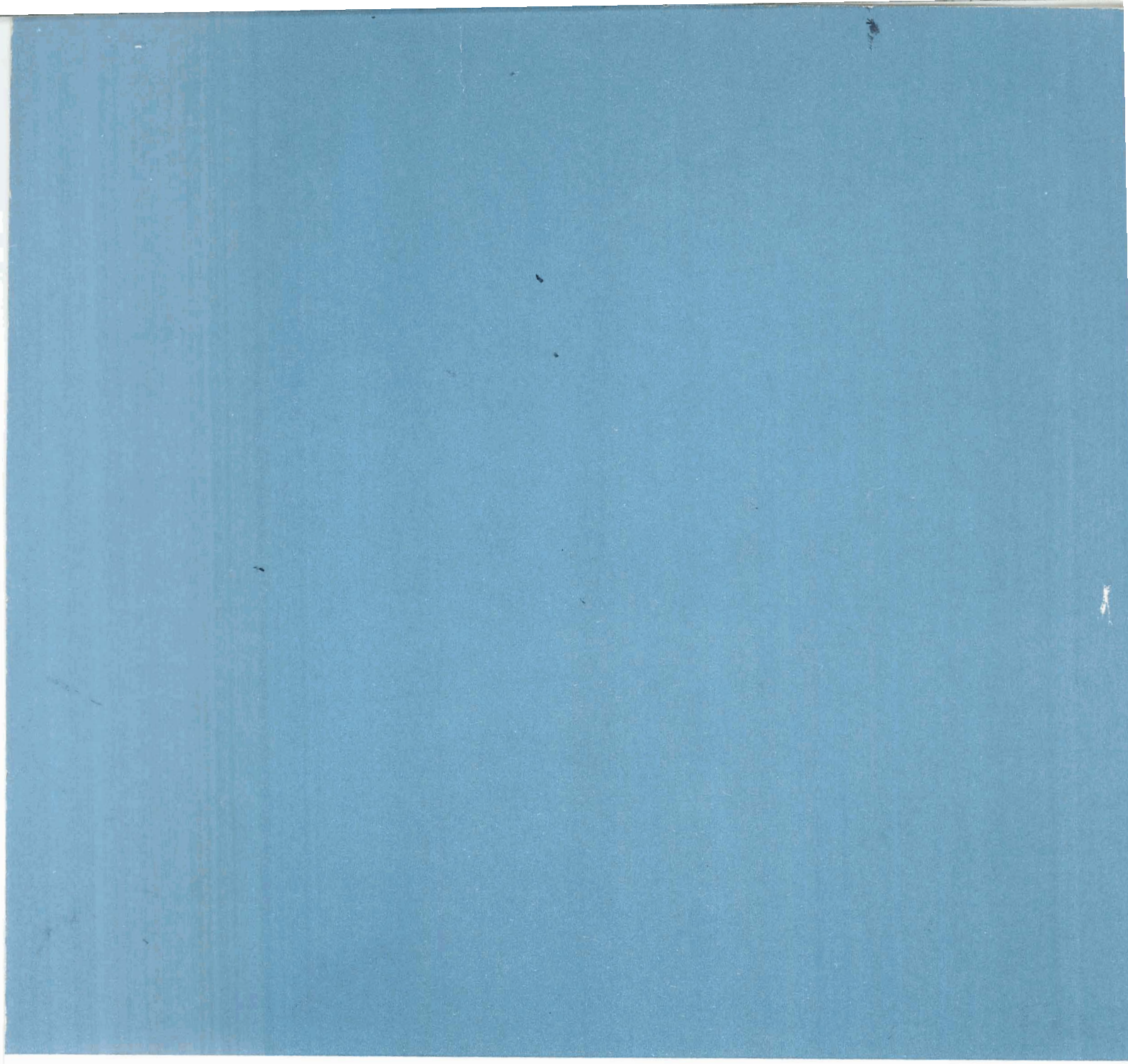
Inconel
    International Nickel Co
    New York, N.Y.

Syton
Hastelloy
    Union Carbide
    New York, N.Y.

Ludox
Positive Sol
    E. I. duPont de Namours
    Wilmington, Del.

Alon
    Cabot Corp.

Triton
    Rohm and Haas
    Philadelphia, Pa.



MCDONNELL DOUGLAS ASTRONAUTICS COMPANY – EAST

MCDONNELL DOUGLAS
CORPORATION